SELECTIVE SURFACE ACTIVATION OF MOTOR CIRCUITRY IN THE INJURED SPINAL CORD

A Dissertation
Presented to
The Academic Faculty

by

Kathleen Williams Meacham

In Partial Fulfillment
of the Requirements for the Degree
Ph.D. in the
School of Biomedical Engineering

Georgia Institute of Technology
December 2008

SELECTIVE SURFACE ACTIVATION OF MOTOR CIRCUITRY IN THE INJURED SPINAL CORD

Approved by:

Dr. Stephen P. DeWeerth, Co-Advisor
Department of Biomedical Engineering
Georgia Institute of Technology

Dr. Shawn Hochman, Co-Advisor
Department of Physiology
Emory School of Medicine

Dr. Robert Butera
School of Electrical and Computer Engineering
Georgia Institute of Technology

Dr. Vivian K. Mushahwar
Department of Cell Biology
University of Alberta - Edmonton

Dr. Robert Lee
Department of Biomedical Engineering
Georgia Institute of Technology

Dr. Lena Ting
Department of Biomedical Engineering
Georgia Institute of Technology

Date Approved: August 22, 2008

To my great-grandmother, Marjorie Lee Luna

ACKNOWLEDGEMENTS

I would like to thank my family and friends for their support, and especially to my father for all of those copies of Science News he would bring home for me. I would like to thank Stephen Adler for recommending neuroscience as one of the great last frontiers for engineers to explore. I would like to thank my husband, Mark, for his kindness and sense of humor. Finally, I would like to all of my teachers and mentors for continually lighting the way.

TABLE OF CONTENTS

LIST OF TABLES

LIST OF FIGURES

LIST OF ABBREVIATIONS

5HT	5-Hydroxy Tryptamine (Serotonin)
CAP	Compound Action Potential
DiI	1,1- Diocytadecyl-3,3,3,3,-tetramethylindocarbocyanine perchlorate
DLF	Dorsolateral Funiculus
FRA	Flexor Reflex Afferent
L2	Lumbar level 2
L6	Lumbar level 6
LF	Lateral Funiculus
MEA	Micro-Electrode Array
RIE	Reactive Ion Etch
SCI	Spinal Cord Injury
T12	Thoracic Level 12
vL2	Ventral Root L2
vL6	Ventral Root L6
VLF	Ventrolateral Funiculus
WMT	White Matter Tract

SUMMARY

Access to and subsequent control of spinal cord function are critical considerations for design of optimal therapeutic strategies for SCI patients. Electrical stimulation of the spinal cord is capable of activating behaviorally-relevant populations of neurons for recovery of function, and is therefore an attractive target for potential devices. A promising method for accessing these spinal circuits is through their axons, which are organized as longitudinal columns of white matter funiculi along the cord exterior. For this thesis, I hypothesized that these funiculi can be selectively recruited via electrodes appropriately placed on the surface of the spinal cord, for functional activation of relevant motor circuitry in a chronically-transected spinal cord. My tandem design goal was to fabricate and implement a conformable multi-electrode array (MEA) that would enable this selective stimulation.

To accomplish this design goal, I participated in the design, fabrication, and electromechanical testing of a conformable MEA for surface stimulation of spinal tracts. I then assessed the fundamental capability of this MEA technology to stimulate white matter tracts in a precise, controlled, and functionally-relevant manner. This was accomplished via *in vitro* experiments that explored the ability of this MEA to locally activate axons via single- and dual-site surface stimulation. The results from these evaluation studies suggest that spinal-cord surface stimulation with this novel MEA

technology can provide discrete, minimally-damaging activation of spinal systems via their white matter tracts.

To test my hypothesis that surface stimulation can be used to recruit distinct populations in the spinal cord, I performed studies that stimulated lateral funiculi in both chronically-transected and intact *in vitro* spinal cords. Results from these studies reveal that selective surface stimulation of white matter tracts in the ventrolateral funiculus (VLF) elicit motor outputs not elicited in intact cords. In addition, I was able to demonstrate that the spinal systems activated by this surface stimulation involve synaptic components and are responsive to spatial, temporal, and pharmacologic facilitation. Corresponding labeling of the axonal tracts projecting through the T12 VLF indicate that, after chronic transection, the remaining spinal neurons whose axons travel through the VLF include those with cell bodies in both the intermediate region and dorsal horn. These electrophysiological results show that surface-stimulating technologies used to control motor function after injury should include focal activation of interneuronal systems with axons in the ventrolateral funiculus. As a whole, these studies provide essential starting points for further use of conformable MEAs to effectively activate and control spinal cord function from the surface of the spinal cord.

CHAPTER 1

INTRODUCTION

Overview

Spinal cord injuries (SCI) sever descending pathways that normally control spinal neuronal circuits including the central pattern generating circuitry (CPG) that generates locomotion. While brain commands are lost, most spinal circuits remain intact. In such cases, alternate access to and control of these remaining circuits is plausible via recruitment of remaining sensory and interneuronal pathways (Jankowska, Jukes et al. 1967; Baldissera, Hultborn et al. 1981; Antonino-Green, Cheng et al. 2002).

Spinal cord stimulation is a promising method for recovery of motor functions lost to injury or disease with demonstrated ability to recruit hindlimb motor systems in multiple animal models. For example, in rat, cat and human, epidural stimulation, with electrodes placed near the dorsal column, has been demonstrated to initiate and control hindlimb movement using single-site stimulation protocols (Dimitrijevic, Gerasimenko et al. 1998; Gerasimenko, Lavrov et al. 2005; Ichiyama, Gerasimenko et al. 2005; Gerasimenko, Lavrov et al. 2006; Lavrov, Dy et al. 2008). This method uses electrodes placed near the dorsal column, and is thought to activate both low-threshold dorsal root afferents as well as propriospinal neurons in the dorsolateral funiculus (Minassian, Jilge et al. 2004; Ichiyama, Gerasimenko et al. 2005; Barthelemy, Leblond et al. 2007; Gerasimenko, Roy et al. 2008).

Another promising method for recruiting spinal motor systems is intraspinal microstimulation. This approach uses microwires placed in gray matter regions within

the lumbosacral enlargement has been demonstrated to activate populations of neurons involved in motor output, including those that generate locomotion (Mushahwar, Gillard et al. 2002). For both approaches axons rather than cell bodies appear to be preferentially recruited, particularly at lower stimulus intensities (Ichiyama, Gerasimenko et al. 2005; Gaunt, Prochazka et al. 2006)(see also (Jankowska, Padel et al. 1975; Ranck 1975; Gustafsson and Jankowska 1976)). Both epidural and intraspinal stimulation approaches highlight the critical contribution of axon recruitment in the production of coordinated motor activity.

Fortuitously, the axon tracts of virtually all functional populations of spinal interneurons, ascending tract cell and descending systems have their axon tracts located near the surface of the spinal cord in anatomically identifiable sites (**Figure 1**). This geometry provides an opportunity for initiation and modulation of spinal circuits via stimulation at the surface of the spinal cord. Such an approach could potentially stimulate specific functional subpopulations of interneurons and augment, but not bypass the intact motor circuitry and sensory feedback. The result may be a system that combines artificial stimulation/control of intact pathways with the natural afferent feedback provided by and reinforcing the initiated movements.

Hence, this thesis represents an exploration of selective white matter stimulation. This thesis had two major objectives, the first of which was a design goal. This goal was to fabricate and implement a conformable multi-electrode array (MEA) for selective recruitment of spinal white axon populations. I hypothesized that a MEA placed in contact with the surface of the spinal cord can be applied to selectively recruit spinal tracts and to selectively activate motor patterns. I fabricated a novel biocompatible MEA on a mechanically conformable (elastic) substrate to facilitate multisite stimulation. I evaluated this device to demonstrate that it conforms to the surface of the cord and can produce robust stimulation of parallel projecting axon tracts.

The second objective was to characterize the ability of site-specific electrical stimulation of white matter sites, devoid of their normal descending projections, to activate spinal motor activity after spinal cord injury. For both objectives, the model system employed was the isolated young rat spinal cord, which can be maintained *in vitro* and contains all the neural elements required for the generation of coordinated motor activity including locomotion (Kiehn and Butt 2003; Kiehn 2006). Experimentally, this preparation provides access to much of the cord surface for selective stimulation of projection pathways that control spinal circuits. Previous studies in the neonatal rat have demonstrated that surface stimulation can activate selected pathways and evoke transient responses including activation of motor patterns consistent with activation of locomotor circuits (Wallis, Wu et al. 1993; Magnuson and Trinder 1997).

As separate classes of interneurons project their axons in a topographically organized manner in white-matter tracts in the spinal cord, I hypothesized that they can be selectively recruited via electrodes appropriately placed on the surface of the spinal cord. I used the chronically-transected rat spinal preparation. I combined axonal tract dye labeling with stimulation of white-matter tracts while recording motor output to characterize the ability of mapped interneurons to reproducibly generate motor patterns that may be of functional utility.

The ultimate goal of this research direction is to initiate and modulate spinal cord motor circuits after SCI via a combination of selective multisite stimulation and of closed-loop control using computational techniques that assess stimulus efficacy. The research undertaken here is a first step toward the development of new approaches for augmenting our selective control of motor circuits to improve the lives of individuals with SCI. It is hoped that the resulting technologies and techniques can be applied to clinically relevant prosthetic devices that reestablish user control of the locomotor CPG after SCI.

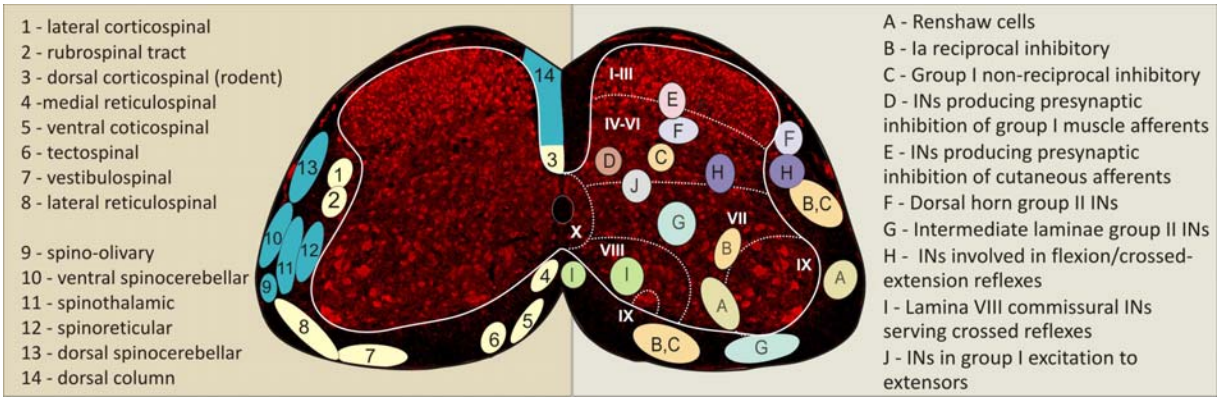

Figure 1.1. Axons in white matter are arranged topographically into tracts that convey ascending, descending, and propriospinal signals to and from brain and spinal cord regions.
Approximate locations in white matter are shown. Some descending (yellow) and ascending pathways (blue) are shown at right. Propriospinal pathways from identified interneurons are shown at left. Spinal neurons are labeled with the neuron specific marker NeuN (red) to exemplify spinal cord neuron architecture. (from Hochman 2007).

Background

Spinal cord injuries (SCI) produce life-long disabling impairments in both sensory and motor function. In the U.S. alone, accidents and violence lead to ~10,000 new injuries/year with more than 200,000 people currently living with SCI. Injuries predominantly affect young adults and healthcare costs often exceed $250,000/year. Scientists have identified five primary SCI research strategies: (i) limiting damage after injury, (ii) regeneration including transplantation, (iii) drug therapies, (iv) rehabilitation, and (v) neural prostheses (NPs). Though SCI research has developed an increased momentum and breadth (Kiehn, Harris-Warrick et al. 1998; Kalb and Strittmatter 2000; Chapin and Moxon 2001; Prochazka and Mushahwar 2001; McKerracher and Doucet 2002; Schouenborg and Kiehn 2002; Edgerton, Tillakaratne et al. 2004; Fouad and Pearson 2004; Rosenzweig and McDonald 2004; Silver and Miller 2004; Kiehn 2006; Edgerton, Courtine et al. 2008) it is still widely accepted that no single strategy can provide complete functional recovery of function, so research in all these fields are remain essential.

This thesis will focus on strategy (v) —neural prostheses (NPs). I introduce an alternate approach to motor control after SCI that engages the spinal cord motor circuits via stimulation of their white matter tracts with surface electrodes in a conformable multi-electrode array (MEA). To that end, I first provide a background introduction to important terms and concepts used to describe spinal cord systems and locomotion. I then describe the spinal cord interneuronal systems and their observed plasticity after SCI to set the stage for studies on the actions of electrical stimulation on locomotion. I then highlight the current approaches to electrical stimulation-based neuroprosthetic (NP) control of motor function highlighting important limitations that compel the creation of novel enabling NP technologies for control of motor function. I then discuss the use of

MEAs in neural interfacing, demonstrating their broad applicability, before prefacing the work undertaken in this thesis.

Spinal Cord

Spinal Cord Anatomy

The spinal cord is the gateway for information transfer between body and brain, and is an integrative center for neuronal circuits that coordinate complex sensory, motor, and autonomic functions. The central gray matter is organized into anatomical layers called laminae (**Figure 1**). White matter surrounds the gray matter and contains axon tracts that relay information throughout the spinal cord and between body and brain. These projections are conveyed in a topographically organized fashion (Figure 1). The spinal cord is segmentally organized. It is comprised of cervical, thoracic, lumbar, and sacral segments. Circuits that control the hindlimbs are dominant in caudal thoracic and lumbar segments. Primary afferent (sensory) neurons enter the spinal cord through the dorsal roots. They synapse onto spinal neurons and also project rostrally and caudally via the white matter axons tracts. The intermediate zone (lamina VII) and ventral horn of the spinal cord contain neural elements associated with the integration of motor output. Many of these neurons have been shown to receive considerable convergent input from both sensory and brain systems. Motoneurons are located in lamina IX and send axons exit via ventral roots to innervate muscles. Interneurons are defined as neurons whose projections are contained entirely in the spinal cord. The majority of interneurons are propriospinal interneurons. They project to other spinal cord segments via the white matter tracts. Ascending tract cells are not classified as interneurons, and are spinal neurons that also project to the brain.

Locomotion

The entire neural network required to generate locomotor activity resides in the spinal cord (Grillner 1981; Kiehn 2006). This network had been called the locomotor central pattern generator (CPG). The isolated intact rat or mouse spinal cord can produce a coordinated hindlimb motor output that spatiotemporally resembles locomotion in the intact hindlimb (Kiehn and Kjaerulff 1996; Kiehn 2006). This activity is referred to as "locomotor-like activity" and motor output recorded from L2 and L5 ventral roots have been shown to correlate well with motor activity in flexors and extensors, respectively (Kiehn and Kjaerulff 1998). The timing of locomotion can be controlled by activating systems that project to pattern generating elements of the CPG. This has been demonstrated following activation of afferent systems. 'Resetting' is said to occur when a stimulus activates the CPG such that the cycle of the locomotor rhythm is shortened or lengthened followed by the return of regular rhythm in a coordinated fashion (Hultborn, Conway et al. 1998). 'Enhancement' is said to occur if the stimulus leads to a transient disturbance of the rhythm following which the original rhythm is reinstated without a maintained phase shift (Hultborn, Conway et al. 1998). 'Entrainment' is said to occur when the frequency of CPG-mediated locomotion is altered by and follows the frequency of an external input to the CPG. Rhythmic afferent inputs have been shown to be able to entrain locomotor activity within a narrow range of frequencies (Andersson and Grillner 1983; Conway, Hultborn et al. 1987; Kriellaars, Brownstone et al. 1994).

Spinal cord neural networks, locomotion, and adaptation

Cellular and network components of vertebrate locomotion have been studied in various vertebrates including several mammalian species (Kiehn, Harris-Warrick et al. 1998). In mammals, classical studies (Sherrington 1910; Brown 1911; Jankowska, Jukes et al. 1967) demonstrated that the isolated spinal cord can generate a locomotor-like activity termed spinal stepping. Later studies have clearly demonstrated that the entire

network required for locomotor activity resides in the mammalian spinal cord including humans (Calancie, Needham-Shropshire et al. 1994; Nicol, Granat et al. 1995; Dimitrijevic, Gerasimenko et al. 1998; Fedirchuk, Nielsen et al. 1998). The very broad general view of locomotion is that 'drive' systems in brain project descending axons to activate the spinal locomotor CPG (Jordan 1998). Once activated the ensuing movements take advantage of multisensory movement-related feedback to the CPG to reinforce network activity thereby minimizing the effort placed on brain systems to maintain locomotion. Importantly, multisensory access sends a continuous stream of cutaneous and proprioceptive feedback to the spinal cord so that unexpected perturbations can reflexively modify ongoing patterns to engage adaptive responses to prevent injury (e.g. the stumble-corrective response). Importantly, locomotor pattern generation does not require descending commands for their initiation or control. The combination of intrinsic spinal cord circuits with sensory input can initiate and control locomotion in all species examined (Kiehn, Harris-Warrick et al. 1998). Thus, access to and recruitment of complex motor circuits including locomotion can be accomplished even after a complete loss of descending controls as seen after SCI (Edgerton, Leon et al. 2001; Rossignol, Giroux et al. 2001).

The central role of propriospinal neurons in motor control

Complex propriospinal (interneuronal) circuitry must exist to coordinate hindlimb motor activity across multiple joints bilaterally. It is not surprising then that propriospinal neurons make up as much as 97% of all cells in the spinal cord (Chung, Kevetter et al. 1984). Motoneurons and ascending tract cells comprise the rest. As stated earlier, propriospinal neurons interconnect via axons projecting as white matter tracts, and account for 1/3 to 2/3 of all white matter axons in the spinal cord (Chung and Coggeshall 1983; Chung and Coggeshall 1988). The organization of the white matter axon tracts of descending and ascending systems are well known (**Figure 1.1**). On the other hand, the

organization for propriospinal projections in the spinal cord is poorly documented and incomplete (Hochman 2007). For example, axons of propriospinal interneurons constitute the majority of all axons in the dorsolateral funiculus (Chung, Langford et al. 1987). However, very little is known about the identity of the propriospinal neurons that use this pathway. All that is known is that they include neurons in lamina I-IV (Petko and Antal 2000), the lateral parts of laminae V-VII (Molenaar and Kuypers 1978), and probably include the interneurons involved in stepping (Jankowska, Jukes et al. 1967). **Figure 1.1** presents a summary map of projection sites of propriospinal interneurons.

Some of the propriospinal neurons active during locomotion have been shown to be distributed via identifiable white matter funiculi over several spinal segments (Jankowska 1992; Jankowska and Edgley 1993). A prediction, then, is that focal electrical stimulation of their axons in the white matter should actually be able to activate these same functional populations of interneurons distributed over several spinal segments. Because these interneurons coordinate motor output across hindlimb joints bilaterally (Baldissera, Hultborn et al. 1981; Jankowska 1992), organized motor patterns should be recruited by such stimuli. Currently, there are no studies that have stimulated the white matter tracts of interneurons to study their ability to produce a coordinated motor output.

Individual populations of interneurons, when selectively recruited, have been shown to provide complex patterns of motor activation. For example, Group I non-reciprocal inhibitory interneurons project in the lateral or ventral funiculi (Czarkowska, Jankowska et al. 1981; Jankowska, Johannisson et al. 1981) and diverge to affect motoneurons of practically all muscles of a limb. They appear to; (i) coordinate activity of muscles operating at different joints, (ii) regulate muscle activity during stepping, and (iii) regulate muscle tension depending on the speed of the gait (Jankowska 1992). Lamina VII group II interneurons project in the ventrolateral funiculus (Bras, Cavallari et al. 1989) and are concentrated in spinal segments where critical elements of the

locomotor CPG are found (Cazalets, Borde et al. 1995; Rosenfeld, Sherwood et al. 1995; Langlet, Leblond et al. 2005) just rostral to those containing most hindlimb motoneurons (Jankowska 1992). Flexor reflex afferent (FRA) interneurons probably project through the dorsolateral funiculus (Jankowska, Jukes et al. 1967). They mediate the flexion and crossed extension reflexes that are provided via the enormous amount of converging afferent input.

An obvious feature of these interneurons is that they have very widespread actions. They coordinate trunk and limb motor activity bilaterally. Practically all categories of interneurons (including those described above) and ascending tract neurons are influenced by them (Eccles, Eccles et al. 1960). FRA interneurons are also thought to be used to mediate centrally initiated complex motor synergies as an integrating interneuronal system (Jankowska 1992).

These examples demonstrate that different functional populations of interneurons serve different motor tasks during ongoing movements, and participate in the organization of widespread motor synergies (Jankowska 1992). It is commonly thought that brain systems control movement by selectively recruiting a subset of these interneuronal populations (Baldissera, Hultborn et al. 1981; Hultborn 2001). Since the axon tracts of these intrinsic propriospinal interneurons travel in a functionally-organized manner, like brain systems, I hypothesize that I can recruit subsets of interneuronal populations by selective stimulation of their axons in white matter tracts.

Electrical Stimulation

I am proposing to control spinal motor circuits in the absence of descending commands via spinal segmental white matter electrical stimulation. Various studies have proven the feasibility of such an approach for activation of locomotor circuits. These are described below.

Sensory afferent-induced recruitment of locomotor-like activity

Studies in lower vertebrates have shown that a sensory stimulus can activate a long-lasting bout of locomotion (Sillar and Roberts 1992; Roberts, Soffe et al. 1998). In the acute spinal cat (after i.v. L-dopa), trains of stimuli to the FRA produce spinal stepping (Jankowska, Jukes et al. 1967). In the isolated neonatal rat spinal cord, sensory stimuli can also recruit an alternating locomotor-like activity but cannot control locomotor frequency (Marchetti, Beato et al. 2001; Strauss and Lev-Tov 2003). Sacral afferents are also capable of activating locomotion via projections in ventral, lateral, and ventrolateral tracts (Strauss and Lev-Tov 2003; Gordon, Dunbar et al. 2008) demonstrating that sensory access to the locomotor CPG occurs via multiple sites.

Sensory input induced resetting and entrainment of CPG activity

Stimulation of sensory input during ongoing locomotion can reset the locomotor rhythm demonstrating that these afferents have direct access to the CPG (McCrea 1998; Schomburg, Petersen et al. 1998; Hultborn 2001; McCrea 2001). Other studies have shown that sensory input provided by hip (Andersson and Grillner 1983; Kriellaars, Brownstone et al. 1994) and ankle afferents (Conway, Hultborn et al. 1987) can entrain the locomotor rhythm over a narrow frequency range.

Direct activation of spinal neurons can induce locomotor-like activity

In the rat, stimulation of the ventrolateral funiculus in lower cervical and thoracic spinal cord regions can induce hindlimb locomotor-like activity (Magnuson, Schramm et al. 1995; Magnuson and Trinder 1997) at via activation of ascending tract spinoreticular neurons and propriospinal interneurons (Antonino-Green, Cheng et al. 2002; Reed, Shum-Siu et al. 2006; Reed, Shum-Siu et al. 2008). Based on this information, I hypothesize that, after chronic spinal injury, surface stimulation of white matter regions

in the thoracolumbar spinal cord will be able to activate spinal motor circuits that go on to elicit hindlimb movement, and potentially locomotor-like activity.

Neural Prostheses

Neural prosthetic devices (NPs) may be defined as artificial extensions to the body that restore or supplement function of the nervous system that is lost during disease or injury. Many NPs stimulate peripheral nerves electrically, either through surface electrodes over nerves or through implanted electrodes near nerves. These NPs have been used on people with hemiplegia to counteract footdrop (Liberson, Holmquest et al. 1961; Kralj, Bajd et al. 1988; Kraft, Fitts et al. 1992; Taylor, Burridge et al. 1999). Stimulators triggered by voluntary electromyographic activity have also been used to facilitate retraining of the motor system (Chae, Bethoux et al. 1998; Francisco, Chae et al. 1998). There are also implantable NPs. However, because of their invasiveness, they must be biocompatible and durable. Dorsal column and deep brain stimulators are implanted to control chronic pain (Kumar, Toth et al. 1997; Waltz 1997) and brain stimulators also treat extrapyramidal disorders (Benabid, Wallace et al. 2005). Others NPs include phrenic nerve stimulators for respiration (Elefteriades, Quin et al. 2002) and sacral root stimulators for bladder control (Brindley, Polkey et al. 1982). In comparison, NPs for restoring motor function after SCI may need to be complex since they require the coordinated actions of many muscles. To date strategies have focused on restoring hand control in quadriplegics either with surface stimulators (Prochazka, Gauthier et al. 1997; Weingarden, Zeilig et al. 1998) or implants (Peckham, Keith et al. 2001) that involve stimulating muscle combinations that produce hand grasps.

Epidural vs. subdural spinal-cord stimulation

Decades ago, the first applied spinal-cord stimulators were used to control chronic pain using direct subdural placement of electrodes on the dorsal column spinal cord

surface (Shealy, Mortimer et al. 1970). While effective pain control ensued, fibrosis and morbidity (Nashold and Friedman 1972; Alo and Holsheimer 2002) led the abandonment of this technique and replacement with epidural electrodes (Alo and Holsheimer 2002). Epidural electrode placement for spinal cord stimulation introduces several complicating variables. They include: (i) a requirement for current to flow first through variable depth cerebrospinal fluid, (ii) unknown electrode placement in relation to spinal cord, and (iii) the need for much larger currents. Technological innovations that include the insertion of multiple electrodes insertions and advances in the programmable modifiability of stimulus delivery have increased effectiveness to this approach. Still, long-term success at pain control has been limited (Alo and Holsheimer 2002). Perhaps subdural electrode placement, the technique abandoned thirty years ago, should be revisited with the advent of newer technologies and enhanced material biocompatibility.

Epidural stimulation for activation of motor systems

In patients with complete cord transection, epidural electrode stimulation over the dorsal surface can elicit coordinated locomotor-like movements (Dimitrijevic, Gerasimenko et al. 1998; Minassian, Persy et al. 2007). Importantly, this suggested that the human CPG for locomotion also resides in the spinal cord and can be activated in the absence of descending commands. Similarly, epidural stimulation at L2 in chronic spinal rats also induces locomotor activity (Ichiyama, Gerasimenko et al. 2005; Ichiyama, Gerasimenko et al. 2005). This segment is thought to be critical to locomotor rhythmogenesis in rodents (Cazalets, Borde et al. 1995; Kjaerulff and Kiehn 1996; Cowley and Schmidt 1997). In cat spinal cord, epidural stimulation-induced locomotion was indistinguishable from the more conventional brainstem stimulation evoked locomotion and which could also be induced after thoracic cord transection (Iwahara, Atsuta et al. 1992) (see also (Gerasimenko, Avelev et al. 2003; Gerasimenko, Lavrov et al. 2005)). Interestingly, even though electrodes are placed over the dorsal columns in

these studies, lesioning experiments demonstrated that it was activation of the dorsolateral funiculus that recruits locomotor-like activity (Gerasimenko, Avelev et al. 2003). The dorsolateral funiculus is dominated by propriospinal neurons of largely unknown function. More recently, Edgerton and colleagues (Lavrov, Gerasimenko et al. 2006; Gerasimenko, Roy et al. 2008) have begun to use epidural stimulation at the sacral spinal cord which is thought to more selectively activate dorsal roots in the spinal column prior to cord entry.

Advantages and disadvantages of epidural stimulation

The greatest advantage of epidural stimulation is it relative lack of invasiveness and ease of application. Disadvantages include those stated above. Additionally, it is unlikely that gross electrical stimulation can afford the control required to manage the numerous subtleties of motor control.

Intraspinal microstimulation

Intraspinal microstimulation (**ISMS**) involves insertion of microelectrodes directly into the spinal cord gray matter. ISMS has been tested in animal models to recruit various motor activities (Bizzi, Tresch et al. 2000; Prochazka, Mushahwar et al. 2001; Mushahwar, Gillard et al. 2002; Mushahwar, Aoyagi et al. 2004). ISMS actions have been examined on bowel (Tai, Booth et al. 2001) and bladder control (Woodford, Carter et al. 1996; Grill, Bhadra et al. 1999; Tai, Booth et al. 2004), penile erection (Tai, Booth et al. 1998) and limb movements (Giszter, Mussa-Ivaldi et al. 1993; Mushahwar and Horch 1998; Tai, Booth et al. 1999; Tresch, Saltiel et al. 1999; Mushahwar and Horch 2000; Mushahwar and Horch 2000; Tai, Booth et al. 2000; Mushahwar, Gillard et al. 2002; Tai, Booth et al. 2003; Aoyagi, Mushahwar et al. 2004; Mushahwar, Aoyagi et al. 2004; Saigal, Renzi et al. 2004). Three groups have been primarily responsible for using ISMS to activate spinal neurons in order to recruit motor behaviors; cat experiments by

Mushahwar and colleagues (Prochazka, Mushahwar et al. 2001) and Roppolo and colleagues (Tai, Booth et al. 2000; Tai, Booth et al. 2001; Tai, Booth et al. 2003; Tai, Booth et al. 2004), and experiments predominantly in frog but also rat by Bizzi and colleagues (Tresch, Saltiel et al. 1999). At lower stimulus intensities, intraspinal microstimulation has been shown to synaptically recruit motor output via activation of intraspinal axons, including those of primary afferents (Gaunt, Prochazka et al. 2006). As many intraspinal axons are highly collateralized, divergent actions are expected to occur and have been demonstrated to extend multiple spinal segments (Gaunt, Prochazka et al. 2006). There is also evidence that local networks of interneurons (including those receiving cutaneous afferent input) are involved in producing the evoked motor outputs (Tresch and Bizzi 1999). Both epidural and intraspinal stimulation approaches highlight the critical contribution of axon recruitment in the production of coordinated motor activity. This is because axons are activated at lower thresholds than their associated cell bodies (Jankowska, Padel et al. 1975; Ranck 1975; Gustafsson and Jankowska 1976).

Advantages of ISMS include: (i) Electrodes can be implanted in a localized and mechanically stable environment (e.g. the lumbosacral spinal region is approximately 5 cm long in humans and the spinal column protects implanted electronics). (ii) As the spinal cord contains all the interneuronal circuits involved in producing coordinated motor behaviors (i.e. standing, locomotion, excretory and sexual function), tapping into these circuits directly may provide for command control of "hard-wired" coordinated behaviors, and thus reduces the number of needed control sites (Giszter, Mussa-Ivaldi et al. 1993; Tresch, Saltiel et al. 1999; Grill and Kirsch 2000; Tai, Booth et al. 2000; Tai, Booth et al. 2003). (iii) Motor recruitment by activation of 'up-stream' spinal circuits may produce more physiologically appropriate recruitment and graded motor activity, with a nearly normal order of motor unit recruitment and reduced muscle fatigue (Mushahwar and Horch 1997; Mushahwar and Horch 2000; Mushahwar and Horch 2000).

Disadvantages of ISMS include: (i) Technical difficulties: Currently electrodes are implanted manually and there is considerable "difficulty in accurately placing 30 μm tips in sub-millimeter precise locations" (Mushahwar, Gillard et al. 2002). (ii) Electrode fixation: Adhesives used to maintain electrode position "can displace the electrodes upwards when it dries"(Mushahwar, Gillard et al. 2002). (iii) Spinal cord damage: Implanting electrodes into the spinal cord is invasive with electrode placement undertaken blindly. Additional surgical concerns include the possibility of intraspinal bleeding, scar formation, and need for additional surgery to fix or replace an inaccurate transplant. (iv) Non-selective control over spinal cord functional systems: ISMS recruits neurons largely by activation of their axons at lower stimulus intensities and then cell somas at higher stimulus intensities. Since axonal and soma excitability is controlled in a state-dependent manner, ISMS of the exact same site can have completely opposite actions on motor output under different spinal states (Lundberg 1969; Aoyagi, Mushahwar et al. 2004; Mushahwar, Aoyagi et al. 2004). Moreover, reflex gating cannot be controlled, and the flexibility to recruit subpopulations of interneuronal systems is lost. Additionally, ISMS activates cell bodies and axons at a specific site yet physiological studies have shown that functional circuits are distributed dorsoventrally and rostrocaudally (Baldissera, Hultborn et al. 1981; Jankowska 1992). Moreover, descending and propriospinal systems channel actions to subpopulations of interneurons while activity in other interneurons are actively inhibited (Lundberg 1967; Lundberg 1979; Baldissera, Hultborn et al. 1981; Lundberg, Malmgren et al. 1987; Jankowska 1992; Hultborn 2001; Jankowska 2001).

Multielectrode array (MEA) stimulation of spinal circuits

Extracellular activation and monitoring of neural circuitry has demonstrated ability to provide significant functional restoration. A common concern however is for NPs has been the inability to produce optimal results with low numbers of stimulation

sites. This restricts many effective electrical stimulation NPs from translating into clinically applicable devices. Reasons for the lack of success of reduced-site models to produce reliable long-term results include: (i) fatigue of activated circuitry, (ii) degradation of the electrode-tissue interface, and (iii) shifting of electrodes from original sites of stimulation (Branner, Stein et al. 2001; Popovic, Curt et al. 2001; Kern, Hofer et al. 2002; Mushahwar, Gillard et al. 2002). In addition, the aforementioned observed plasticity of neural systems, including those that follow SCI, is also a challenge for implantable NPs of limited electrode number. This is because stimulation sites that may have initially elicited a desired function may change in functionality or completely cease to functional (Wolpaw and Carp 1993). A more adaptable and diverse interface is required if implanted electrode approaches can be used to restore lost spinal cord function.

Multi-electrode arrays (MEAs) use can address the several challenges facing implantable neural devices for chronic stimulation. MEAs provide multiple selective sites at which activation can occur (Veraart, Grill et al. 1993; Rutten, Smit et al. 1999; Tarler and Mortimer 2004). Moreover, multi-site interleaved stimulation enables activation at lower electrical intensities than single sites. Such an approach has been shown to produce less-fatigable and smoother motor activation (McDonnall, Clark et al. 2004). Last, multi-site stimulation paradigms can confer recruitment patterns not achievable with single-site stimulations (Tyler and Durand 2002). While epidural stimulation can activate locomotor patterns, the greater range and sophistication of spatiotemporal stimulation that can be provided by MEAs has been shown to improve the coordination of advanced motor control such as that underlying locomotion (Mushahwar and Horch 2000; Mushahwar and Horch 2000).

Applications of commercially available MEAs

Several fields of neural prosthetic research have achieved clinical success using multi-electrode stimulation and recording, including implants for hearing (Clark 1999; Spelman 1999), respiratory (Lanmuller, Sauermann et al. 1999), bladder (Boyer, Sawan et al. 2000; Dalmose, Bjarkam et al. 2003), bowel (Amaris, Rashev et al. 2002; Rashev, Amaris et al. 2002), and postural function (Davis, Houdayer et al. 1999). In the cortex, multi-electrode arrays provide spatiotemporal signaling patterns that can be translated into control signals for a robotic arm (Nicolelis 2001). In addition to these impressive advancements, there is also significant potential for multi-electrode implants to reduce spasticity, pain, and influence growth patterns in tissue engineering grafts (Shealy, Mortimer et al. 1967; Shealy, Taslitz et al. 1967; Mortimer, Shealy et al. 1970; Shealy, Mortimer et al. 1970; Levin and Hui-Chan 1992; Hesse, Reiter et al. 1998; Al-Majed, Neumann et al. 2000; Zhong, Yu et al. 2001). Implantable MEAs, such as those developed at the Universities of Utah and Michigan, are commercially available and have been used widely by neurophysiologists towards both basic science and clinical ends (Maynard, Nordhausen et al. 1997; Normann, Warren et al. 2001; Rousche, Pellinen et al. 2001; Warren, Fernandez et al. 2001; Hetke 2003; Hillman, Badi et al. 2003; Kipke, Vetter et al. 2003; Branner, Stein et al. 2004; Stein, Aoyagi et al. 2004; Vetter, Williams et al. 2004; Warren and Normann 2005). Single-site and several-site stimulation approaches have elicited motor patterns via intraspinal access (Saigal, Renzi et al. 2004) (Guevremont L, Renzi CG, Norton JA, Kowalczewski J, Saigal R, Mushahwar VK. 2006) as well as stimulation of the ventrolateral funiculus (Magnuson, Schramm et al. 1995; Magnuson and Trinder 1997) and dorsal column tracts (Ichiyama, Gerasimenko et al. 2005).

Flexible and conformable MEAs

One of the primary limitations of typical rigid MEAs is that differences in mechanical properties of electrodes and tissue can lead to significant tissue damage. Consequences range from reduced interface integrity to irreversible loss of function. Tissue/electrode property mismatches—including differences in material compliance, damping, and density—are a significant issue for all long-term implantable devices. Measures have been implemented to reduce electrode rigidity in part by creating flexible wires, jointed rigid interfaces, and slower penetration methods (Kennedy, Mirra et al. 1992; Kennedy, Bakay et al. 2000; Branner, Stein et al. 2001; Holman G. 2002). Flexible MEAs have also been developed, and they primarily use polyimide as a substrate (Gonzalez and Rodriguez 1997; Stieglitz, Beutel et al. 1997; Rousche, Pellinen et al. 2001). However, while polyimide thin-film arrays exhibit varied levels of flexibility and have been applied to various interfaces in the neuromuscular system (Boppart, Wheeler et al. 1992; Stieglitz, Beutel et al. 1997; Rousche, Pellinen et al. 2001; Rizzo, Wyatt et al. 2003; Rizzo, Wyatt et al. 2003; Lapatki, Van Dijk et al. 2004; Takeuchi and Shimoyama 2004), they are not sufficiently flexible to confront the challenge of chronic surface stimulation of the spinal cord. This is primarily because the material does not conform to the topographically complex surface of the cord. Further, it does not allow for oxygen to diffuse through which would likely lead to oxygen deprivation and cell death. In contrast, an MEA fabricated of conformable and oxygen-permeable material would minimize mechanical mismatch, provide uniform contact around the circumference of the cord (Maghribi M.

2002), and provide the necessary oxygen supply. In addition, for spinal cord activation, conformable surface electrodes would enable more selective access to the majority of spinal functional systems along the rostrocaudal and circumferential axes of the cord. Such an MEA has yet to be fully developed.

Advantages of conformable MEAs for surface stimulation

Newly developed materials and microfabrication techniques are available to support creation of a spinal cord interface that possesses a greater adaptability as compared to traditional rigid and polyimide MEAs, and also provide a conformable substrate that allows for optimal contact with multiple spinal tracts.

There are additional advantages to using a conformable MEA. The combination of surface stimulation of the spinal cord with conformable multi-electrode arrays provides a novel and potentially powerful method for controlling and improving upon motor behaviors after SCI. Less invasive than ISMS, it provides a clear topographical target for site-specific stimulation. Since functional systems are organized topographically around the spinal cord, differential control of numerous functional systems could allow expression of a greater repertoire of behaviors. As an example, one could recruit Ia inhibitory interneurons in the lateral funiculus as a means to control whether the motor output of flexor and extensors is alternating or co-activated. Alternating activity would promote locomotion (Grillner 1981; Petersen, Morita et al. 1999) while silencing of Ia inhibitory interneurons would allow co-contraction of antagonist muscles in order to stabilize a joint (Crone and Nielsen 1994). As MEAs offer numerous contact sites, neural interfacing is probably only hindered by physiologic rather than design limitations. This thesis serves to begin to understand the physiologic limitations faced following the development of a novel conformable MEA.

Subsequent organization of this thesis

The following 3 chapters are presented as three independent but related research projects that define the thesis. Chapter 2 describes the conceptualization, development, characterization, and testing of a novel MEA technology for conformable access of spinal surface tracts. Chapter 3 involves further optimization of the MEA and then focuses on its testing in the isolated spinal cord. This chapter also shows that MEA can be used for

surface stimulation of white matter regions with the same selectivity seen with more conventional rigid electrodes. In Chapter 4, I facilitate future applications of this MEA as a spinal cord prosthetic by examining evoked responses following stimulation of the injured spinal cord surface. As our ultimate goal is to control spinal cord motor output using the propriospinal systems that remain following SCI, experiments focused on stimulation studies in the chronically-transected spinal cord. I have identified the ventrolateral funiculus as an effective site for motor control after SCI and use tract tracing to anatomically identify the populations of spinal neurons with axons in the ventrolateral funiculus in both chronic-transected and intact cords. Chapter 5 provides a short synthesis of my results and suggests future directions for continued study.

CHAPTER 2:

FABRICATION AND TESTING OF A NOVEL, ELASTOMER-BASED MICRO-ELECTRODE ARRAY FOR SURFACE STIMULATION OF THE SPINAL CORD

Parts of this chapter are published as:

Meacham, K.W., Richard J.Giuly, Liang Guo, Shawn Hochman, Stephen P. DeWeerth

A Lithographically-Patterned, Elastic Multi-electrode Array for Surface Stimulation of the Spinal Cord. Biomedical Microdevices.

Summary

A new, scalable process for microfabrication of a silicone-based, elastic multi-electrode array (MEA) is presented. The device is constructed by spinning poly(dimethylsiloxane) (PDMS) silicone elastomer onto a glass slide, depositing and patterning gold to construct wires and electrodes, spinning on a second PDMS layer, and then micropatterning the second PDMS layer to expose electrode contacts. The micropatterning of PDMS involves a custom reactive ion etch (RIE) process that preserves the underlying gold thin film. Once completed, the device can be removed from the glass slide for conformal interfacing with neural tissue. Prototype MEAs feature electrodes smaller than those known to be reported on silicone substrate (60 μm diameter exposed electrode area) and were capable of selectively surface stimulating the surface of the *in vitro* isolated spinal cord of the juvenile rat. Stretchable serpentine traces were also incorporated into the functional PDMS-based MEA, and their implementation and testing is described.

Specific contributions to this section:

R. J. P. Giuly (Former research engineer, Georgia Institute of Technology):

- Microfabrication of prototype devices August 2004 – August 2005
- Optimization of fabrication steps, including reactive ion etch parameters
- Serpentine trace design and stretch-testing evaluation
- Listed as co-first author on associated publication

L. Guo (Graduate student, Wallace H. Coulter Department of Biomedical Engineering):

- Microfabrication of devices: 2006 - present
- Impedance testing of non-conical well MEA
- Creation of conical-well MEA and optimization of fabrication steps

K. W. Meacham:

- Microfabrication of devices: March 2005 – October 2005
- Design and conceptualization of devices, including choice of materials and isolation well features
- Stretch-testing evaluations of first version of MEA
- Design of electrical testing protocols, assistance in implementation
- Electrode trace design
- Post-microfabrication processing of MEA for *in vitro* testing
- All *in vitro* testing, analysis, and protocol development
- All associated data reporting and analysis

Introduction

Neural prostheses (NPs) that electrically activate central and peripheral systems have shown significant promise in supplementing function lost to disease or injury (Chapin 2000; Prochazka, Mushahwar et al. 2001; Stein and Mushahwar 2005). Clinical advancements made possible by NP technology include those that restore hearing (Clark, Tong et al. 1977; Kessler 1999; Spelman 1999), respiration (DiMarco 2001), bladder voiding (Brindley, Polkey et al. 1982; Grill, Craggs et al. 2001), and upper and lower extremity control (Liberson, Holmquest et al. 1961; Kralj, Bajd et al. 1988; Kraft, Fitts et al. 1992; Prochazka, Gauthier et al. 1997; Weingarden, Zeilig et al. 1998; Taylor, Burridge et al. 1999). A subset of these prostheses communicates with neural tissue via penetrating multiple-electrode arrays (MEAs), which can provide highly specific and robust activation of the targeted neurons (Branner, Stein et al. 2001; Tyler and Durand 2002; Hillman, Badi et al. 2003; McDonnall, Clark et al. 2004). Multi-electrode NPs that penetrate neural tissue, however, have been shown to incur acute and chronic damage, which in turn can result in degradation of both the interfaced tissue and the implanted device (Edell, Toi et al. 1992; Schmidt, Horch et al. 1993; Polikov, Tresco et al. 2005). There has been a variety of successful efforts to minimize the adverse effects of MEA invasiveness, including those using specialized device geometries and protective surface coatings (Naples, Mortimer et al. 1988; Zhong, Yu et al. 2001; Holman G. 2002; He and Bellamkonda 2005).

The damage sustained by NP interfacing can be minimized by stimulating exclusively from the surface of the interfaced neural tissue. This approach eliminates damage associated with electrode penetration, but potentially loses direct accessibility to the targeted neuronal circuitry. For certain prosthetic applications, however, this loss in

accessibility can be ameliorated by the inherent organization of the neuronal systems. For example, the sub-fascicular organization of the peripheral nerve has been successfully tapped into by surface electrodes to elicit functionally-specific muscle activation (Leventhal and Durand 2003; Leventhal and Durand 2004). In an analogous manner, spinal-cord NPs might utilize the topographical organization of spinal axons into bundles (i.e., white matter tracts) to recruit specific motor outputs via surface stimulation. The relevance of this approach has been supported by studies in which spinal cord surface stimulation has been used effectively to elicit coordinated motor responses—including locomotion—in both rats and humans (Magnuson, Schramm et al. 1995; Magnuson and Trinder 1997; Ichiyama, Gerasimenko et al. 2005; Gerasimenko, Lavrov et al. 2006).

The specificity with which surface-stimulating NPs activate neural circuitry may also be augmented by tailoring the electrode's physical properties for optimal tissue interfacing. A critical factor in this interaction specificity is the degree of isolation between electrodes and their targeted neural tissue, which should be minimized to reduce signal leakage to adjacent tissue and extracellular space (Stein and Pearson 1971; Loeb and Peck 1996; Struijk, Thomsen et al. 1999). For this reason, surface-stimulating MEAs whose designs confer a closer fit of their electrodes to the tissue surface may have potential for improving the selectivity with which their targeted neural systems are activated. Towards this end, numerous MEAs have been developed with specialized flexible substrates. **Table 2.1** is a summary of some of the more recently reported flexible-substrate, multi-electrode NP technologies, which use as substrates the biocompatible polymers polyimide, parylene, and polydimethylsiloxane (PDMS).

Table 2.1: Comparison of MEA technologies for surface stimulation of neural tissue.

Source/Type of MEA	**Reported Electrode Size** (μm)	**Substrate Material**	**Interfaced Neural Tissue Type**
Stieglitz et al. (Stieglitz 2001)	10 μm diameter	Polyimide	Various
Rodger et al. (Rodger 2006)	150 μm diameter	Parylene	Spinal cord and Retina
Maghribi et al. (Maghribi, Hamilton et al. 2002)	300-350 μm diameter	PDMS	Retina
Fraunhofer Institute, 18 polar array (Schuettler and Stieglitz 2000)	500 μm diameter	Polyimide-PDMS hybrid	Radial Nerve
Sahin et al (Sahin, Haxhiu et al. 1997)	500μm by 1mm rectangular	PDMS	Peripheral Nerves
Tsay et al. (Tsay 2005)	100μm to 1 mm squares	PDMS	Hippocampal Culture
Schuettler et al. (Schuettler, Stiess et al. 2005)	600 μm square	PDMS	Various

The MEA substrate PDMS, with a Young's modulus of 0.4-1.0 MPa, is significantly more elastic than parylene and polyimide, whose Young's moduli are approximately 4-4.5 GPa and 2.3-2.8 GPa, respectively (Yang 1998; Armani 1999; Rousche, Pellinen et al. 2001; Suzuki 2003). Because of its greater elasticity, PDMS can confer not just flexible but also conformable interfacing with neural tissue. In addition, the oxygen-permeability and improved mechanical impedance matching properties of PDMS have potential to augment the viability of the MEA/neural tissue interface. Other groups have demonstrated successes using PDMS-based MEAs for activation and recording of neural circuitry (Maghribi, Hamilton et al. 2002; Maghribi, Hamilton et al. 2002; Leventhal and Durand 2004; Schuettler, Stiess et al. 2005; Cater, Gitterman et al. 2007); however, these MEAs have not been able to achieve the same electrode size resolution as demonstrated in polyimide and parylene MEAs.

In this chapter, we present the design, fabrication, and preliminary testing of an elastic MEA with electrode diameters (<60 μM) smaller than previously reported using a PDMS substrate. To achieve this feature size, we implement a novel, customized Reactive Ion Etch (RIE) fabrication process. Our functional PDMS-based array exhibits properties that enable close, mechanically conformable contact with the surface of the spinal cord for selective stimulation of axonal tracts. To confer an even greater elasticity, we implement a serpentine pattern that allows the traces to stretch along with the PDMS substrate; this helps us to minimize electrode trace elasticity issues seen with previous fabrication techniques (Maghribi, Hamilton et al. 2002; Schuettler, Stiess et al. 2005).

Fabrication Process

Our fabrication approach consists of layering patterned gold between two thin sheets of PDMS and using a novel reactive ion etch (RIE) step to expose the gold electrode contacts. We eliminate the need for gold-to-PDMS adhesion by bordering exposed electrode contacts with PDMS, which prevents the gold from lifting off. As a means to pattern the gold electrodes, we use standard photolithography because it can generate small features reliably. To create orifices in the upper PDMS layer, we use a protective aluminum mask layer along with RIE techniques. Our fabrication steps use standard microfabrication techniques on a novel (PDMS) substrate and are designed to enable scaling of the MEA to a very large number of small-feature size (<60μm diameter) electrodes.

Fabrication Step 1: Preparation of PDMS and Rigid Substrate

To prepare the elastomer substrate, we mix PDMS (Sylgard 184©, Dow Corning) at 10:1 PDMS prepolymer to curing agent ratio and store the mixture at -20 °C to slow curing. The cooled mixture remains liquid for several days. No degassing under vacuum is required because air bubbles rise out during the first five hours of storage. Prior to use, we allow the mixture to sit at room temperature for 15 minutes to reduce the formation of condensation.

We use a 75x50x1mm glass slide as a rigid substrate for fabrication, and prepare it through sequential rinsing with trichloroethylene, acetone, isopropanol, and deionized water. We then evaporate 250 Å of gold onto the slide to create a non-stick layer (Figure 3.1a). All evaporation is performed with a CVC Products, Inc. Electron Beam Evaporator. The initial gold layer facilitates future removal of the finished elastomer-based array from the glass slide, a technique originally described by Maghribi et al. for their retinal array (Maghribi, Hamilton et al. 2002). Prior to the evaporation step, we

place transparent adhesive tape around the perimeter of the glass slide to form a 3mm-thick border. After removing the tape, the bare glass bonds to the subsequent PDMS layer more strongly than to the anti-adhesion gold layer. This configuration prevents fabrication chemicals from seeping under the array, which subsequently prevents the device from delaminating off the glass slide during processing.

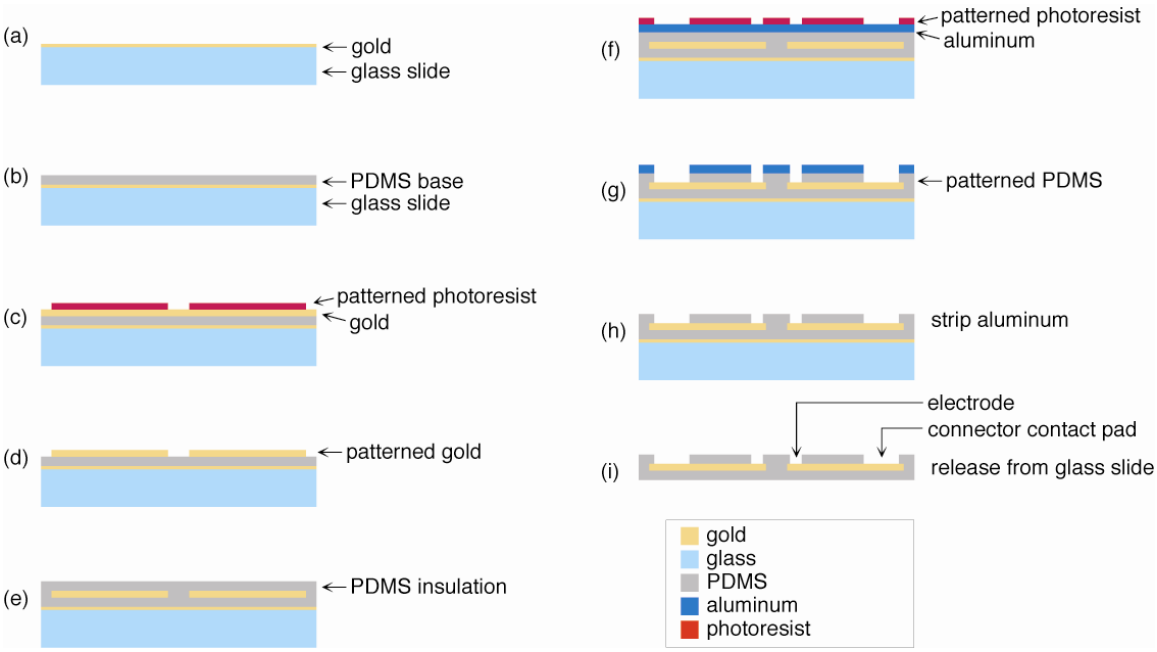

Figure 2.1: Fabrication Steps for a PDMS-Substrate Multi-Electrode Array (MEA). (a) Deposition of gold anti-adhesion layer onto glass slide. (b) Spin coating of PDMS. (c) Gold conductor layer deposition and positive photoresist defining conductor pattern. (d) Etching of gold and photoresist removal. (e) Spin coating of insulating PDMS. (f) Aluminum deposition for RIE mask and photoresist defining the mask pattern. (g) Etching of Aluminum and reactive ion etching to remove PDMS. (h) Stripping of aluminum. (i) Removal from glass slide.

Fabrication Step 2: Creation of PDMS Base Layer

Following removal of the adhesive tape border, we spin the PDMS mixture onto the slide at 1500 rpm for 15 seconds, using a 1000 rpm/s ramp rate. We then allow the PDMS layer to settle for one minute and cure it in a 95 °C oven for 15 minutes. This produces a PDMS film approximately 70 μm thick (**Figure 2.1b**).

Fabrication Step 3: Deposition and Patterning of Gold Film

To create the electrodes and wire traces, we first evaporate a 5000 Å thick gold film onto the PDMS layer. 5000 Å was found to be the maximum thickness achievable by evaporation while maintaining good film quality; we use this maximal thickness in order to improve the robustness of the MEA, which ultimately must survive the mechanical stresses and electrolytic corrosion of repetitive, long-term use. Following evaporation of the gold film, we use standard photolithography techniques to transfer the electrode pattern into a positive photoresist (Shipley Microposit 1813) (**Figure 2.1c**). We etch the gold layer by first dipping the patterned device in Transene GE-8148 Gold Etchant and then rinsing it in DI water. Because no adhesion layer is used between the gold and PDMS, we avoid delamination by spin drying the device at 2000 rpm for 30 seconds rather than jet drying with a nitrogen gun. In addition, we flood expose the sample (no mask used) and then soak it in developer (Microposit MF319) to remove the photoresist (Figure 3.1d). These steps eliminate the need for solvent strippers (e.g. acetone) that can swell the PDMS. After removing the photoresist, we rinse the sample again by dipping in water and then we spin dry and bake at 80 °C to remove moisture.

Fabrication Step 4: Creation of PDMS Insulating Layer

To create the second layer of PDMS, we spin the PDMS mixture onto the patterned gold at 6000 rpm for 150 seconds, with a 100 rpm/s ramp rate. This film is then

cured in an oven for 24 hours at 95 °C to create a thin PDMS layer of approximately 9.5 μm (**Figure 2.1e)**.

Fabrication Step 5: Deposition and Patterning of Aluminum Mask Layer

To protect the PDMS surface during the ensuing reactive ion etch (RIE) step, we deposit and pattern an aluminum mask. We accomplish this by evaporating aluminum (1500 Å at 0.5 Å/s) onto the PDMS and then patterning with positive photoresist. For accurate placement of the holes above the gold electrodes, we carefully align our second mask to gold-patterned alignment marks under the PDMS. These alignment marks have been protected during the aluminum evaporation using transparent adhesive tape, which is subsequently removed. The protective mask pattern is then defined using Transene Type A aluminum etchant.

Fabrication Step 6: Reactive Ion Etch (RIE)

To create openings in the upper PDMS layer for the gold electrodes and electrical contacts, we use a custom two-step reactive ion etch (RIE) process (Plasma-Therm Reactive Ion Etcher). During this dry etching, the aluminum layer serves as a protective mask and the gold film acts as an etch-stop layer. The first of our two steps uses a 10% CF_4 and 90% O_2 mixture for 240 minutes (**Table 2.1b**); this step etches through most of the PDMS and strips away the photoresist. For our second step, a 3% CF_4 and 97% O_2 mixture (Table 3.2c) is applied for 150 minutes to etch any remaining PDMS without damaging the underlying gold (**Figure 2.1g** and **Figure 2.2**).

We use RIE parameters modified from a rate-optimized PDMS etch recipe developed by previous research (**Table 2.2a**) (Shao and Miller; Garra, Long et al. 2002). These previously-established parameters were optimized more for speed than selectivity and were not suitable for our purpose because they attack the underlying gold film. To cleanly etch away the PDMS film while leaving the gold layer intact, we use the

following modifications: (1) We decrease CF_4 concentration and increase oxygen to eliminate the tendency to redeposit polymer (Madou 2002), (2) We reduce the power and increase the pressure, under the assumption that a more chemical—rather than physical—etching process would have less effect on gold and therefore tend to etch PDMS with more selectivity, and (3) We use two etching steps: one that removes the bulk of the PDMS (**Table 2.2b**) and another slower etch that cleans off any residue without attacking gold at an appreciable rate (**Table 2.2c**).

Table 2.2: Parameters used for reactive ion etching process.
We use a customized, two-step process that etches holes in the upper PDMS layer of our device without damaging the underlying gold electrodes.

	Gas Pressure (mTorr)	RF level (W)	O2 Flow Rate	CF_4 Flow Rate	PDMS Etch Rate (□m/hour)	Etches Underlying Gold:
(a) PDMS Etch, Rate-Optimized	47	270	25% (50 sccm)	75% (12.5 sccm)	18	Quickly
(b) Our Step 1	200	70	90% (27 sccm)	10% (3 sccm)	2 (approximate)	Slightly
(c) Our Step 2	200	70	97% (29 sccm)	3% (1 sccm)	1 (approximate)	Negligibly

We use a dry etch process to open the orifices in the PDMS insulating film because wet etching of PDMS can be more difficult to control (Maghribi, Hamilton et al. 2002). We suspect that Recipe A etches the patterned gold layer while the film of PDMS remains on top of it, and that this phenomenon is related to the gas-permeable properties of PDMS. A similar effect is described by Subrebost et al., where silicon is dry etched underneath a layer of PDMS (Subrebost, Rosenbloom et al. 2002). This problem is exacerbated by the fact that the PDMS etch rate, which starts at approximately 18 μm per hour, decreases as the PDMS layer thins to about 1 μm. This allows ample time for the RIE to attack the gold film underlying the permeable PDMS layer.

Because of high selectivity of the fabrication methods shown in **Table 2.2b** and **2.2c**, the RIE can run approximately 1.5 times as long as typically necessary without danger of over-etching into the gold. This is important because the exact time needed to fully etch is difficult to determine: not only do loading effects change the etch rate, but, in the presented fabrication process, the PDMS layer is not always exactly the same thickness from one device to another.

Another advantage of the recipes shown in **Table 2b** and **2c** is that they do not etch aluminum at an appreciable rate as does the recipe shown in **Table 2a** (Shao and Miller; Garra, Long et al. 2002), so the 1500Å mask holds up for over 6 hours. Incidentally, we tested same recipe with SF_6 in place of CF_4 and it also gave satisfactory results. Our primary goals were reliability and repeatability rather than speed, but we suspect that more future work could be done to optimize the speed of the RIE process and still maintain feature precision.

Testing indicates that our novel dry etch process works reliably. **Figure 2.2** shows a Scanning Electrode Microscope image of orifices etched through PDMS with our recipe; it can be seen that the underlying gold film is cleanly exposed and intact.

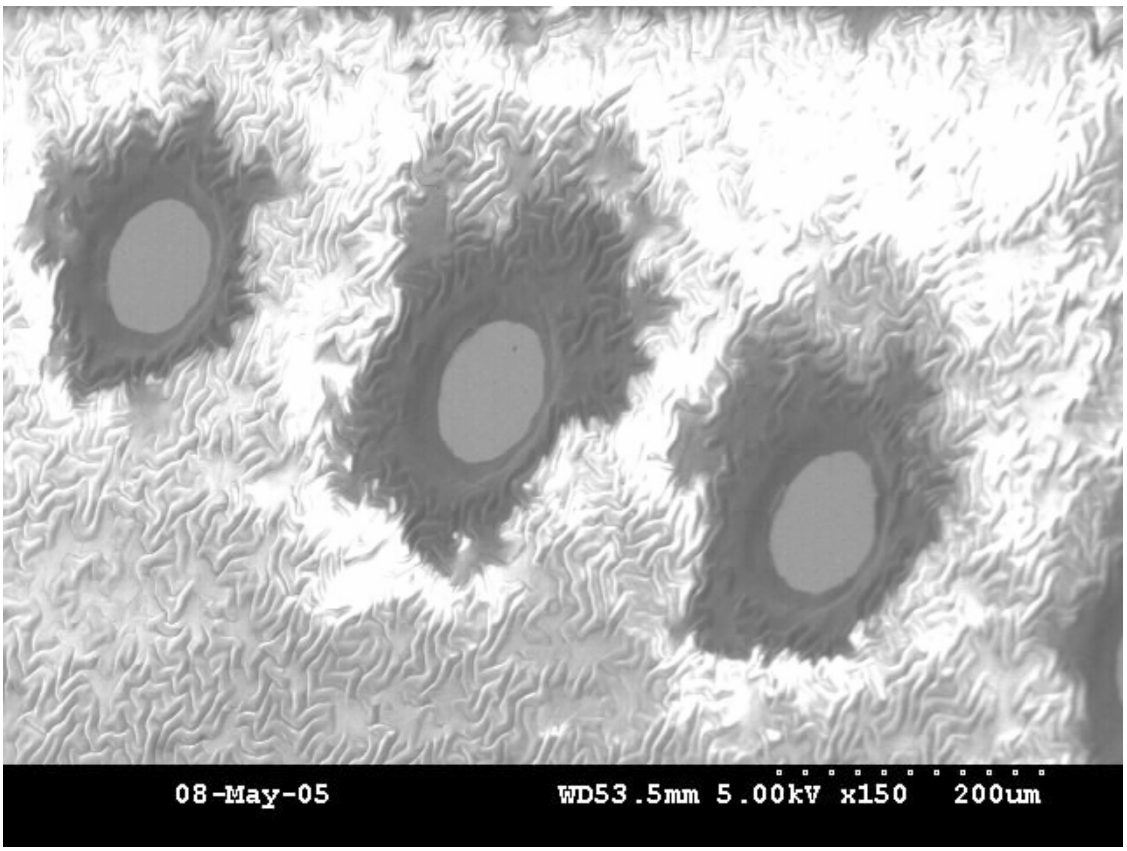

Figure 2.2: Scanning electron microscope image of etched electrode contacts. Three PDMS-substrate MEA electrodes are shown following the reactive ion etch step. The upper PDMS layer has been etched to expose the underlying gold electrode contacts (circular areas above) without incurring any damage to the gold. The lighter area indicates the prior presence of an aluminum mask, which was used to prevent etching of the PDMS insulation over electrode wires and was subsequently stripped before imaging.

Fabrication Step 7: Stripping of Aluminum Layer

Following the dry etch of holes into the insulating PDMS layer, we strip the protective aluminum mask layer in a bath of aluminum etchant. During this process, we ramp the bath temperature from 25 °C to 70 °C (**Figure 2.1h**).

Fabrication Step 8: Removal from slide

To reduce the force required to remove the finished MEA from the glass slide, we first excise the 3 mm array border that is on bare glass. For subsequent manual removal of the array from the glass slide, we wedge a razor blade under a corner to start the delamination and then very gently peel off the device by hand (**Figure 2.1i**). We then soak the MEA in DI water for a minimum of 24 hours to remove any residual fabrication chemicals before *in vitro* use. **Figure 2.3** shows an initial functional prototype of the completed PDMS-based MEA.

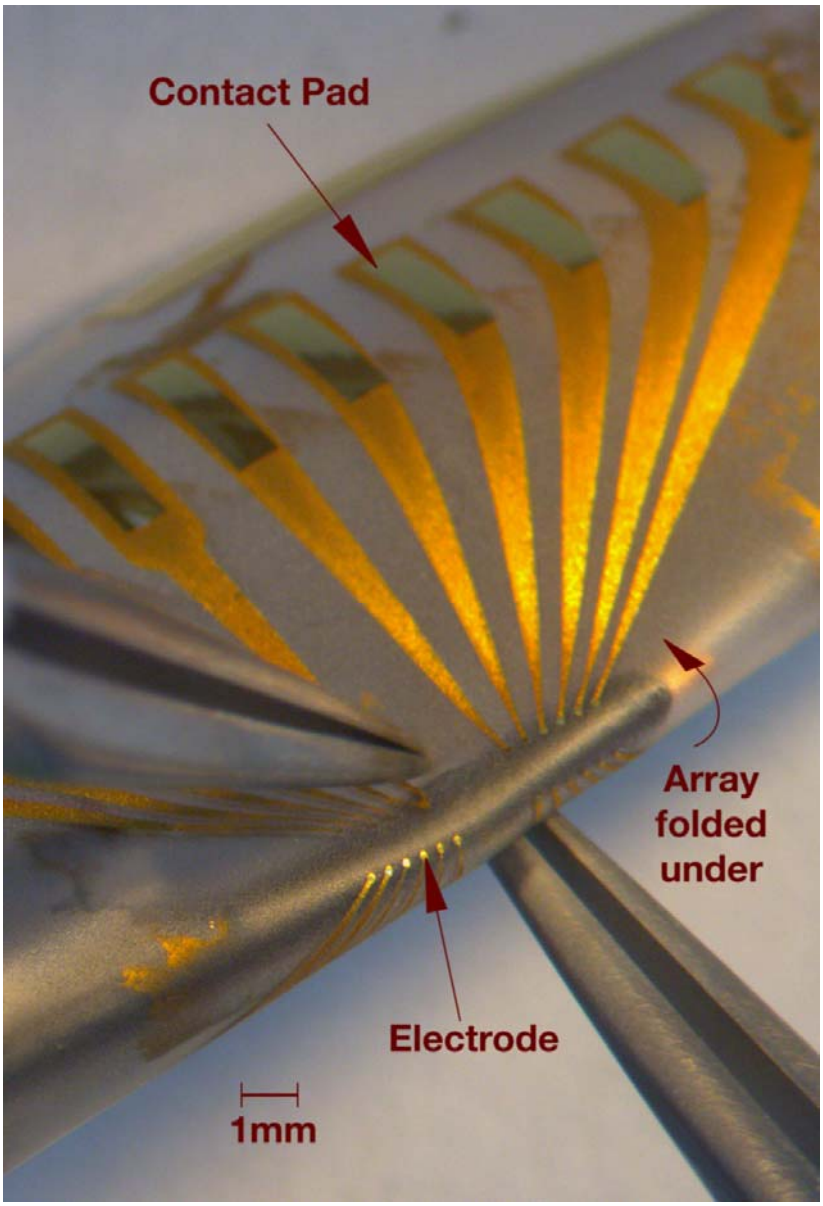

Figure 2.3: Fabricated PDMS-substrate MEA.
A final product of our fabrication process is shown wrapped around a wire of similar diameter (2mm) to that of the neonatal intact or hemisected juvenile *in vitro* rat spinal cord.

Array Evaluation

In order to assess the capabilities and limitations of our fabricated MEA, we conducted a series of electrical, mechanical, and neural interfacing tests. These tests were designed to assess the MEA under conditions pertinent to its imminent use as an *in vitro* electrophysiology tool. Neural interfacing assessment focused on measuring the MEA's ability to selectively activate white matter tracts when wrapped around an *in vitro* isolated rat spinal cord, as this will be the first *in vitro* application for which the MEA will be used.

Electro-Mechanical Testing

We characterized the electrical impedances of exposed electrodes and insulated for each of eight traces on a fabricated MEA. We measured impedances using a spectrum analyzer (SRS Dynamic Signal Analyzer, SR785) at frequencies from 100Hz to 100KHz. For all experiments, electrical interfacing between spectrum analyzer and MEA was accomplished by placing a drop of saline over the electrode and insulated trace sites and then placing spectrum analyzer leads into the saline drops (**Figure 2.4**). Results for impedance testing of the electrode contacts and insulated wire traces are given in **Figure 2.5**, and show that the electrode impedances are uniform across electrodes and compare favorably to properties of rigid-MEA electrodes (Oka, Shimono et al. 1999; Heuschkel, Fejtl et al. 2002). Impedance measurement results also indicate that the PDMS insulating layer acts well as an insulator (**Figure 2.5a**).

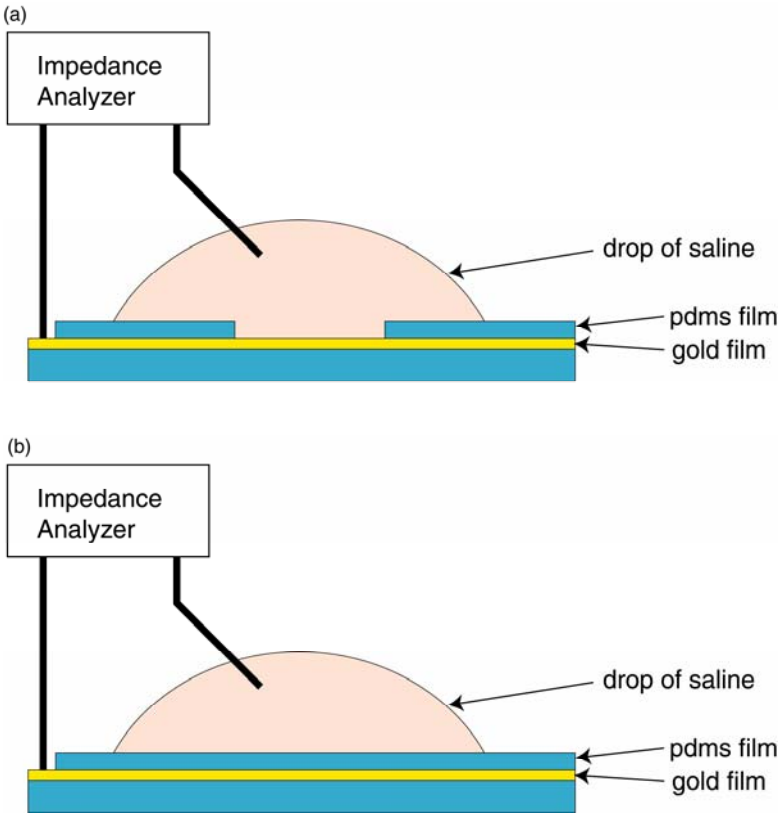

Figure 2.4: Experimental apparatus for electrical evaluation of MEA.
To evaluate the electrical properties of the MEA, we measured impedances using a spectrum analyzer at frequencies from 100Hz to 100KHz. A drop of saline was used to interface between the MEA and the spectrum analyzer lead. (a) Configurations for measuring impedance of an electrode contact (a) and the insulating PDMS film (b) are shown.

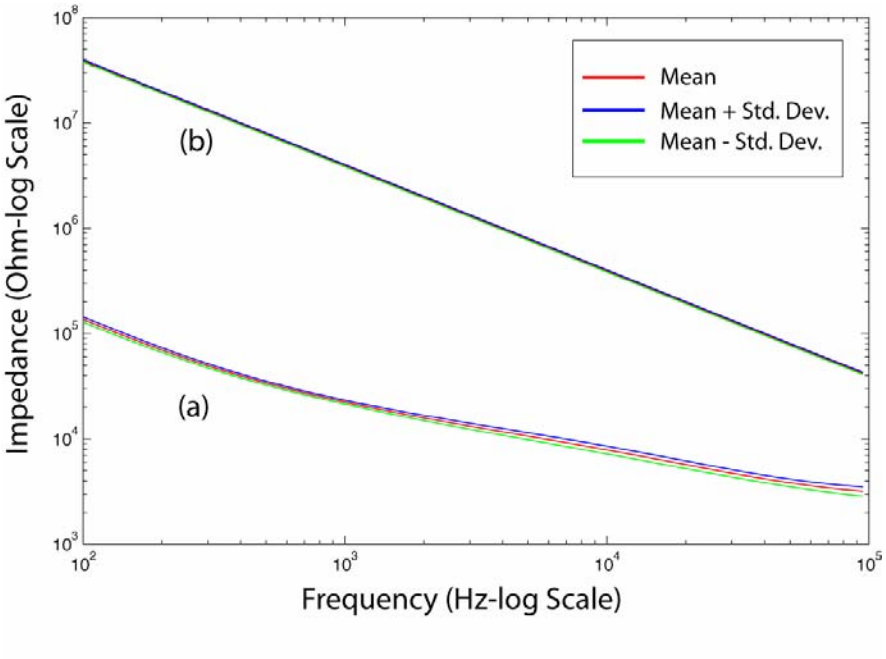

Figure 2.5: Results for electrical impedance testing of MEA electrodes.
MEA electrodes consistently exhibited impedance values comparable to those of rigid MEAs (Oka, Shimono et al. 1999; Heuschkel, Fejtl et al. 2002) (a). The PDMS-covered traces demonstrated impedance values indicative of insulation (b).

The elasticity of the MEA was evaluated by measuring the impedance properties of the device's electrodes both during and after repeated uniaxial loading. For these tests, both straight electrode trace patterning and serpentine electrode trace patterning were evaluated. To stretch the MEA, we used a custom-built apparatus that clamped to two ends of the array (**Figure 2.6**). The stretching device was used to manually increase the strain along the length of the electrode traces at intervals of 1%. At each stretching increment, impedances were measured at frequencies ranging from 100Hz to 100KHz. Our measurements were not precise enough to detect the continuous increase in impedance accompanied by strain near the failure point, but were sufficient to measure total trace failure. Impedance of 60 kΩ or less was considered acceptable; when failure occurred the impedance rose by a factor of approximately 100.

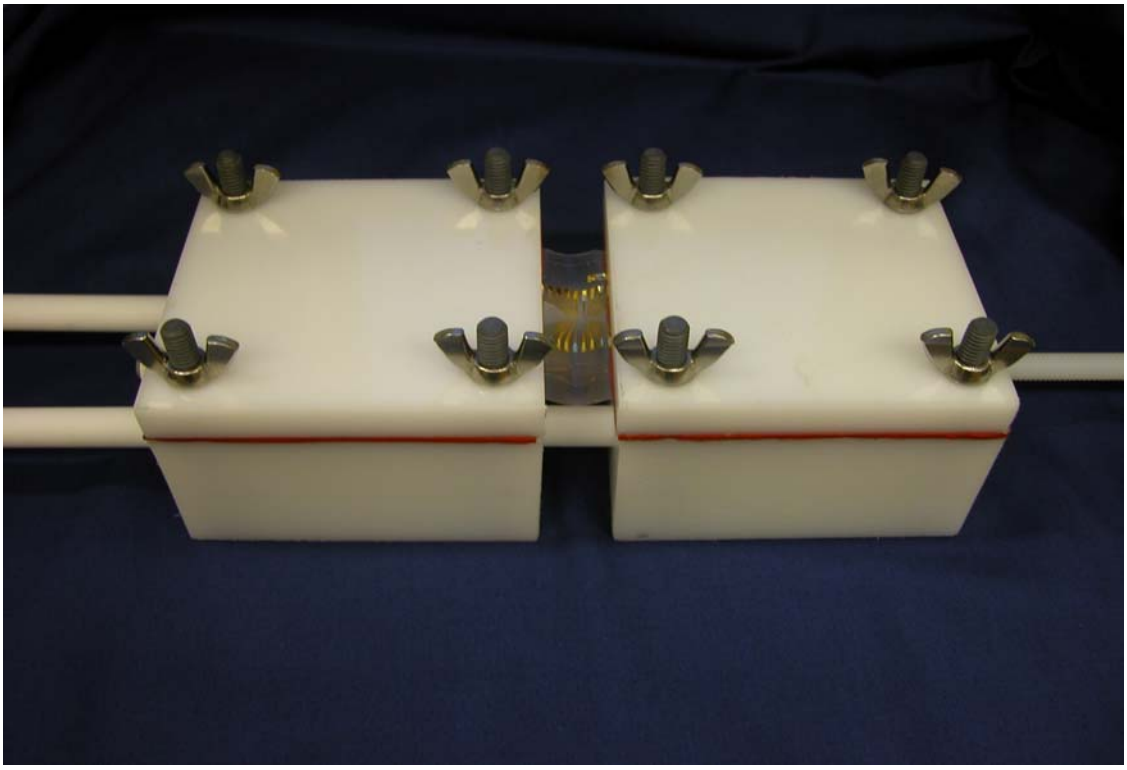

Figure 2.6: Uniaxial strain device for electro-mechanical evaluation of the PDMS-based MEA.
The custom-made apparatus shown was used to clamp the MEAs and apply uniaxial strain in 1% increments.

We found that the intersecting serpentine electrode trace design shown in Figure 7 performed better than the other tested patterns, withstanding 8% strain while continuing to conduct at impedances similar to rigid MEA electrodes. Serpentine traces performed better than straight electrode traces (**Figure 2.7**), which failed at 3% strain. These observed strain limits are lower than those reported for other, PDMS-based stretchable electrodes that have been designed for the study of traumatic brain injury (Tsay 2005; Cater, Gitterman et al. 2007). Nonetheless, these strain limits appear to be above those imposed upon the devices during repetitive use as a conformable, multi-electrode interface to the *in vitro* spinal cord, as over repetitive interfacing use the MEAs have not failed due to excessive strain.

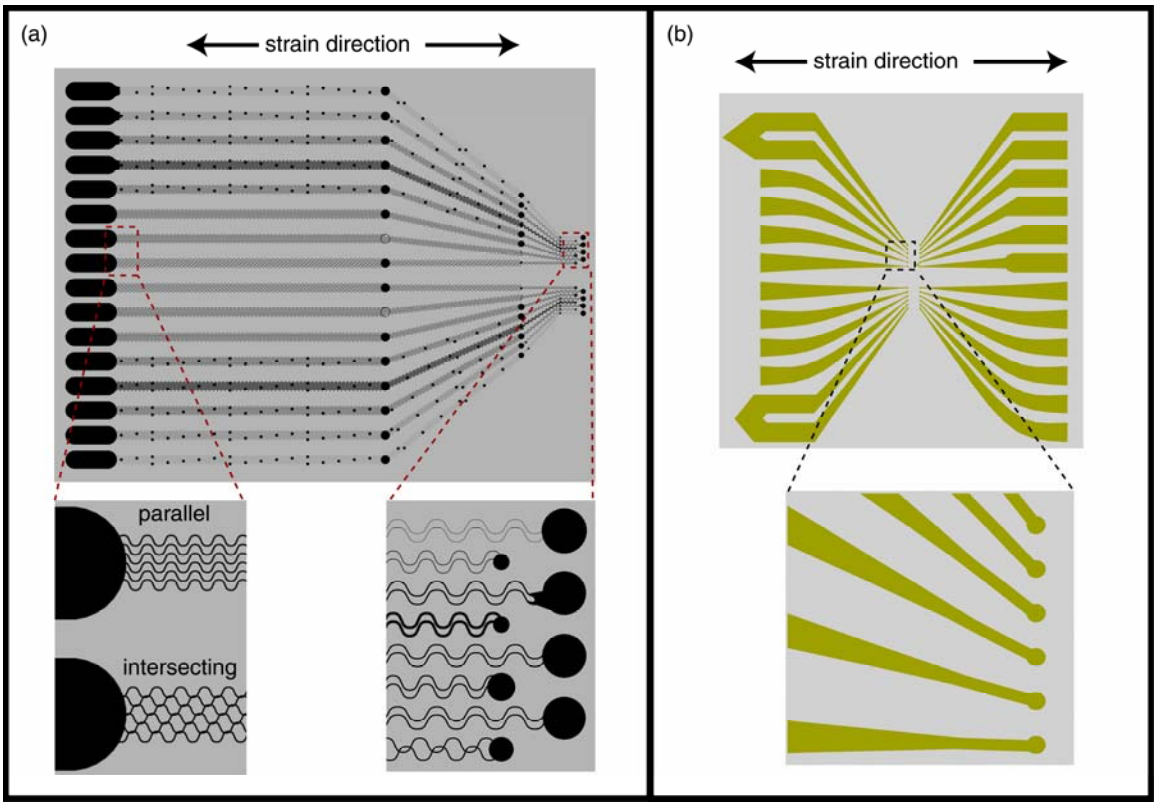

Figure 2.7: Serpentine Trace Design for MEA Electrode Traces.
(a) An intersecting, serpentine electrode trace pattern confers a greater elasticity to the PDMS-based MEA (electrode trace conductivity failure at > 8% strain, recoverable upon relaxation) than does a (b) non-serpentine pattern of electrode traces (failure at > 3% strain, no recovery). The parallel, serpentine electrode trace pattern shown in (a) conferred no functional elasticity advantages when compared to the non-serpentine pattern (b).

We also tested the ability of the PDMS substrate to conform to shapes similar to that of our targeted neural substrate (the *in vitro* isolated spinal cord). Arrays fabricated using both PDMS and polyimide as substrates were wrapped around plastic tubing of diameter (2mm) similar to that of the isolated neonatal rat spinal cord and the hemisected juvenile rat spinal cord. **Figure 2.8a** demonstrates the superior conformability of a PDMS film to the bending tube, while **Figure 2.8b** shows a polyimide film bending and folding in multiple places, providing a less continuous contact with the bending tube surface.

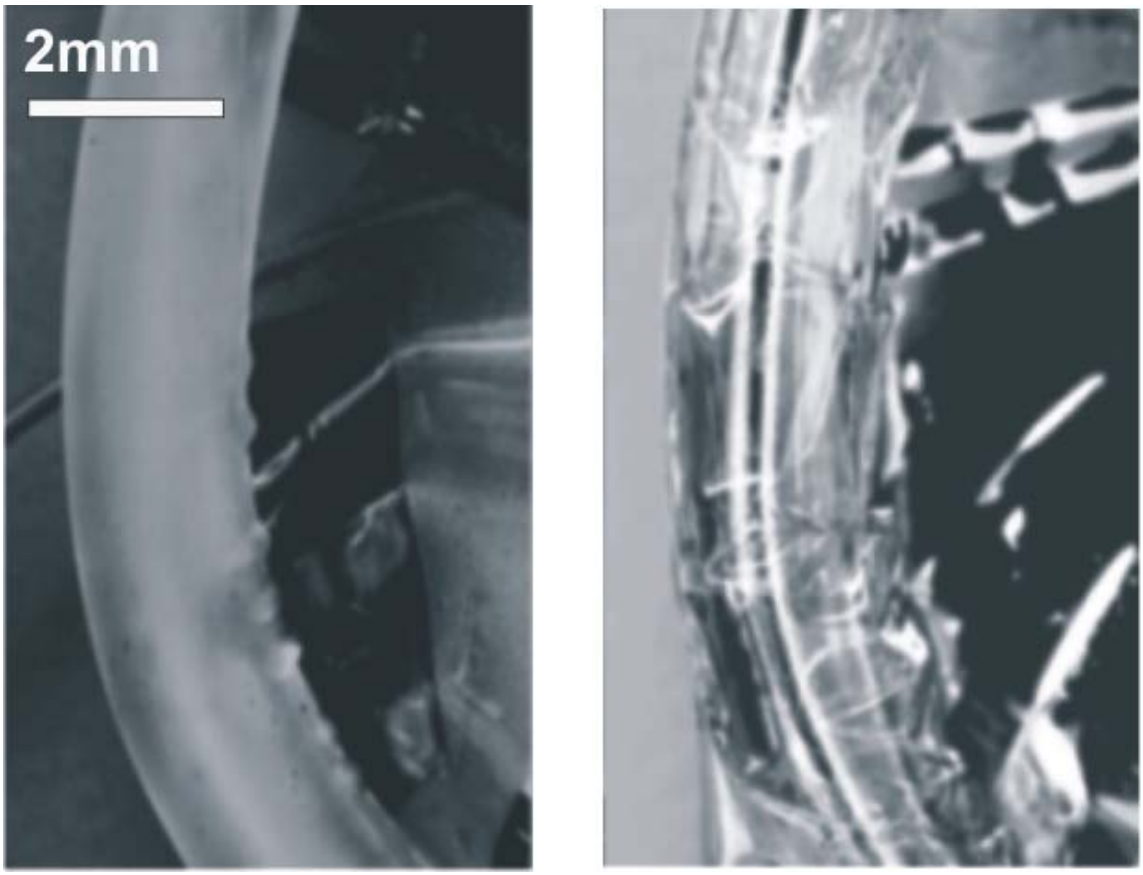

Figure 2.8: Bending of polyimide and PDMS arrays.
We visually compared the ability of PDMS and polyimide array substrates to conform to a bending tube of the same approximate diameter as our *in vitro* spinal cords. (a) Polyimide film wrapped around a 2mm-diameter tube shows buckling of the polyimide film along the tube. (b) PDMS film wrapped around a 2mm tube conforms more uniformly to the bending tube.

Neural Interfacing

Studies were performed to demonstrate the capacity of our elastic MEA to activate a specific region of longitudinally-oriented axonal bundles (spinal white matter tracts) in the *in vitro* rat isolated spinal cord (**Figure 2.9**). We determined this degree of selectivity by delivering single-site MEA stimuli to the surface of the cord and then recording the evoked compound action potential (CAP) response 11.5 mm distal to the site of activation (on adjacent white matter tracts). To determine stimulus selectivity, we measured the strength of evoked CAPs as we increased recorded lateral distance from the site of maximal white matter tract CAP activation.

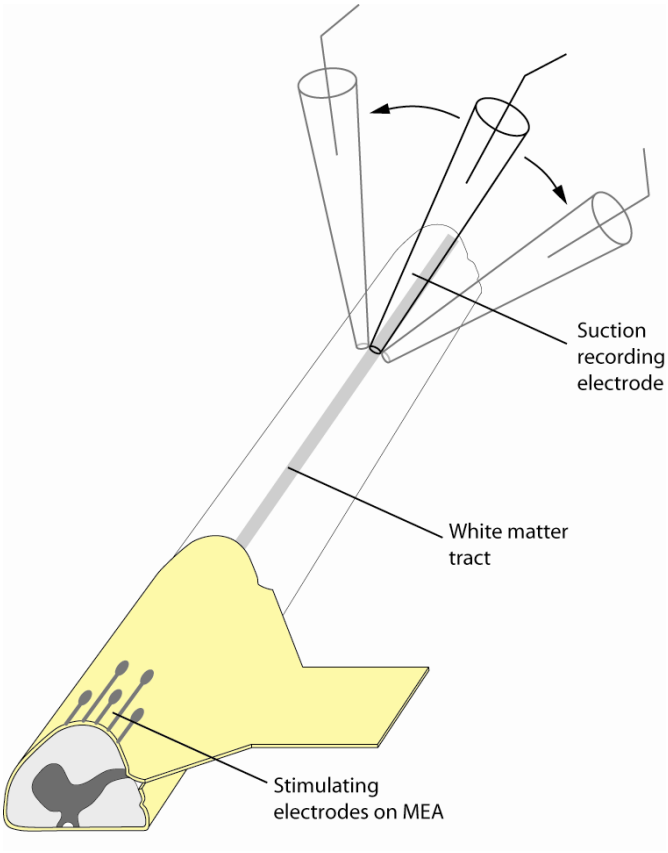

Figure 2.9: Experimental setup for surface stimulation of the *in vitro* isolated rat spinal cord (hemisected).

The MEA was wrapped around the isolated *in vitro* spinal cord of a postnatal day 11 rat and two adjacent MEA electrodes (bipolar configuration) were used to stimulate the 5th thoracic segment's ventrolateral funiculus. The degree of stimulus spread was assessed by recording surface compound action potentials (CAPs) at multiple circumferential sites distant to the site of activation. For recording, a glass suction electrode (40-50 μm internal diameter) was placed 11.5 mm caudal to the stimulation site to record CAP responses in 50 μm lateral increments from the site of the peak response.

To prepare for *in vitro* spinal cord interfacing, we used a protocol adapted from Shay et al. (Shay, Sawchuk et al. 2005), in which a juvenile (postnatal day 11) Sprague-Dawley rat was first anesthetized with 10% wt./vol. urethane (2.0 mg/kg injected intraperitoneally) and then submerged in an ice slurry for five minutes to decrease body temperature. Following decapitation, the cervical to sacral spinal cord was isolated along with ventral and dorsal roots. The cord was then pinned ventral-side up in a Sylgard-coated (Dow Corning) Petri dish containing cold (4°C), oxygenated (95% O2, 5% CO2) high sucrose-containing solution [(in mM): sucrose 250; KCl 2.5; $NaHCO_3$ 26; NaH_2PO_4 1.25; D-glucose 25; $MgCl_2$ 3; CaC_{l2} 1]. Spinal cord dura was carefully removed and a sagittal hemisection was performed using insect pins (1.0 mm, Fine Science Tools). The spinal cord was then placed in room-temperature, oxygenated (95% O_2, 5% CO_2), artificial cerebrospinal fluid (aCSF, in mM: NaCl 128; KCl 1.9; D-glucose 10; $MgSO_4$ 1.3; $CaCl_2$ 2.4; KH_2PO_4 1.2; and $NaHCO_3$ 26]) and allowed to equilibrate for 1 hour prior to further experimentation.

To prepare for stimulation and recording, the MEA was connected to an STG-2008 stimulation unit (MultiChannel Systems) using a custom-built press fit connector. Exposed electrodes on the MEA were then wrapped around the 5th thoracic segment of the cord such that the stimulating electrodes were on the ventrolateral funiculus (Figure 9). To secure the MEA in this configuration, insect pins (1.0mm, Fine Science Tools) were used to pin non-electrode containing parts of the MEA (i.e. flaps of PDMS film adjacent to the MEA electrode traces) to the bottom of the dish. A reference ground electrode was placed in the bath near the caudal end of the spinal cord. A glass suction electrode (40-50 μm internal diameter) was used to record stimulus-evoked CAPs as they conducted along the surface of the spinal cord white matter. This electrode made bipolar recordings using chloridated silver wires: one placed within the glass and the other placed immediately outside the glass.

Two adjacent MEA electrodes were used to deliver a single, bipolar, charge-balanced current pulse to the surface of the spinal cord. To measure the subsequent evoked CAP, a recording electrode was placed 11.5 mm caudal to the stimulation site, starting at the circumferential location that responded with the greatest evoked CAP response. The minimum current value at which a CAP was visible at this recording site was defined as the threshold stimulus value (for this experiment, 700 μA/500 μs). Between single-pulse stimuli at this threshold value (and several values greater than threshold, increasing in 20 μA increments), the recording electrode was moved in 50 μm lateral increments from the site of the peak response to record CAP responses on laterally adjacent tracts. The strength of the evoked CAP response at these different sites along the cord was calculated based on the baseline-subtracted, rectified and integrated signal (μV*μs) averaged over ten trials for each recording site (**Figure 2.10**, standard error bars shown).

Results indicate that, for reliable activation of visible CAP responses along the ventrolateral funiculus, the minimum charge-balanced current pulse required using our MEA was 700μA/500μs. This compares to a threshold value of 300μA/100μs determined using a conventional bipolar tungsten electrode (5μm tip diameter, 10μm inter-electrode distance) pressed firmly onto the cord surface. When the MEA was not placed conformably around the cord but instead placed loosely on top of the cord within the aCSF bath, no recruitment of white matter tracts was discernable at any single-pulse, bipolar-configuration current value within the range of our stimulator (800μA/200ms).

Selectivity of tract stimulation using the MEA was demonstrated with a decremented—and eventually absent—evoked CAP on laterally adjacent axonal tracts (Figure 10). The stimulus selectivity of the MEA compared favorably to that evoked with a tungsten bipolar stimulating electrode (**Figure 2.10**), in that the rate at which

evoked CAP response strength decreased over recording distance compared favorably to the trendline for threshold stimulation with a bipolar tungsten electrode control (R^2 =0.8201). These results indicate a similarity in the stimulus selectivity between the MEA and a conventional bipolar tungsten electrode in direct contact with the spinal cord surface. At stimulus values incrementally greater than threshold value for the MEA, we observed incrementally greater recruitment of white matter tracts (as shown by higher-strength CAP responses, **Figure 2.10**).

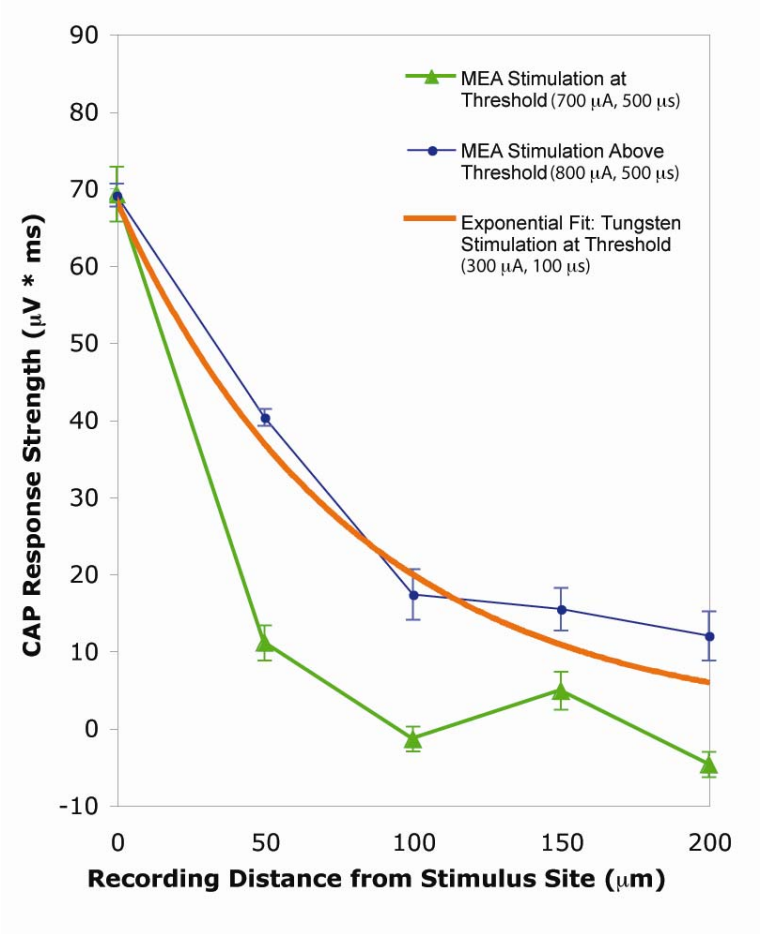

Figure 2.10: Spinal cord white matter response to MEA surface stimulation. MEA (vs. tungsten control) stimulus-evoked compound action potentials (CAPs) on white matter tracts are plotted over lateral recording distance from the site of peak CAP response. Recordings were made 11.5 mm caudal to the site of ventrolateral funiculus stimulation, in 50 μm lateral increments. Strength of CAP response was quantified by finding the area under the baseline-subtracted, rectified traces of the CAP recording. Shown are responses to MEA stimuli at threshold value (700 μA/500 μs single current pulse) as well as at 800 μA/500 μs, demonstrating an increase in white matter tract recruitment at greater stimulus values. To compare stimulus selectivity, also shown is the logarithmic trendline for threshold stimulation (300μA/100μs) using a conventional tungsten bipolar electrode. The rate at which evoked CAP response strength decreased over recording distance compared well to the logarithmic trendline for tungsten bipolar stimulation ($R^2 = 0.8201$), indicating a similar stimulus selectivity between the two methods.

Discussion

Our fabrication approach enables reliable and rapid production of MEAs with various desired electrode geometries and includes a novel reactive ion etch (RIE) process that makes possible our 60 μm diameter electrode resolution. Our fabrication process differs from previous work in silicone micro-array fabrication in that we use a customized reactive ion etch process for opening electrode and electrical contact orifices in a membrane of PDMS. This process removes PDMS cleanly and does not etch away the underlying gold electrode. To our knowledge, no previously published RIE recipes for dry etching PDMS are capable of selectively removing the PDMS and leaving an underlying gold thin film intact.

Also novel to PDMS MEAs, we use serpentine electrode traces to increase overall elasticity of the electrode array. Although PDMS silicone stretches easily, metal traces have limited the elasticity of previous silicone MEAs (Maghribi, Hamilton et al. 2002; Schuettler, Stiess et al. 2005). Such gold serpentine traces on silicone have been investigated (Madou 2002; Gray, Tien et al. 2004), but they have not previously been incorporated into a stretchable multi-channel electrode array. Traces with intersecting serpentine patterns were capable of stretching 8% without failure (versus 3% for MEAs with straight electrode traces). For our *in vitro* spinal cord interfacing work thus far, the elasticity of both the intersecting serpentine-trace and straight-trace MEAs has been sufficient for repetitive handling and use; however, the additional elasticity that the intersecting serpentine trace arrays may become more critical for future neural interfacing scenarios (e.g. *in vivo* implantation). Future work to fully characterize the multi-axial strain limits of the MEA might be helpful for determining the array's overall potential for future applications to other types of biological interfacing.

We demonstrated that our fabrication process produces MEAs with uniform electrical properties and that our devices can selectively activate white matter tracts in an *in vitro* isolated spinal cord preparation. Our results also indicate that a close, conformable fit of the array to the surface of the cord is a critical factor in its ability to evoke compound action potentials with spatial precision, presumably because it gives the stimulating electrodes a closer, semi-isolated proximity to the cord surface. Future work is planned to more thoroughly characterize the role of the MEA substrate in promoting selective activation of white matter tracts, in particular in relation to flexible-substrate (but non-elastic) MEA technologies. Furthermore, we plan to assess the electrical and mechanical stability of the MEA over extended usage and incubation periods as a first step towards determining its potential as an *in vivo* device.

Future MEA design improvements will focus on augmenting the isolated delivery of electrical stimuli to the cord surface, using techniques including fabrication of raised PDMS isolation wells around individual electrodes. We will also be applying modified geometries of single electrodes and multiple electrode configurations and evaluating their influence on MEA stimulus selectivity. Our ultimate goal is to use this technology as part of a multi-site interface for selective, closed-loop recruitment and control of spinal cord functional systems.

CHAPTER 3

SELECTIVE ACTIVATION OF THE SPINAL CORD USING A SURFACE-STIMULATING MICRO-ELECTRODE ARRAY

Summary

Electrical stimulation of the spinal cord is capable of activating behaviorally-relevant populations of neurons for recovery of function. A promising method for accessing these spinal circuits is through their axons, which are organized as longitudinal columns of white matter funiculi along the cord exterior. To selectively stimulate white matter columns at multiple sites, we have developed a novel microelectrode array (MEA) that wraps conformably around the spinal cord. To further isolate the electrode-tissue microenvironment, this MEA features isolation wells around each electrode. We used an isolated rat spinal cord preparation maintained *in vitro* to demonstrate that electrical stimulation with the MEA can activate specific white matter regions with the dorsal column with a spatial selectivity that compared well to tests with a rigid, bipolar Tungsten electrode. Dual-site stimulation of adjacent electrode pairs could recruit spatially distinct populations of axons. Site-specific stimulation of the ventrolateral funiculus was capable of synaptically recruiting motor circuits. We conclude that for surface stimulation the conformable MEA functions analogously to rigid electrodes. This MEA should minimize mechanical trauma following surgical implantation, and allow for therapeutic stimulation of spinal cord functional systems.

Introduction

Recovery of motor function lost to disease or injury is an important goal for many of the 250,000 people in the United States who have spinal cord injury(NSCISC 2008). For many individuals, control of motor function remains a key component for improving quality of life (Barbeau, Ladouceur et al. 2002; Mushahwar, Jacobs et al. 2007). To accomplish this recovery, several electrical stimulation technologies have been implemented to restore motor function (Peckham and Knutson 2005). These devices typically activate each muscle or peripheral nerve independently, and are often referred to as functional electrical stimulation (FES) devices.

One of the limitations of muscle and peripheral nerve stimulation strategies is their inability to replicate the nuanced, multiple-muscle movements naturally coordinated by upstream spinal circuitry (Mushahwar and Horch 1997; Emmanuel Pierrot-Deseilligny 2005). Therapeutic methods that directly activate this spinal circuitry have the advantage of drawing upon the richness of connectivity inherent in spinal cord to produce whole limb movements.

Importantly, experiments in spinal cord-transected cats and rats have shown that the spinal neural circuits known to organize and control motor behaviors such as locomotion remain intact and accessible following injury(Grillner and Zangger 1979; Grillner 1981; Kiehn and Butt 2003). For example, the spinal cord has been shown to evoke alternating hindlimb motor outputs when stimulated either externally, using epidural stimulation (Iwahara, Atsuta et al. 1992; Dimitrijevic, Gerasimenko et al. 1998; Minassian, Jilge et al. 2004; Lavrov, Dy et al. 2008), or internally, using intraspinal microstimulation (Eccles, Eccles et al.; Tresch and Bizzi 1999; Mushahwar and Horch 2000; Barthelemy, Leblond et al. 2007). In epidural stimulation studies, electrodes are placed near the dorsal column, and are thought to activate both low-threshold dorsal root afferents and/or propriospinal interneurons in the dorsolateral funiculus (Eccles, Eccles et

al.; Minassian, Jilge et al. 2004; Gerasimenko, Roy et al. 2008). Intraspinal microstimulation studies have used microwires placed in various gray matter laminae within the lumbosacral enlargement, and have been shown to activate motor neurons via intraspinal axons including those of sensory afferents whose collaterals extend many spinal segments (Gaunt, Prochazka et al.). There is also evidence that local interneuronal networks are involved in producing the evoked motor outputs (Tresch and Bizzi). For both epidural and intraspinal stimulation, it is assumed that the axons of neurons are activated at lower thresholds than their associated cell bodies (Jankowska 1975; Ranck 1975; Gustafsson and Jankowska 1976; Gaunt, Prochazka et al. 2006).

Since the longitudinal white matter axon tracts that control spinal cord function surround the gray matter, and also have lower thresholds of recruitment than cell bodies (detailed above) their selective recruitment may be easily accomplished via surface electrical stimulation. As axons of functionally similar populations of neurons travel in the same approximate location (Hochman 2007), a method for local activation of axon fibers may recruit subpopulations of neurons with greater precision as compared to epidural or intraspinal stimulation. Quasi-selective recruitment of functional subpopulations of spinal interneurons via their white matter tracts should allow a greater degree of spinal circuit control. Such an approach would be facilitated by an electrode interface that provides very close contact with the spinal cord for regionally-selective stimulus delivery (Stein and Pearson 1971; Loeb and Peck 1996; Struijk, Thomsen et al. 1999; Rutten). Moreover, implantable arrays of such electrodes could provide multi-site searches of the cord surface for location of effective stimulus locations that recruit many functional subpopulations of neurons. This also affords the possibility of multi-electrode stimulus protocols to more precisely recruit control 'modular' elements of spinal cord function in different spatiotemporal combinations to provide a more flexible control of motor function.

As the spinal cord is a soft tissue, ideal multi-electrodes arrays for surface stimulation would not produce mechanical or anoxic damage. This has motivated our development of a novel surface-stimulating, microelectrode device for conformal interfacing with excitable tissue (Guo 2007). To further isolate the space between electrode and interfaced tissue, each multi-electrode array (MEA) electrode is surrounded by a raised isolation well (**Figure 3.1**). The MEA is comprised of gold traces and electrodes that are photo-patterned between layers of thin-film polydimethylsiloxane (PDMS). PDMS is a gas-permeable elastomer with well-characterized biocompatibility (Mirzadeh, Khorasani et al. 1994; Yang 1998; Belanger and Marois; Peterson, McDonald et al. 2005). In addition, its elasticity is orders of magnitude greater than more traditional flexible electrode array materials, including parylene and polyimide (Yang 1998; Armani; Rousche, Pellinen et al. 2001; Suzuki 2003).

In this chapter, we evaluate the ability of this MEA to locally activate axons via single- and dual-site surface stimulation. Selectivity is tested in the isolated young rat spinal cord maintained *in vitro*. These studies quantify the orthogonal (lateral) spread of activated white matter tracts, and compare results with those obtained with traditional rigid bipolar electrodes. Single-pulse MEA electrical stimulation is then tested on circuits that require synaptic activation by examining evoked responses in motor nerve roots.

Methods

All animal procedures were performed in accordance with policies of the Association for the Assessment and Accreditation of Laboratory Animal Care International and approved by Emory University's Institutional Animal Care and Use Committee. Each rat was administered 10% wt./vol. urethane (2.0 mg/kg injected intraperitoneally) and, following confirmation of anesthesia, submerged in an ice slurry for five minutes to decrease body temperature. Following decapitation and evisceration, the cervical-to-sacral spinal cord was isolated along with ventral and dorsal roots and placed in an oxygenated (95% O_2, 5% CO_2) bath of artificial cerebrospinal fluid (aCSF, in mM: NaCl 128; KCl 1.9; D-glucose 10; $MgSO_4$ 1.3; $CaCl_2$ 2.4; KH_2PO_4 1.2; and $NaHCO_3$ 26). Further isolation procedures were specific to whole-cord vs. hemisected-cord experiments and are described in the following sections.

The spinal cords of 17 Sprague-Dawley juvenile rats (postnatal days 10-14) were isolated and maintained *in vitro* for MEA and rigid electrode interfacing and evaluation. The following subsections describe the steps used in implementation of these experiments. Details concerning the subsequent data processing and analysis procedures are then provided.

Preparation for MEA-Spinal Cord Interfacing

The fabrication steps for the conical-well MEA have been reported previously (Guo 2007), and its stepwise processes are shown schematically in **Figure 3.1.** In brief, our fabrication process involves lift-off patterning gold features onto a PDMS substrate cured on a glass slide, lithographically defining sacrificial posts where electrode and contact pad openings are to be made in assisting the formation of conical wells, covering the sample with another thinner PDMS layer for encapsulation, and then removing the sacrificial posts to expose the electrodes and contact pads.

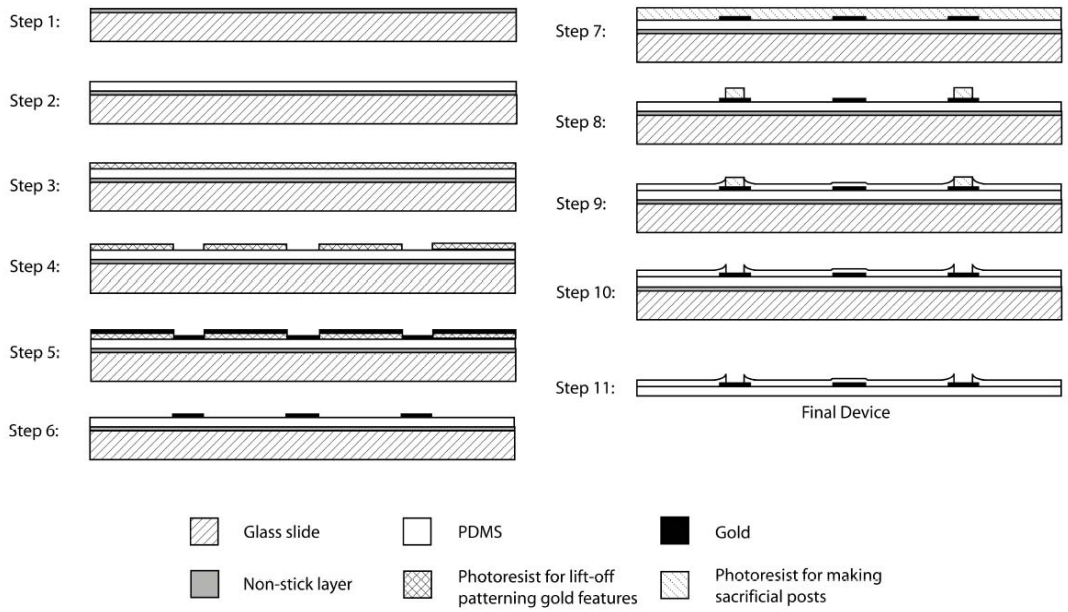

Figure 3.1: Schematic illustration of stepwise fabrication processes for the PDMS-Based conical-well microelectrode array.
1) A cleaned glass slide is coated with a PDMS non-stick gold layer in E-beam Evaporator to facilitate device peeling-off in the end. 2) A PDMS layer is spun on the glass slide to serve as device substrate. 3) After brief PDMS surface activation in oxygen plasma, positive photoresist is spun onto the PDMS substrate. 4) The photoresist layer is processed to form a negative mask for lift-off patterning gold features, then the photoresist mask is flood-exposed. 5) Primed by 150Å adhesion-enhancing titanium, a 5000Å gold film is deposited in E-beam Evaporator. 6) The photoresist mask and extra gold films are lifted off in corresponding photoresist developer, leaving the desired gold features. 7) After brief PDMS surface activation, a thick negative photoresist layer is formed on the sample. 8) The photoresist layer is processed to leave sacrificial posts where electrode and contact pad openings are to be made. 9) After brief PDMS surface activation, another PDMS layer is spun on for encapsulation with thickness smaller than the height of sacrificial posts, and the sample is subsequently baked with a well-defined recipe. 10) The sacrificial posts are removed in acetone, exposing the electrodes and contact pads. 11) The device is peeled off the glass slide in isopropanol and fabrication is completed.

The total substrate thickness for the MEA is approximately 100 μm (no including isolation well height). Inter-electrode spacing for the version of the MEA used in these studies was 200 μm (**Figure 3.2**).

Prior to *in vitro* testing, our MEA was soaked in deionized water for at least 24 hours to ensure removal of any fabrication or handling residue. Contacts on the MEA were adapted to leads for the MCS STG-2008 stimulator (MultiChannel Systems), using 32 AWG wires (Belden, Inc.) bonded to each contact using conductive epoxy (CircuitWorks CW2400) and sealed with a thin layer of Sylgard (Dow Corning). PDMS tabs were cut out of the MEA substrate on either side of the five electrode exposures prior to interfacing; these tabs facilitated conformal attachment of the MEA to a single segment of the spinal cord (**Figures 3.3** and **3.4**). A customized mounting device secured the MEA such that it could be easily wrapped, exposures facing down, around an upper-thoracic spinal segment.

Electrophysiology, Part 1: Whole-Cord Experiments

The first series of experiments assessed the degree to which adjacent axonal tracts were activated by single-site MEA stimulation (**Figure 3.3**). Immediately following isolation, the whole cord was secured using insect pins (1.0 mm, Fine Science Tools) in a Sylgard-coated Petri dish containing cold (4°C), oxygenated aCSF. Dura was carefully and thoroughly removed, and the cord was given an hour to equilibrate at room temperature before further experimentation.

To stimulate the cord, MEA electrodes were placed directly on the center of the dorsal column at thoracic levels 6, 7, or 8. The dorsal column is responsible for conveying somatosensory information, and was chosen for evaluating regional selectivity because its axon composition is well-characterized (Chung, Langford et al. 1987; Willis 2004). For comparison, a conventional tungsten bipolar electrode (5μm exposed tip

diameter, 10μm inter-electrode distance; Harvard Apparatus, Inc.) was pressed firmly onto—but not penetrating—the cord surface at the same longitudinal tract location as the MEA electrode pair, as determined electrophysiologically (**Figure 3.3**). For a subset of these experiments, an additional, adjacent pair of MEA electrodes was also used to stimulate the cord. This was done to determine the white matter tract selectivity achievable between adjacent MEA electrode pairs.

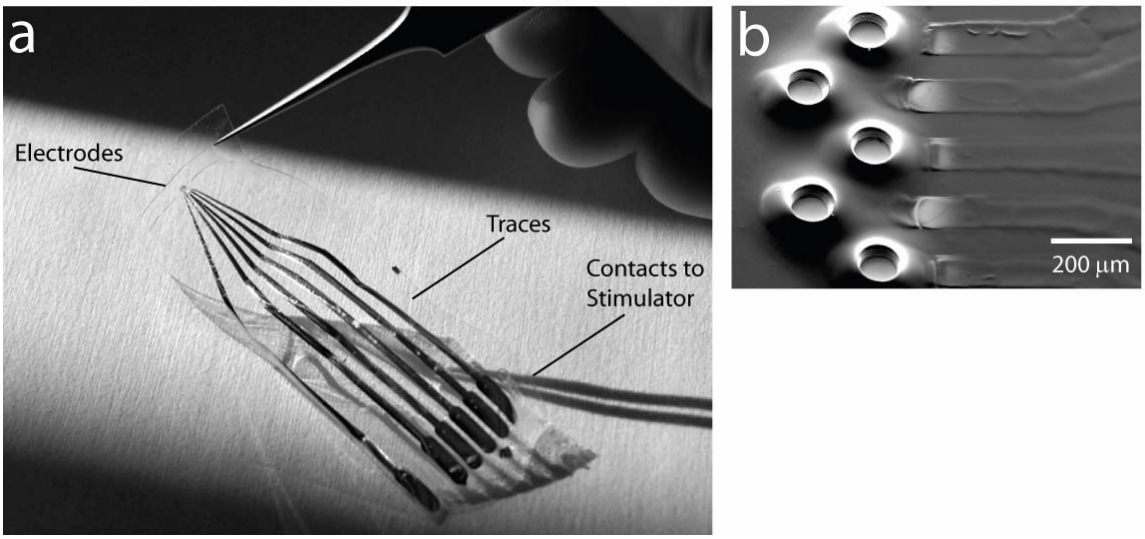

Figure 3.2: A polydimethyl siloxane (PDMS)-substrate micro-electrode array (MEA) with conical isolation wells. This configuration has five electrodes.
a. Photograph of the whole MEA, indicating the location of cord- interfacing electrodes, traces, and contacts to external stimulating hardware**.**
b. Scanning electron micrograph of the exposed gold stimulating electrodes, showing the raised PDMS wells around each electrode area. The raised PDMS wells surrounding each electrode help to further isolate the space between a given electrode and its interfaced soft-tissue surface.

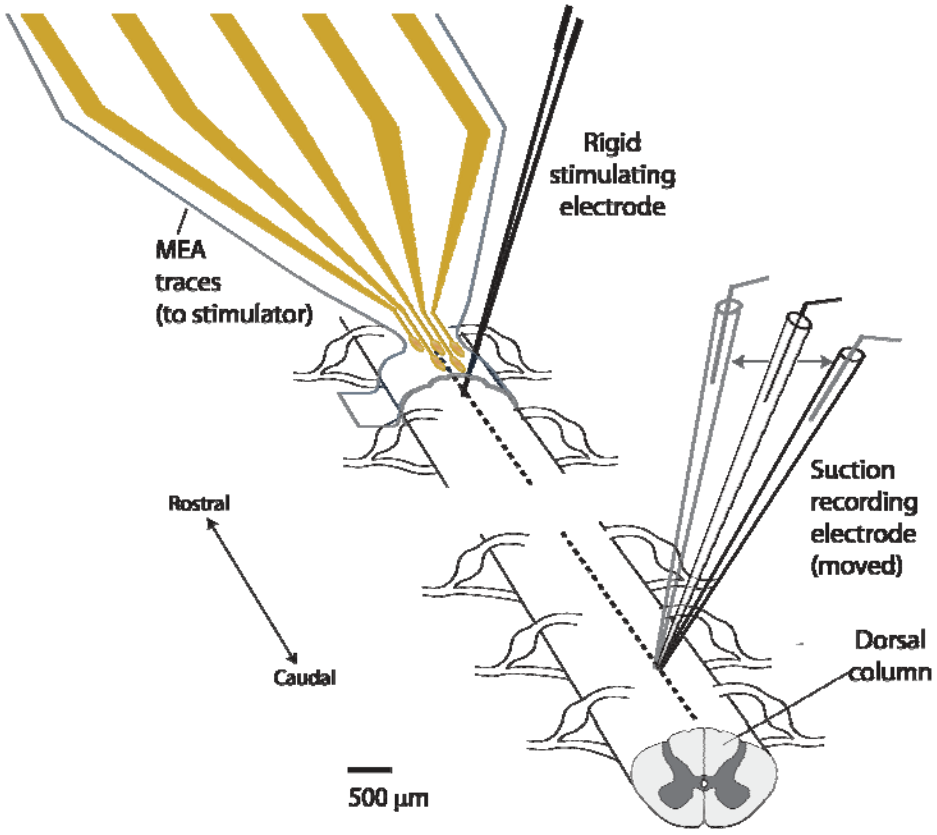

Figure 3.3: Experimental setup for measuring degree of lateral stimulus spread (anatomical selectivity).
Studies were performed to demonstrate the capacity of our conformable MEA to activate a specific region of longitudinally-oriented axonal bundles (spinal white matter tracts) in the *in vitro*, isolated spinal cord of postnatal days 10-15 rats (n=9). We determined this degree of anatomical stimulus selectivity by delivering single-site MEA stimuli to the surface of the cord (thoracic levels 6-8) and then recording the evoked compound action potential (CAP) response on adjacent white matter tracts located 10-15 mm (approximately 8 spinal segments) caudal to the site of activation.

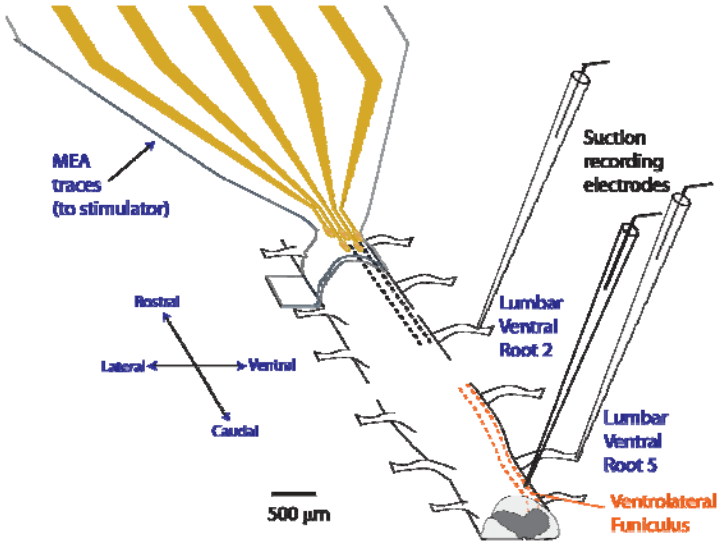

Figure 3.4: Experimental setup for measuring motor outputs evoked by adjacent MEA electrodes on the ventrolateral funiculus (VLF).
The MEA was wrapped around the isolated, hemisected *in vitro* spinal cord of postnatal days 10-12 rats. Two adjacent MEA electrodes (bipolar configuration) were used to stimulate the 12th thoracic segment's VLF using adjacent electrodes (200 µm inter-pair distance). For recording, glass suction electrodes (70-100 µm internal diameter) were placed on ventral roots at the 2nd and 5th lumbar level, as well as on the surface of the spinal cord at the 6th lumbar level VLF.

To measure activation of axonal tracts, a single glass recording suction electrode was used to record evoked compound action potentials (CAPs) in 50 μm lateral increments across the cord surface (MO-10 One-axis Oil Hydraulic Micromanipulator, Narishige International USA). The recording electrode (40-50 μm internal diameter glass, silver chlorided wire differential recording) was placed 10-15 mm caudal to the stimulation site (typically spinal lumbar level L2) to allow for temporal separation of stimulus artifact and the evoked CAP. For all electrophysiology, a reference ground electrode was placed in the bath near the caudal end of the spinal cord.

For all white matter tract selectivity studies, the delivered stimuli were single, biphasic, bipolar current pulses. The minimum current value at which a CAP was visible on the white matter tract with the greatest evoked response was defined as the threshold stimulus value (T). Amplitude multiples of these threshold values (1.0T to 2.0T in .2T increments) were used to stimulate the cord to evoke increasingly stronger evoked CAPs, and this series of stimuli were repeated as the recording electrode was moved incrementally across the surface of the cord.

Electrophysiology Studies, Part 2: Hemisected Spinal Cord

For the second series of experiments, which measured motor responses to MEA surface stimulation (**Figure 3.4**), Hemisection was required to ensure sufficient surface area exposure for complete oxygenation of all spinal gray matter. Mid-sagittal hemisection was accomplished using insect pins and was performed immediately after isolation and placement of the cord into a bath of ice-cold, oxygenated, high sucrose-containing aCSF (in mM: sucrose 250; KCl 2.5; $NaHCO_3$ 26; NaH_2PO_4 1.25; D-glucose 25; $MgCl_2$ 3; $CaCl_2$ 1). Following hemisection, the spinal cord was placed in room-temperature, oxygenated aCSF and allowed to equilibrate at room temperature for at least 1 hour before commencement of MEA testing.

Following placement of the MEA on the ventro-lateral funiculus between thoracic roots 11 and 12, single monophasic current pulses were applied at each of the two electrode pair sites at a stimulus value of 500 μA/50 μs, which corresponds with known thresholds for activating myelinated fibers of all diameters in peripheral nerve (Thompson, King et al.). Motor outputs were recorded at the ventral root at the second and fifth lumbar lumbar levels (L2 and L5, respectively). Previous work by Kjaerulff and Kiehn (1996) has shown that recordings from these roots are associated with hindlimb flexor (L2) and extensor (L5) motor output (Kiehn and Kjaerulff). Ventral root recording was accomplished using bipolar glass suction electrodes (90-150 μm internal diameter glass, silver chlorided wire differential recording). All extracellular responses were amplified by 10,000 and recorded using pClamp data acquisition software (MDS Analytical Technologies).

Signal Analysis

Seven to ten trials were recorded for a given stimulus source and current intensity. Data were analyzed post-experiment using custom MATLAB routines. The strength of evoked responses for both CAPs and ventral-root responses was quantified by rectifying and integrating the signal for the time window of 100 ms post-stimulus, starting immediately after the end of a given stimulus artifact. To adjust for baseline noise, 100 ms worth of rectified, integrated pre-stimulus recording was subtracted from each value. For white matter tract selectivity comparisons across animals, values were also amplitude normalized such that the maximal response was equal to 1.

The time to onset and duration of a given response was also calculated using a custom MATLAB routine. The detection algorithm used a combination of threshold detection and time windowing to identify the onset and offset of a given response. Visual verifications of response onset and offset values were performed for each trial used in analysis, and the consistency of response across trials was also verified visually.

However, small triphasic spikes at longer-latencies were seen whose amplitude was comparable to peak-to-peak noise amplitudes. These spikes were not detected by the threshold detection technique and were not included in calculations of conduction velocity. Values for delay and duration of evoked response were subsequently used, in combination with distance measurements, to calculate axonal fiber conduction velocities.

Results

In the analysis of the in *vitro* stimulation efficacy of the MEA, three different capabilities of the MEA were assessed: anatomical selectivity, size selectivity, and 'functional' selectivity. We define anatomical selectivity as the ability of the MEA to stimulate axons with a pattern of spatial selectivity that compares to conventional rigid stimulating electrodes. We use the term size selectivity to describe the MEA's ability to preferentially stimulate axonal fibers of different diameters, as measured by their correlated conduction velocities (Hursh 1939; Rutten 2002). We define functional selectivity as the MEA's ability to synaptically-recruit a select population of neurons in the spinal cord, as measured by ventral root responses associated with motor activity. The following sections describe the results of these analyses and evaluate the fundamental capability of our MEA to stimulate white matter tracts in a precise, controlled, and functionally-relevant manner.

Part 1. Anatomical Selectivity

Anatomical selectivity was first demonstrated by the ability of the MEA to evoke compound action potentials (CAPs) on axonal surface tracts with a site of peak recruitment and progressive bilateral reductions in CAP amplitude with lateral distance (**Figure 3.5a**, n=9). This activation profile selectivity of the MEA compared favorably with that evoked with a rigid, metal (tungsten) bipolar stimulating electrode (5 □m exposed tip diameter, 10 μm inter-electrode distance) in direct contact with the cord surface (tested at multiples of threshold and normalized). For both array and rigid electrode, increasing the stimulus amplitude increased the magnitude of CAP responses in a graded, controllable manner (**Figure 3.5b,** n=9).

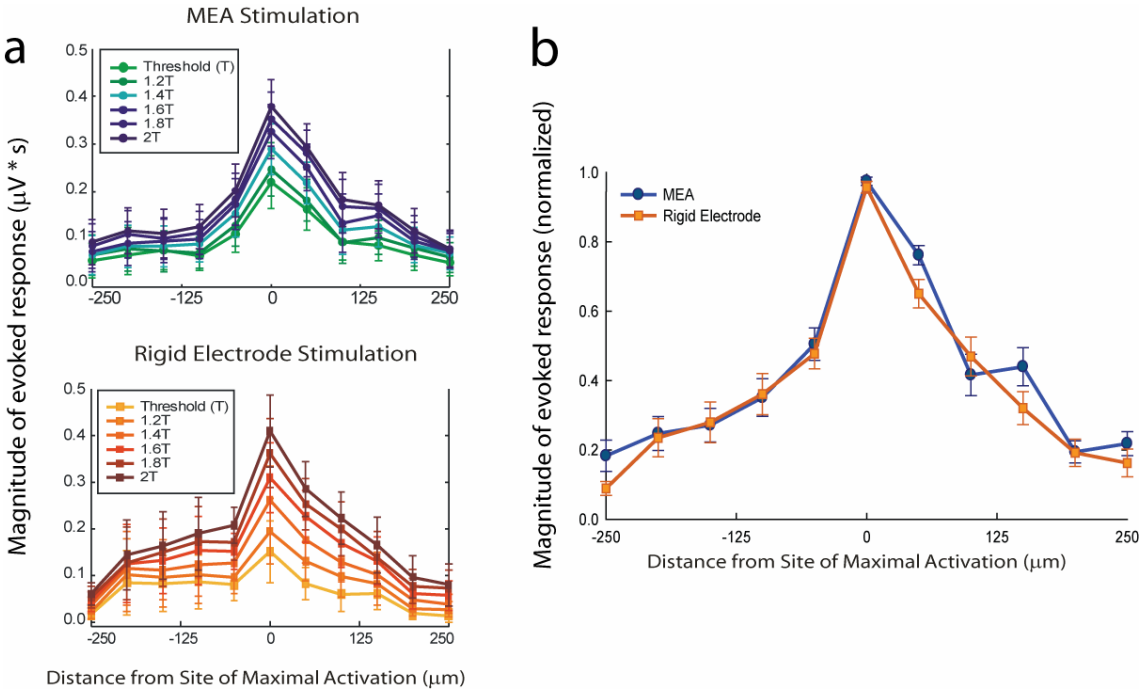

Figure 3.5: Anatomical stimulus selectivity of MEA vs. rigid tungsten electrode. The magnitude of evoked compound action potentials (CAPs) (μV*ms) was measured over lateral distance from site of maximal CAP response. CAP response magnitudes were calculated using the rectified, integrated, and baseline-subtracted responses for a fixed time window following the stimulus artifact. These values were then averaged over ten trials for a given recording site on the dorsal column.
a. We used both MEA and rigid electrodes to stimulate the cord surface while increasing current amplitude (biphasic pulses, 500 μs duration biphasic), and recorded the evoked CAPs at incremented lateral distances from the site of maximal activation. Stimulus amplitudes were chosen as multiples of threshold, which we defined as the minimum current amplitude required to elicit a visible evoked CAP. The resulting graded recruitment properties of MEA vs. rigid tungsten electrode stimulation are shown.
b. For comparison of region-of-activation between MEA and rigid electrodes, the recruited CAPs for a given animal at a given multiple of stimulus threshold were amplitude-normalized such that the maximal response was equal to 1. Standard error bars are shown. The magnitudes of evoked CAPs for both the MEA electrode pair and the rigid electrode decreased to below 50% within approximately 100 μm of either side of the site of maximal activation.

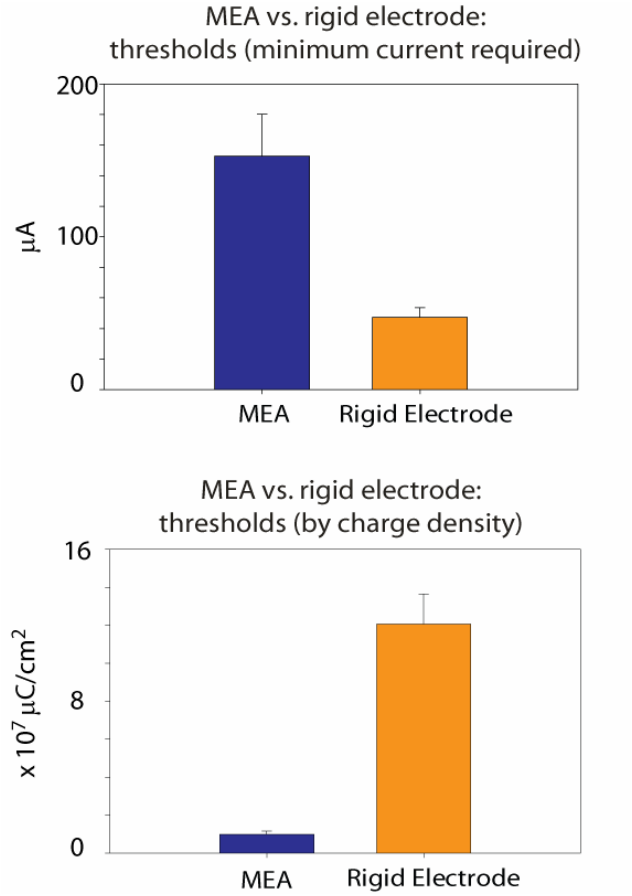

Figure 3.6: Stimulus (threshold) strengths required to elicit a detectable compound action potential: MEA electrode pair vs. rigid electrode pair.
Standard deviation bars are shown (n=14).
a. The threshold current stimulus value was higher for the MEA than the rigid electrode.
b. The threshold current required at each electrode, expressed as current density.

The average threshold current required for the MEA electrode pair was greater (170 μA) than for the rigid electrode pair (51 μA) (**Figure 3.6a**, n=14). However, when electrode surface area was accounted for by measuring the threshold current density (μC*cm^2), the threshold for the MEA was less than for the rigid electrode pair (**Figure 3.6b**). Taken together with our stimulus selectivity data (**Figure 3.5**), these results show that the MEA electrode pair can stimulate the surface of the spinal cord with similar resolution than a standard, rigid bipolar microelectrode, and at a lower threshold current density.

For a subset of experiments, an additional MEA pair was used to stimulate a second site on the dorsal column surface (**Figure 3.7**, n=3). For each of the two electrode pairs (400 μm distance between pairs), stimuli were applied independently, using minimum current values for evoking a visible evoked CAP volley (i.e. at threshold). Evoked CAPs were recorded at orthogonally-incremented locations approximately 8 segments caudal to the site of maximal activation. For all three animals, distinct peaks in CAP response magnitude were found (**Figure 3.7**). The spacing of these peaks was the predicted ~400 μm in 2 out of the 3 animals, and less than 400 μm for the third. These results demonstrate the MEA's capability to recruit distinct white matter tract populations using adjacent electrodes along the dorsal column.

To further test the ability of the MEA to selectively activate spinal cord surface tracts, dual-electrode stimulation was then tested at a more lateral location on the dorsal surface (**Figure 3.8**, n=2). These electrode pairs did not activate anatomically-distinct tracts; instead, the more lateral electrode pair seemed to evoke its CAP peak at the site anatomically-identical to the more medial electrode pair. Interestingly, current requirements for threshold intensity were ~2.5 times higher in the lateral electrode pair, whose location may coincise with placement over Lissauer's tract. This tract contains largely high threshold afferents (Lidierth 2007). This suggests that lower-threhsold

afferents more distant to the stimulating electrode are recruited before high-threshold afferents closest to the electrode. Alternatively, we may have been stimulating populations of axons at the dorsal root entry zone that then enter the cord to travel along the same more medially-located group of axons. These issues are explored in further detail in the Discussion section.

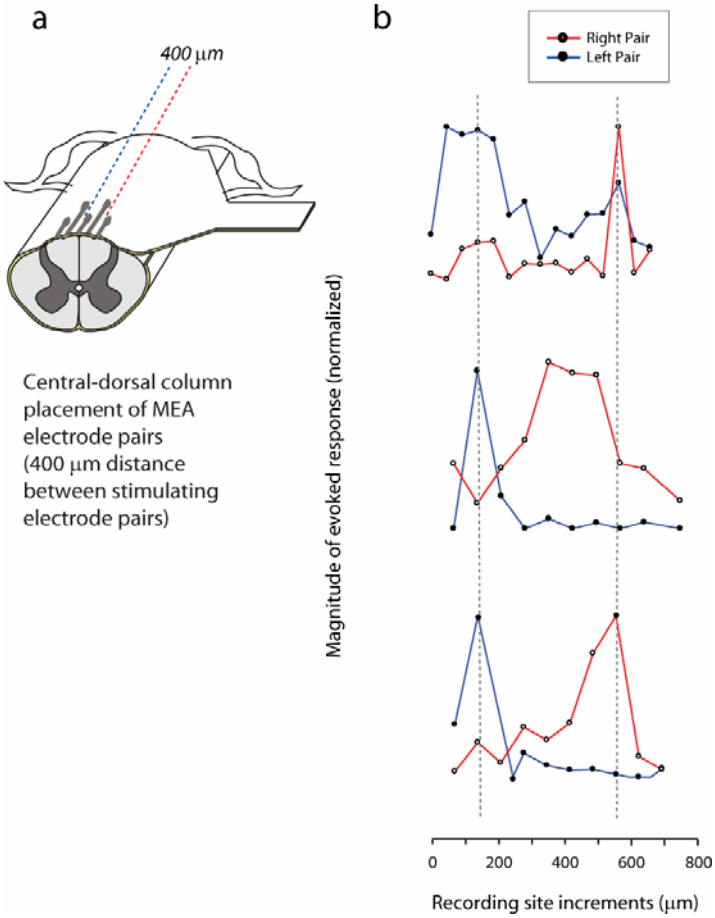

Figure 3.7: Adjacent-pair MEA stimulation of the dorsal column activates regionally-distinct tracts.
a. The MEA was placed on the central-dorsal column for stimulation of white matter tracts by adjacent pairs of MEA electrodes (400 µm distance between pairs). For each pair, stimuli were applied independently, using minimum current values (biphasic pulses, 500 µs duration) for evoking a visible evoked CAP. For each of the two stimulus pairs, the evoked CAPs were recorded at incremented lateral distances from the site of maximal activation. Response magnitudes were calculated as the rectified, integrated, and baseline-subtracted responses for a fixed time window following the stimulus artifact. These magnitudes (µA*ms) were then averaged over ten trials for a given recording site (error bars not shown) on the dorsal column and, for a given stimulus value, amplitude-normalized such that the maximal response was equal to 1.
b. Results shown above (n=3) have been aligned to the peak response elicited by the left pair of electrodes. The dashed lines indicate a trend in relative location of CAP response magnitude peaks. This demonstrates the array's ability to recruit distinct white matter tract populations using adjacent electrodes.

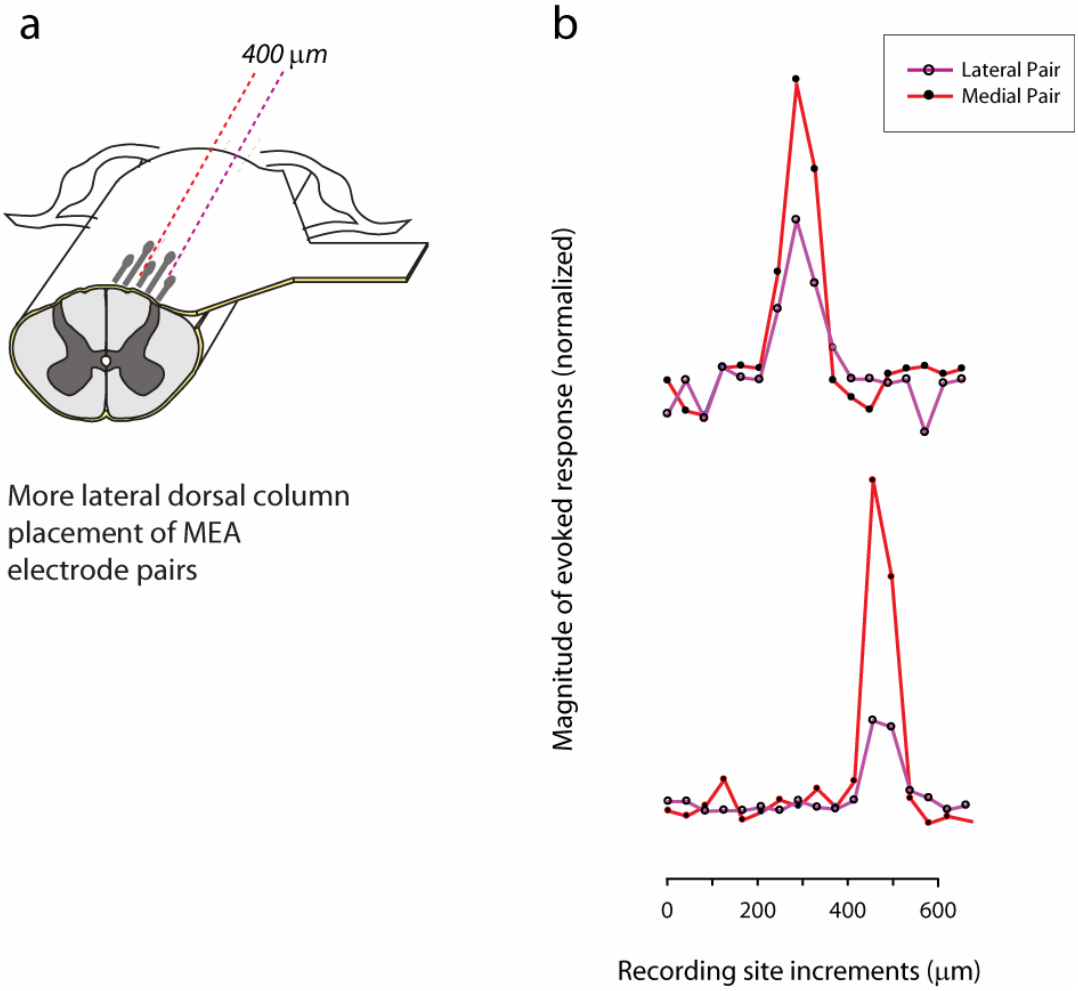

Figure 3.8: Lateral-dorsal column stimulation using MEA electrode pairs activates a single tract (or converging tracts).
a. The MEA was placed on the lateral aspect of dorsal column for stimulation of white matter tracts by adjacent pairs of MEA electrodes (400 µm distance between pairs). For each pair, stimuli were applied independently, using minimum current values (biphasic pulses, 500 µs duration) for evoking a visible evoked CAP (threshold). For each of the two stimulus pairs, the evoked CAPs were recorded at incremented lateral distances from the site of maximal activation. Response magnitudes were calculated as the rectified, integrated, and baseline-subtracted responses for a fixed time window following the stimulus artifact. These magnitudes (µA*ms) were then averaged over ten trials (error bars not shown) for a given recording site on the dorsal column and, for a given stimulus value, amplitude-normalized such that the maximal response was equal to 1.
b. Results shown above (n=3) suggest that the MEA electrode pairs are activating the same lower-threshold tract (that is closer to the medial pair of electrodes, or are activating two tracts that converge before reaching the more-caudal evoked-CAP recording site.

Part 2: Size Selectivity

We next determined the extent to which our MEA could recruit surface tracts in order of their axonal fiber size (**Figure 3.9** and **Figure 3.10**, n=9). Larger-diameter axons are known to be recruited at lower thresholds than axons with smaller diameters; for this reason, size selectivity can provide insight into the MEA's ability to stimulate white matter axons in order of axon diameter. Because there is also a direct relationship between axonal fiber diameter and the speed at which its compound action potentials propagates (Hursch 1939), we used calculations of conduction velocities to assess afferent fiber populations.

Figure 3.9b demonstrates that, even at threshold stimulus intensity, slow conducting fibers are recruited. However, with increased intensities of stimulation, there was a trend toward recruitment of progressively slower conducting afferents in both the rigid and MEA electrodes. In comparison, the fastest conducting axons were recruited at the lowest stimulation intensities (not illustrated).

In addition, we compared conduction velocity range of axons recruited as a function of lateral distance from the peak CAP response. **Figure 3.10** shows that the MEA recruits the slowest-conducting fibers only at sites closest to the site of maximal response. This relation to proximity was not observed for faster-conducting fiber populations (as indicated by maximum conduction velocities). A similar pattern was observed for stimulation with the rigid electrode. This lack of a clear recruitment pattern for lower-threshold, faster-conducting fibers on the cord surface indicates that at least some of the fastest conducting axons are recruited at distant sites.

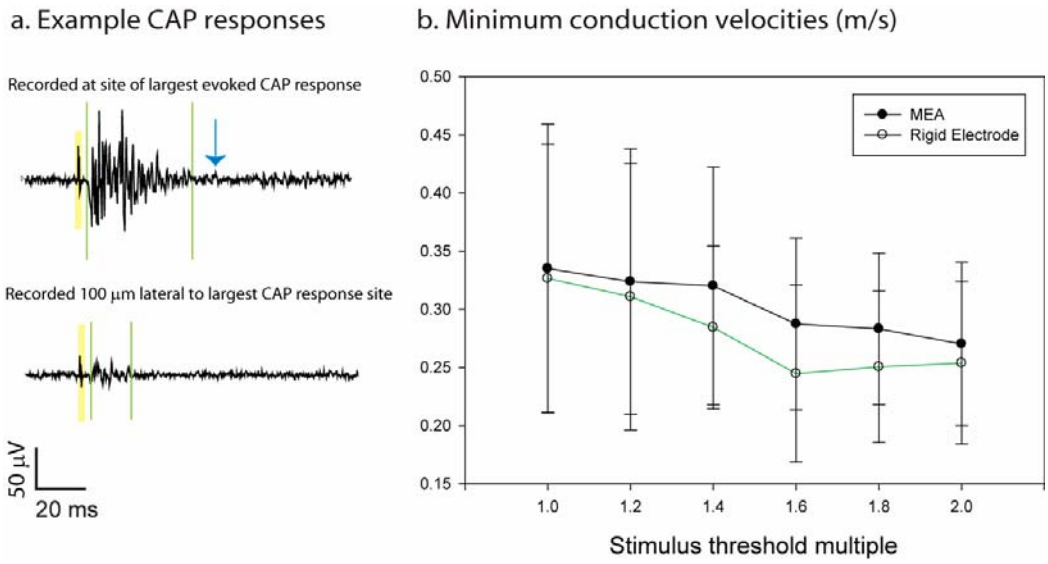

Figure 3.9: MEA stimulation of axonal fibers: Size selectivity.
A single pair of MEA electrodes was used stimulate the dorsal column, and the evoked CAPs were recorded at incremented sites as described in **Figure 3.2**.
a. Two CAPs, evoked at twice the threshold stimulus value, are shown. The top trace was recorded on the site of maximal recorded CAP (i.e., site of maximal activation) and the bottom trace was recorded on a white matter tract 100µm lateral to the site of maximal activation. The yellow overlay highlights the presence of stimulus artifact, and the vertical lines surrounding the responses indicate the onset and offset of the evoked CAP. Minimum and maximum conduction velocities for the evoked CAPs were calculated using stimulus-to-recording distance values and latency to onset and offset of evoked responses, using customized MATLAB scripts described in the **Methods** section.
b. At the site of maximal recorded CAP, the minimum conduction velocity is shown in relation to the current stimulus amplitude (defined in multiples of threshold, T). With increased intensities of stimulation, there was a trend toward recruitment of progressively slower conducting afferents in both the rigid and MEA electrodes. In comparison, the fastest conducting axons were recruited at all (including the lowest) stimulation intensities above threshold for activation (not illustrated).

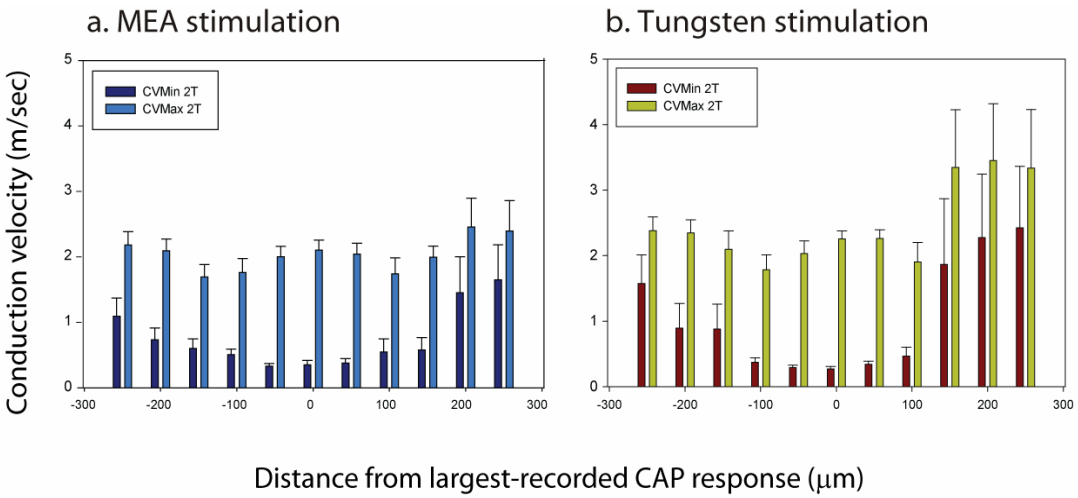

Figure 3.10. Minimum and maximum conduction velocities evoked by 2 times threshold (2T) and recorded along the dorsal column.
For both MEA and rigid electrode, the conduction velocity ranges were calculated for each recorded CAP site (incremented distances from the site of maximal activation). Standard error bars are shown (n = 9). Note that the slowest conducting fibers are recruited near the site of peak CAP. Note also that a stimulus intensity of 2T appears to be of sufficient strength to recruit the fastest conducting axons with considerable lateral spread.

Part 3: Functional Selectivity

Functional selectivity of the MEA was assessed in terms of its ability to differentially activate motor outputs using electrode pairs on the same array placed on or near the ventrolateral funiculus at thoracic level 12 (electrode pairs spaced 200 μm apart, **Figure 3.4**). We evaluated functional responses by measuring ventral root motor activity at the second and fifth lumbar level, as they have known correlation with hindlimb flexor and hindlimb extensor movements, respectively. In addition, CAPs evoked on the surface of the ventrolateral funicuclus (VLF) were recorded at the sixth lumbar level. Motor output responses to separate stimuli from adjacent MEA electrode pairs were evaluated in four cords. MEA placement onto the cord surface was not precise enough to evoke motor output responses that were comparable across samples; however, all four cords tested could produce a differential activation of L2/L5 responses at adjacent electrode pairs, of which one example is shown (**Figure 3.11**). This example also demonstrates differences in the VLF activity pattern.

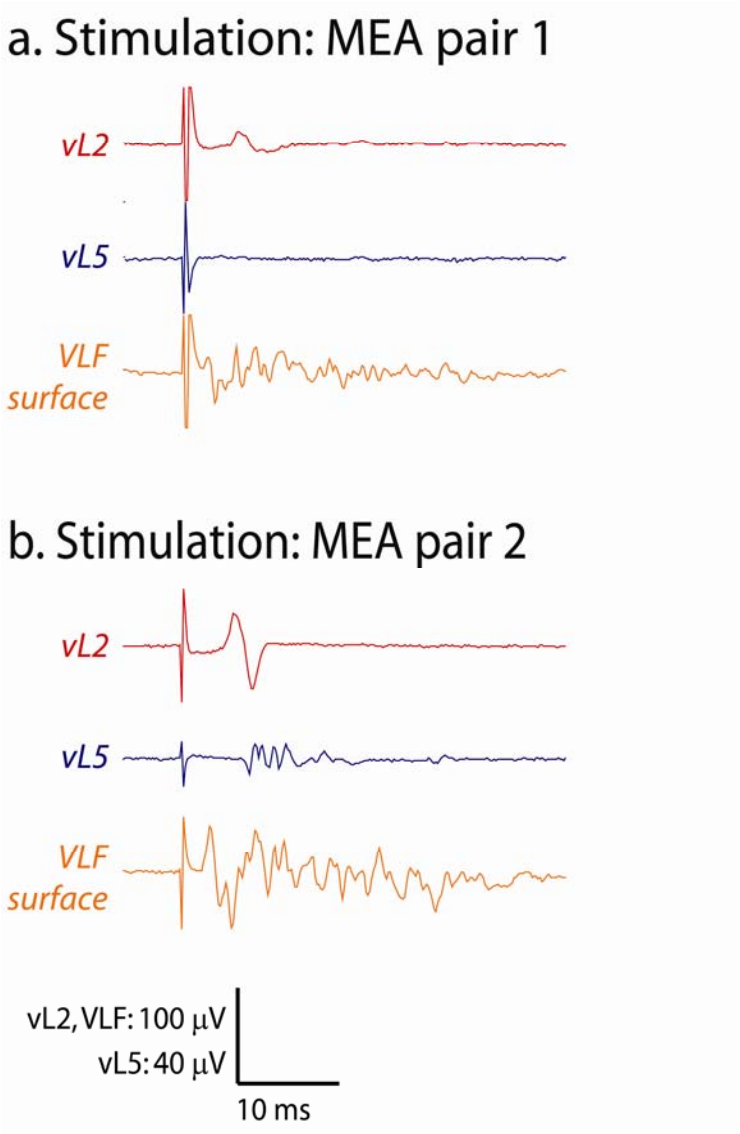

Figure 3.11: Example evoked motor responses to adjacent MEA electrode stimulation.
Using the experimental setup illustrated in Figure 3, electrode pairs spaced 200 µm apart (sharing a central electrode) each delivered separate stimuli to the T12 ventrolateral funiculus. Recordings of responses at vL2 and vL5 were made in order to determine the ability of the MEA to activate distinct motor patterns based on electrode positioning. The compound action potential at the surface of the ventrolateral funiculus (VLF) at L6 was also recorded. Example evoked responses to the more dorsally-placed electrode pair (a) versus the more ventrally-placed pair (b) for one cord are shown.

Discussion

The results presented in this Chapter demonstrate the ability of an elastomer-based MEA to stimulate white matter surface tracts with the same precision as rigid electrodes, and so serves as a starting point for further applications of conformable surface-stimulation technologies. While the minimum current required for evoking a visible compound action potential was higher for the MEA, than that required by the rigid electrode; however, when electrode surface area was accounted for by measuring the threshold current density ($\mu C*cm^2$), the threshold for the MEA was less than for the rigid electrode pair (**Figure 3.6b**). Taken together with our stimulus selectivity data (**Figure 3.5**), these results demonstrate that the MEA electrode pair can stimulate the surface of the spinal cord with similar resolution than a standard, rigid bipolar microelectrode, and at a lower threshold current density.

Unlike the rigid electrode, it was impossible to visually verify direct physical contact of MEA electrodes to the spinal cord surface, so variability in distance between MEA electrodes and spinal cord surface could account for their greater variability in measured threshold stimulus values.

Anatomical selectivity of the MEA was clearly demonstrated by non-overlapping activation of parallel tracts using adjacent MEA electrodes positioned at more medial sites on the dorsal column (**Figure 3.6**). However, this spatial selectivity appeared lost when the MEA was placed on more lateral aspects of the dorsal surface (**Figure 3.7**). More lateral electrode locations likely correspond to placement over Lissuaer's tract which contains axons of high-threshold afferents (Chung and Coggeshall 1982). As tests were conducted at low threshold (2T) stimulus intensity, which should correspond to selective recruitment of large diameter axons, few Lissuaer's tract axons would be recruited. On the other hand, at this location the MEA may recruit large-diameter dorsal root afferents near their entry zone that subsequently travel to the more medial dorsal column before projecting rostrocaudally (and recorded at the more medial site).

One limitation to the present anatomical selectivity studies, which applies to conventional rigid electrodes as well, is the possibility that surface stimulation may also directly activate spinal neurons in the gray matter interior. We view this as unlikely as we stimulated axons at low threshold and it us known that axons are activated at lower thresholds than their associated cell bodies (Jankowska, Padel et al. 1975; Ranck 1975; Gustafsson and Jankowska 1976; Gaunt, Prochazka et al. 2006).

As many stimulated axons (or collateral branches) exit the white matter to synapse on and activate numerous spinal neurons, it is likely that at least some activated postsynaptic spinal neurons project axons back in the dorsal white matter and account for a component of the CAP. This is particularly likely for postsynaptic dorsal column tract cells (Willis 2004). One consequence is that the recorded spatial spread of CAPs in adjacent white matter regions (**Figures 3.4 and 3.6**) may be partly due to synaptically recruited fibers within the dorsal column. Another consequence is that estimates of slower conduction velocities may be contaminated by synaptically activated faster conducting axons. Indeed in several experiments recording CAPs in the ventrolateral funiculus where synaptic transmission was minimized in a high Mg^{2+}/low Ca^{2+} aCSF, longer latency components of the CAP were abolished confirming their synaptic origin (presented in **Chapter 4** of this thesis). However, the VLF contains highly heterogeneous populations of axons from ascending tract, descending tracts and interneuronal systems so the possibility for synaptic interactions is considerable. In contrast, the dorsal column (aside from the deepest white matter) contains only primary afferents and postsynaptic dorsal column tract cells. As the dorsal column tract cells convey their projections only rostrally (Willis 2004) and we recorded CAP that propagated caudally at least 6 spinal segments, it seems very unlikely that any evoked responses were mediated synaptically.

The range of conduction velocities estimated here in the dorsal column at 2T with the MEA range from an average 2.4 to 0.32 m/s. This conduction velocity range compares well to that reported in doral roots in the in a similar preparation at the same

age range ((Shay, Sawchuk et al. 2005); 2.3 and 0.24 m/s, respectively). The slowest conduction velocities are consistent with recruitment of C fibers as previously reported dorsal roots in vitro (Hedo, Laird et al. 1999; Lu and Perl 2003). Afferents in the dorsal column of C fiber conduction correspond to visceral afferents (Willis, Al-Chaer et al. 1999), the only pain-encoding afferents in the dorsal column. A possible explanation for recruitment of slow conducting fibers at low threshold intensities may be due to the choice of electrical stimulus delivery. We purposefully chose to stimulate with a longer duration (500 μs) bipolar charge balanced stimulus. Longer duration stimulus pulse widths and bipolar current delivery may be a less effective at discriminating between axons of different diameters.

The ability of the MEA to synaptically-activate different populations of spinal neurons in a spatially restricted manner was demonstrated via recording of ventral root L2 and L5 responses. When MEA electrodes were placed on the lower-thoracic ventrolateral funiculus, motor activity was recruited via stimulation with MEA electrode pair, but not from its adjacent MEA electrode pair (spaced 200 μm apart). Axons traveling in this region of the cord have been associated with multiple motor-coordinating systems (Reed, Shum-Siu et al.), and surface stimulation of this region has been shown to elicit fictive locomotion in neonate in vitro rat models (Antonino-Green, Cheng et al.). Identification of the spinal neurons with axons in the ventrolateral funiculus has been studied by Magnuson and colleagues (Antonino-Green, Cheng et al. 2002; Reed, Shum-Siu et al. 2006; Reed, Shum-Siu et al. 2008), and labeling studies in **Chapter 4** of this thesis describe populations of neurons present in the ventrolateral funiculus in control and chronic spinal injured spinal cord that reflect putative neurons responsible for the observed L2/L5 evoked responses.

CHAPTER 4

SURFACE STIMULATION OF THE VENTROLATERAL FUNICULUS FOR EVOKING MOTOR OUTPUT IN THE CHRONIC-TRANSECTED SPINAL CORD

Summary

Spinal cord injuries (SCI) can often sever communication lines between brain and body, including the descending pathways that initiate movement. However, most spinal circuits remain intact below the site of injury, and are capable of independently generating complex motor outputs, including locomotion. Therapeutically, then, there is great opportunity to regain function through direct stimulation of remaining spinal motor systems. Multiple approaches have been developed to stimulate both intra-spinally and extra-spinally to activate these motor outputs, but significant work remains before electrical stimulation methods can adequately replicate natural (pre-injury) movements. An ongoing limitation to existing spinal-cord stimulation methods is a lack of complete access to its inherent motor-generating and motor-coordinating circuitry, much of which is ventrally located. These populations are difficult to reach using rigid electrodes via surgical implantation, which must proceed via openings (laminectomies) in the dorsal spine. To overcome this access challenge, we have developed (Chapter 2) a new conformable array technology that can wrap around the spinal cord to reach more lateral and ventral surface sites. We have demonstrated that this new technology is capable of focally stimulating the surface of the spinal cord (Chapter 3).

In this chapter, we investigate whether a particular site on the ventro-lateral surface of the chronic-transected (injured) spinal cord is effective for tapping into motor output associated with hindlimb flexor and extensor activity. This region is known to

contain axons of interneurons involved in motor coordination, including those for locomotion.

This work generated three important findings. First, we found that surface stimulation of the ventrolateral funiculus (VLF) was capable of reliably activating ipsilateral L2 (flexor) and L5 (extensor) motor outputs in an asynchronous manner. Secondly, we found that, at segmental level L6 (caudal to direct pathways to L2/L5 motor neurons), T12 VLF stimulation also evokes a longer-duration (>30 ms), synaptically-mediated surface compound action potential. Finally, we found that that the chronic-transected cord's L2/L5 responses to T12 VLF stimulation can be facilitated for creation of more complex, potentially rhythmic motor outputs. Together, these results suggest that stimulation of the T12 VLF is a promising method for activating dynamic motor output associated with hindlimb flexors and extensors in the chronic-transected cord.

Introduction

Several approaches presently exist that use electrical stimulation to restore function following spinal cord injury (SCI), and which share a common goal of replicating the robust and coordinated actions produced naturally by intact systems. A subset of these approaches, which stimulate muscle and peripheral nerve directly, have been used successfully for therapeutic ends including hand grasp (Prochazka, Gauthier et al. 1997; Peckham, Keith et al. 2001; Peckham and Knutson 2005; Kilgore, Hoyen et al. 2008), bladder and bowel function (Brindley, Polkey et al. 1982; Ganio, Masin et al. 2001; Spinelli, Malaguti et al. 2005), standing support (Fisher, Miller et al. 2006), and counteracting foot-drop (Liberson, Holmquest et al. 1961; Kralj, Bajd et al. 1988; Kraft, Fitts et al. 1992; Taylor, Burridge et al. 1999). These actions, however, require minimal access to deep musculature or coordination across muscles. There is a potentially fundamental limitation to adapting this approach for production of the power and multiple-muscle coordination required for more complex behaviors such as walking.

An alternative approach to muscle or peripheral nerve stimulation is direct stimulation of the spinal cord to elicit movement. Methods that utilize this approach have been successful in restoring locomotor ability to spinal-cord injured humans (Dimitrijevic, Gerasimenko et al. 1998; Minassian, Persy et al. 2007), cats (Saigal, Renzi et al. 2004; Guevremont, Renzi et al. 2006), and rats (Ichiyama, Gerasimenko et al. 2005; Ichiyama, Gerasimenko et al. 2005). These methods are currently capable accessing subsets of the motor-coordinating circuitry that remain intact post-SCI through placement at different sites external or internal to the spinal cord. The exclusive application of these different methods are limited by trade-offs between selectivity and invasiveness. Epidural stimulation of the spinal cord dorsal column can produce multi-joint, multi-muscle hindlimb movements via sensory afferent activation, but cannot focally activate spinal axons without first activating lower stimulus-threshold afferent populations

(Ichiyama, Gerasimenko et al. 2005; Gerasimenko, Roy et al. 2008; Ichiyama, Gerasimenko et al. 2008; Lavrov, Dy et al. 2008). Intraspinal microstimulation (ISMS), which stimulates via microwires inserted (through the dorsal aspects of the cord) into motor neuron pools in the ventral horn, has demonstrated the ability to elicit locomotor actions with with a nearly normal order of motor unit recruitment and reduced muscle fatigue (Mushahwar and Horch 1997; Mushahwar and Horch 2000; Mushahwar and Horch 2000; Bamford, Putman et al. 2005). However, these successes must be balanced with an increased invasiveness of approach.

Another promising, but relatively under-explored, method for evoking multi-joint, multi-muscle movements in the post -SCI cord is through direct stimulation of remaining ascending and propriospinal axonal tracts, many of which are located in the more lateral and ventral aspects of the cord (Davidoff 1983). These remaining axons connect to cell bodies that are caudal to the site of injury and which remain anatomically (and functionally) intact following SCI. The more lateral and ventral white matter tracts have been shown contain axons of neuronal populations sufficient for controlling of motor function, as locomotion is retained in spinal cord devoid of the dorsal half of the cord (Kjaerulff and Kiehn 1996).

A potentially significant advantage of stimulating more lateral and ventral tracts on the spinal cord is an enhanced ability to recruit spinal neurons independent of their sensory input. For example, epidural stimulation may recruit locomotion exclusively via activation of primary afferents (Lavrov, Dy et al. 2008), which may include recruitment of those involved in pain transmission (Gerasimenko, Lavrov et al. 2006; Lavrov, Gerasimenko et al. 2006).

In non-injured cords, the ventrolateral funiculus is known to contain axons that are critical to generation of rhythmic hindlimb motor output, and the putative systems involved include ascending and propriospinal systems that would remain intact post-SCI. In the neonatal (non-injured) rat, *in vitro* stimulation of the ventrolateral funiculus has

been shown to activate rhythmic alternating motor outputs thought to be associated with the locomotor CPG(Magnuson, Schramm et al. 1995; Magnuson and Trinder 1997; Antonino-Green, Cheng et al. 2002); the activated circuitry has been shown to involve both reticulospinal and spinoreticular systems (Magnuson, Green et al. 1998; Antonino-Green, Cheng et al. 2002; Reed, Shum-Siu et al. 2008). Cat studies stimulating the lateral funicular "stepping strip" have also demonstrated success in eliciting rhythmic limb movements (Yamaguchi 1986; Kinoshita and Yamaguchi 2001).

Other ascending tracts present in the VLF include the anterior spinocerebellar, spinothalamic, and spinoolivary tracts (Davidoff 1983). Among other functions, the spinoolivary and spinocerebellar tracts have demonstrated involvement in motor coordination; the spinothalamic tract is associated primarily with transmission of sensory (pain and temperature) information. Ascending tract axons typically also project local collaterals for additional segmental actions (Magnuson, Green et al. 1998), and may undergo plastic changes in their integrative properties which may include sprouting and synaptic stripping (Gustafsson, Pinter et al. 1986).

The VLF is also known to contain propriospinal tracts of significance to motor coordination. Propriospinal populations present include Renshaw cells, Group I non-reciprocal inhibitory interneurons, deep dorsal horn and intermediate laminae Group II interneurons, and FRA interneurons (Davidoff 1983; Hochman 2007). Many interneurons will also be partly axotomized and their function may be altered in a manner analogous to ascending tract cells. Last, many interneurons below the lesion will not incur direct injury. Overall, it is clear that studies are required to determine how these events affects the spinal anatomy and physiology of remaining networks relative to an uninjured control. While many studies have examined various plastic events associated with chronic spinal cord injury (Edgerton, Tillakaratne et al. 2004), specific injury-induced changes associated with axonal populations in DLF, LF and VLF remain to be studied.

In the chronic-transected spinal cord, tract degeneration following SCI may improve surface access to remaining (ascending and propriospinal) axonal tracts in the VLF. Following SCI, axon tracts of descending systems distal to the lesion site are severed from their cell bodies and completely degenerate via Wallerian degeneration (Raff, Whitmore et al. 2002; Saxena and Caroni 2007). Ascending tract neurons will have their major axon branch axotomized but have been shown to survive transaction in the neonatal rat (Bryz-Gornia and Stelzner 1986). Within the VLF, therefore, the lateral reticulospinal and vestibulospinal tracts would be disconnected from their cell bodies, and their associated tracts would degenerate. This degeneration of tracts may leave a potentially greater region of ascending and propriospinal tracts closer to the surface of the cord. This change may improve access to these remaining tracts following SCI, especially in more ventral regions of the cord where many descending tracts will degenerate post-SCI.

We hypothesize that surface stimulation of the lower-thoracic VLF in the chronic-transected cord can be used to elicit motor output. Our prediction is that single-pulse stimulation at this site is capable of evoking transient, combined flexor activity (reported at lumbar level 2) and extensor activity (as reported by ventral root lumbar level 5), as might be expected in the case of low-level activation (i.e. one "cycle") of rhythm-generating interneuronal circuitry. Stimulation at the pre-lumbar enlargement may be particularly important for initiating locomotion (Cazalets, Borde et al. 1995; Cowley and Schmidt 1997; Minassian, Jilge et al. 2004; Langlet, Leblond et al. 2005) and is positioned between forelimb and hindlimb, which is likely a critical site in coordinate their activity during locomotion (Kawashima, Nozaki et al. 2008).

To test our hypothesis, we first compared surface stimulation of the T12 VLF in chronic-transected vs. intact (control) responses to determine whether stimulation of the transected spinal cord at this site reliably activates L2 and L5 motor neuron populations. The relative latencies-to-onset and durations of the evoked L2 and L5 segmental

responses were also analyzed. A non-concomitant activation of these flexor- and extensor- associated motor outputs suggests that these single-pulse, single-site evoked responses could be built upon to sustain a pattern using more complex stimuli.

Next, we investigated the anatomical location of spinal circuits activated by T12 VLF stimulation. These experiments involved both electrophysiological studies as well as tract-tracing imaging of associated neurons whose axons travel in this region of the spinal white matter. We found that T12 VLF surface stimulation in the chronic-transected spinal cord spinal includes synaptic activation of pathways caudal to those leading directly to L2 and L5 motor neuron pools. Tract-tracing study results, while preliminary, suggest that tracts of propriospinal populations in both the dorsal horn and intermediate regions of the spinal gray manner are activated by T12 VLF stimulation.

Finally, we investigated whether the single-pulse T12 VLF stimulus evoked responses could be built upon to sustain a pattern. Sensory co-stimulation and pulse trains were both effective in facilitating activation of L2 and L5 motor outputs, with single-pulse sensory co-stimulation demonstrating potential to activate rhythmic, alternating output.

Combined, the results from these studies suggest that single-pulse focal surface stimulation of the chronic-transected cord at T12 VLF is capable of activating motor circuitry post-SCI in a manner that can be built upon to evoke rhythmic motor output. The T12 VLF site has previously been difficult to selectively stimulate *in vivo*, but can be readily accessed (and stimulated in a focal manner) by the MEA technology presented in Chapter 2 and Chapter 3 of this thesis. In the final section of this chapter, future studies are suggested that use this novel MEA for *in vivo* stimulation of the T12 VLF for re-activation of motor circuitry in the post-SCI rat.

Methods

The following experiments were conducted to investigate the ability of T12 VLF surface stimulation to activate motor circuitry in the chronic-transected spinal cord. A total of 38 chronic-transected rats and 32 intact (control) rats were studied, using animal procedures in accordance with policies of the Association for the Assessment and Accreditation of Laboratory Animal Care International and approved by Emory University's Institutional Animal Care and Use Committee.

We performed transection surgeries on rats at postnatal days 2-3, followed by 7-12 days of recovery (**Figure 4.1**). On a subset of the chronic-transected cords (n=14), *in vitro* experiments were then performed (**Figure 4.3**). The remaining 24 chronic-transected cords were labeled using lipophilic dye placement at three segmental levels (T12, L4, and S1) at the VLF, LF, DLF, and VF (2 cords were labeled at each of the 12 sites). Imaging of dye-labeled cords was conducted > 3 months following labeling in order to allow for complete migration and labeling of cells connected to axons traveling in these white-matter tract regions (**Figure 4.4**).

Thoracic Transection of Spinal Cord

Rats, postnatal days 2-3, were anesthetized with isoflurane via inhalation. Following dorsal laminectomy to expose lower-thoracic segments of the cord, one segment of the cord between T8-T10 was removed using surgical iridectomy microdissection scissors. Completeness of transection was verified visually by the withdrawal of both ends of the spinal cord towards the rostral and caudal axes. Gel foam was placed in the site of transection to maintain the gap between rostral and caudal cord. Rats recovered for 7-12 days (a mean of 9 days) before further electrophysiological experimentation or lipophilic dye labeling of axonal tracts at postnatal days 10-15 (a mean of 12 days). The minimum duration of recovery used has been demonstrated to

provide sufficient time for the Wallerian degeneration of severed descending axonal tracts (Raff, Whitmore et al. 2002; Saxena and Caroni 2007).

The ratio of white-matter to gray-matter areas in sections from two control cords and three transected cords did not indicate a significant difference in the relative presence of gray matter vs. white matter (**Figure 4.2,** 0.65 white matter/ gray matter ratio for control cords, 0.61 for chronic-transected, Student's two-tail t-test assuming equal variance, p-value of 0.20). Because descending axons contribute very little to the overall cross-sectional area of spinal white matter (Chung and Coggeshall 1983; Chung, Kevetter et al. 1984), these findings do not conflict with the degeneration of descending tracts in the case of our chronic-transected cords.

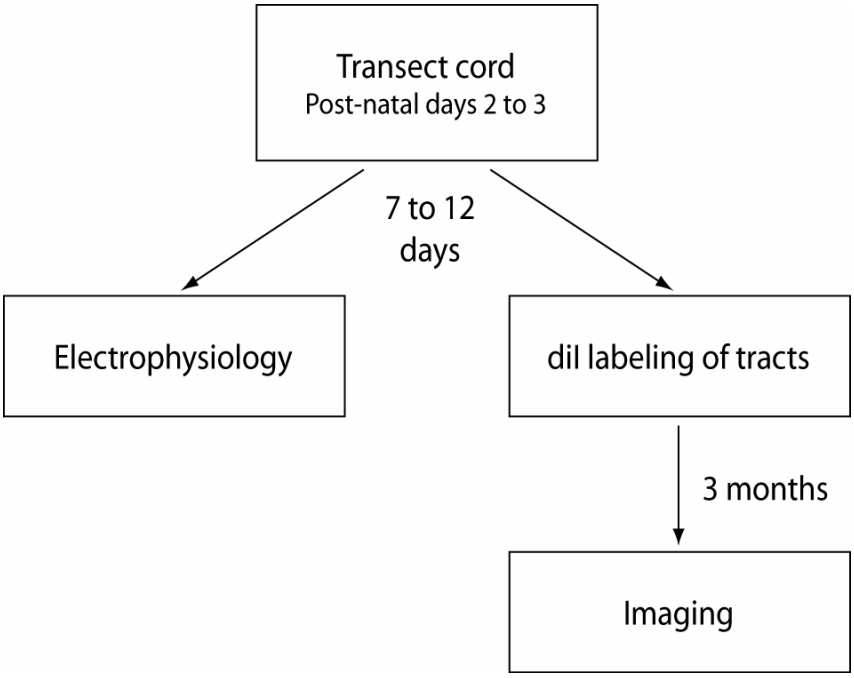

Figure 4.1: Methods Overview.
A timeline is presented for transection procedures and subsequent investigation of the chronic-transected cord (n=38 transected cords). One segment of the cord between T8-T10 was removed, and 7-12 days of recovery was used to allow for Wallerian degeneration of severed axonal tracts. Electrophysiological experiments studying the chronic-transected cord (isolated *in vitro*) to were then performed on a subset of the chronic-transected rats (n=14) (**Figure 4.3**). The remaining 24 chronic-transected cords were labeled using lipophilic dye placement at three segmental levels (T12, L4, and S1) at the VLF, LF, DLF, and VF (2 cords were labeled at each of the 12 sites). Imaging of dye-labeled cords was conducted >3 months following labeling in order to allow for complete migration and labeling of cells connected to axons traveling in these white-matter tract regions (**Figure 4.4**).

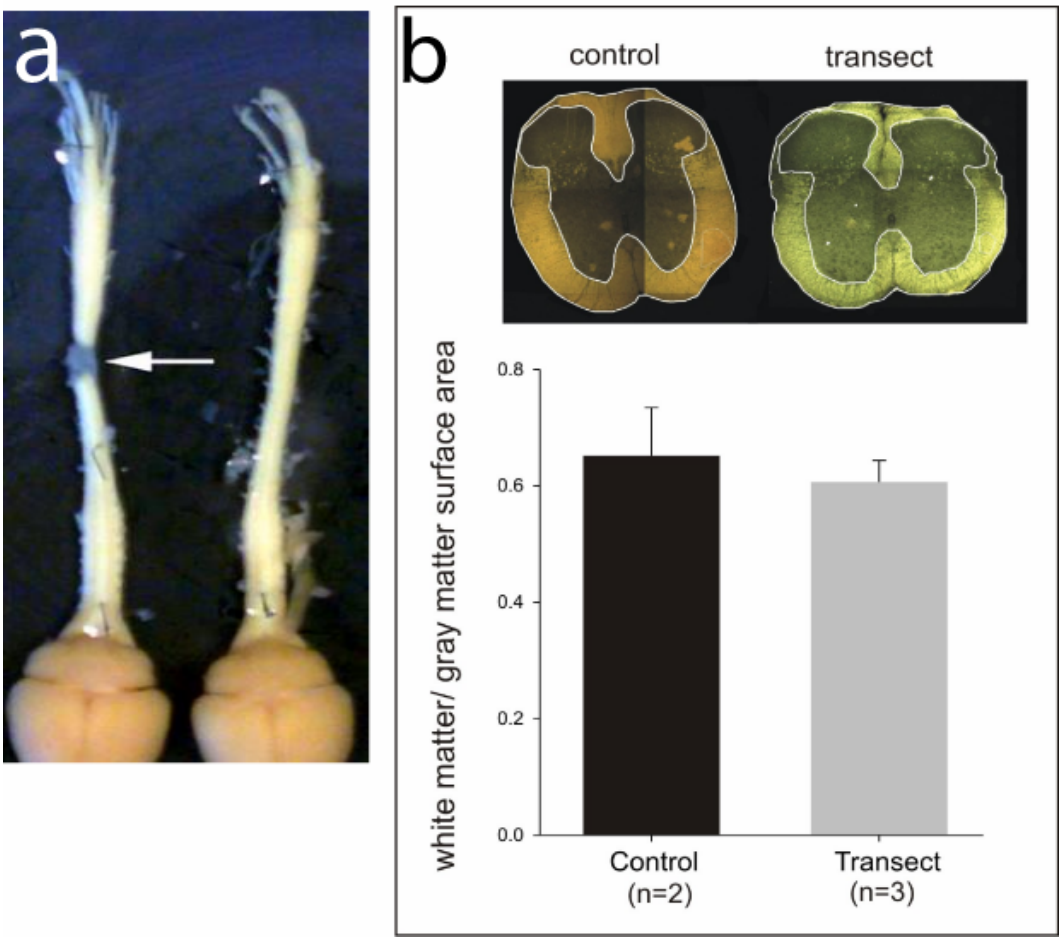

Figure 4.2: Results from chronic transection of the spinal cord.
a. Photograph of isolated chronic-transected cords and a control (non-transected) spinal cord. An arrow indicates the site of lesion.
b. Photographs are shown of transverse sections of lumbar spinal cord in a control animal and one having undergone chronic spinal transection**,** along with quantification results from the remaining ratio of white matter to gray matter area at L4. Measurement of white matter/gray matter ratio indicates that there is no significant difference 7-10 days after thoracic cord transection (2 control, 3 chronic-transected cords), which is in accordance with knowledge that axons from descending tracts constitute a small fraction of the white matter surface area in the lumbar cord.

Electrophysiology

The spinal cords of 22 juvenile rats were used for the following *in vitro* electrophysiology studies. 14 of these cords were transected at 7-12 days prior to experimentation, and 8 of these cords were not transected and were instead used as controls. To ensure sufficient surface area exposure for complete oxygenation of all spinal gray matter, spinal cords were midsagittally hemisected. Preparation involved initially administering 10% wt./vol. urethane (2.0 mg/kg injected intraperitoneally) and, following confirmation of anesthesia, submerging the rat in an ice slurry for five minutes to decrease body temperature. Following decapitation and evisceration, the cervical to sacral spinal cord was isolated along with ventral and dorsal roots within a bath of ice-cold, oxygenated, high sucrose-containing aCSF (in mM: sucrose 250; KCl 2.5; $NaHCO_3$ 26; NaH_2PO_4 1.25; D-glucose 25; $MgCl_2$ 3; $CaCl_2$ 1) within a Sylgard-coated dish (Dow Corning). Following thorough removal of dura mater, sagittal hemisection was accomplished using insect pins (1.0 mm, Fine Science Tools). The spinal cord was then placed in room-temperature, oxygenated aCSF and allowed to equilibrate at room temperature for at least 1 hour before further testing.

To stimulate the cord, a metal (Tungsten) bipolar microelectrode (5μm exposed tip diameter, 50μm inter-electrode distance; Harvard Apparatus, Inc.) was pressed gently onto the cord surface (**Figure 4.3**). At each stimulation site, this microelectrode was used deliver single, monophasic current pulses at a stimulus value of 500 μA/50 μs, which corresponds with known thresholds for activating all myelinated afferent fibers in peripheral nerve (Thompson, King et al. 1990). For a subset of these experiments, current pulses at stimulus values corresponding to selective recruitment of large diameter myelinated axons (100μA/100μs) were also delivered(Thompson, King et al. 1990). For all experiments where responses could be mistaken for stimulus artifact, polarity was reversed on the bipolar microelectrode to verify that the observed responses were not dependent on stimulus polarity.

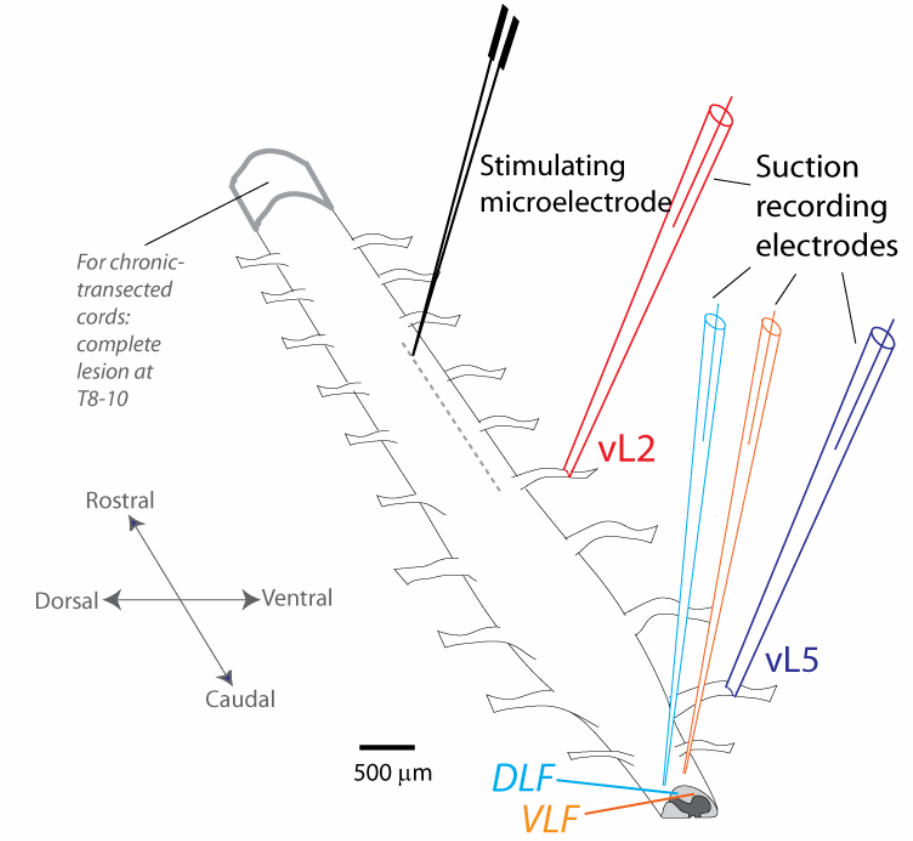

Figure 4.3: Setup for *in vitro* electrophysiological studies of the isolated, hemisected cord (chronic-transected vs. intact/control).
A tungsten bipolar stimulating electrode was used to stimulate the surface of the isolated, hemisected, *in vitro* spinal cord. Shown is placement of the stimulating electrode on the VLF at a site equidistant to the T12 and T13 root exit points (we call this site the T12 VLF for the remainder of the paper). Suction electrodes were used to record evoked responses at four locations; electrodes at ventral roots L2 (vL2) and L5 (vL5) record motor activity in motoneuron populations that are predominantly flexor and extensor-related respectively; small suction electrodes are also used to record the compound actions potential (CAPs) in the VLF and DLF at the L6 lumbar segment.

Motor outputs evoked from surface stimulation were recorded via ventral root electroneurograms (ENGs) at segmental levels L2 and L5, which have been shown to correspond to recruitment of hindlimb flexor (L2) and extensor (L5) motor activity(Kiehn and Kjaerulff 1996). Ventral root recording was accomplished via bipolar glass suction electrodes (90-150 μm internal diameter glass, silver chlorided wire differential recording). To measure activation of surface axonal tracts, two glass recording suction electrodes (40-60 μm internal diameter) were placed on the DLF and VLF surfaces at segmental level L6. For all electrophysiology experiments, a reference ground electrode was placed in the bath near the caudal end of the spinal cord. Prior to all surface-stimulation protocols, a glass stimulation electrode (70-120 μm internal diameter) was placed on dorsal roots at L2 and L5 to test for evoked segmental reflexes (500 μA/50 μs). The presence of long-lasting responses to dorsal root stimulation was not uncommon, and correlates with what has been observed in other studies using chronically-spinalized animals (Li, Harvey et al. 2004).

Initial experiments were performed to determine the extent to which T12 VLF stimulation focally activates axonal tracts for eliciting L2 and L5 motor output. A metal rigid microelectrode was used to stimulate the VLF, DLF, and LF at exactly halfway between thoracic levels 12 (T12) and 13 (T13). (**Figure 4.4**). The locations at which to stimulate these three adjacent funiculi were determined by measuring the distance from dorsal midline to ventral midline of the *in vitro* hemisected cord via a calibrated grid reticule. The DLF, LF, and VLF stimulus locations were determined so that DLF stimulus location was one-fourth, the LF location was one-half, and the VLF location was three-fourths the distance from dorsal midline to ventral midline. Results from these data (n=3 transected cords) confirm that stimulation of the T12 VLF most reliably evokes a combined L2 and L5 motor output when compared to the T12 DLF and T12 LF.

The focal involvement of T12 VLF axonal tracts (versus other proximal, potentially lower-threshold axons) in activating L2 and L5 circuitry was further confirmed by stimulation of tracts 200 μm to the left and right of the T12 VLF (**Figure 4.5**). For a total of 4 chronic-transected cords, the micro-electrode was placed at the T12 VLF and at sites 200 μm immediately dorsal and ventral to the T12-VLF (MO-10 One-axis Oil Hydraulic Micromanipulator, Narishige International USA). Results from these experiments indicate that stimulating 200 μm closer to the dorsal aspect of the cord elicits a significantly smaller vL2 response (mean L2 response strengths of 0.018 μV*ms for chronic-transected cords, 0.003 μV*ms for control cords, paired student's T-test assuming equal variance, p-value < 0.01). The vL5 response is also significantly reduced when the stimulus location is moved 200 μm closer to the ventral aspect of the cord (mean L5 response strengths of 0.050 μV*ms for chronic-transected cords, 0.017 μV*ms for control cords, paired Student's T-test assuming equal variance, $p < 0.01$). These results confirm that stimulation within 200 μm of T12-VLF is necessary to evoke the observed spinal motor outputs, which is consistent with the observation of Magnuson and colleagues in their studies of VLF stimulation-evoked motor responses in the neonatal rat (Magnuson and Trinder 1997).

As a final confirmation of the involvement of focal axonal tracts in the T12 VLF in eliciting the observed L2/L5 motor responses, experiments were performed on 4 chronic-transected cords evaluating the T12-VLF evoked responses at vL2 and vL5 prior to, and then following, isolation of the lateral-funicular white matter (**Figure 4.6**). Following recording of pre-tract isolation responses, isolation of the ventrolateral portions of the cord existing rostral to L1 was performed using small diameter insect pins. Viability of segments caudal to these isolated tracts was confirmed via evoked segmental reflexes. Following isolation, exact re-positioning of the stimulating microelectrode on the T12 VLF was accomplished using a calibrated microscope grid

reticle that enabled recording of the distance coordinates of this site in relation to the L2 segment's dorsal and ventral roots prior to isolation.

Shown in the right column of **Figure 4.6** are the four tested spinal cords with approximate locations of isolated white matter tracts, which were fixed in 2% paraformaldehyde (0.1M phosphate, pH 7.4) and later measured using a calibrated microscope grid reticle. In the top two cords, evoked responses were essentially unchanged. For the bottom two cords, on one occasion evoked responses increased and on one occasion decreased. These results, while preliminary and limited to the variability of the region of tract isolated, indicate that stimulation of tracts immediately subadjacent to the T12-VLF surface is sufficient for activated the observed spinal motor outputs at L2 and L5.

The remainder of electrophysiology experiments used a single rigid bipolar electrode to further explore the capabilities of the T12 VLF to evoke motor outputs, using sub-procedures that are described in conjunction with their experimental results.

Signal Conditioning and Analysis

Extracellular responses were amplified by 10,000, band-pass filtered at 300 Hz to 30 kHz, sampled at a minimum of 2 kHz, and recorded using pClamp data acquisition software (MDS Analytical Technologies, formerly known as Axon Instruments). Seven to ten trials were recorded for a given stimulus source and current intensity. Data were analyzed post-experiment using custom MATLAB routines. The strength of evoked responses for both CAPs and ventral-root responses was quantified by rectifying and integrating the signal for the time window of 100 ms post-stimulus, starting immediately after the end of a given stimulus artifact. To adjust for baseline noise, 100 ms worth of rectified, integrated pre-stimulus recording was subtracted from each value.

The time to onset and duration of a given response was also calculated using a custom MATLAB routine. The detection algorithm used a combination of threshold

detection and time windowing to identify the onset and offset of a given response. Visual verifications of response onset and offset values were performed for each trial used in analysis, and the consistency of response across trials was verified visually. Values for delay and duration of evoked response were subsequently used, in combination with distance measurements, to calculate axonal fiber conduction velocities.

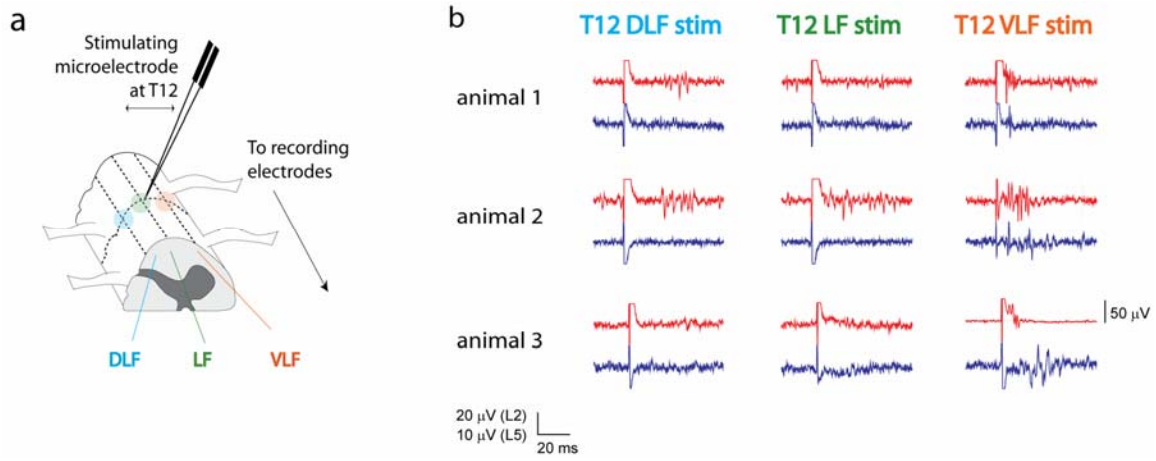

Figure 4.4: At segmental level T12, VLF stimulation was most effective at eliciting a combined ventral root L2 and L5 response, as compared to T12 DLF or T12 LF stimulation.
a. The schematic shows the three stimulation sites investigated, all at T12 and all in the chronic-transected cord (n=3 chronic-transected cords).
b. For each animal, example responses are shown. VLF stimulation-evoked responses in both L2 and L5 ventral roots were greater than those evoked following stimulation of the LF or DLF.

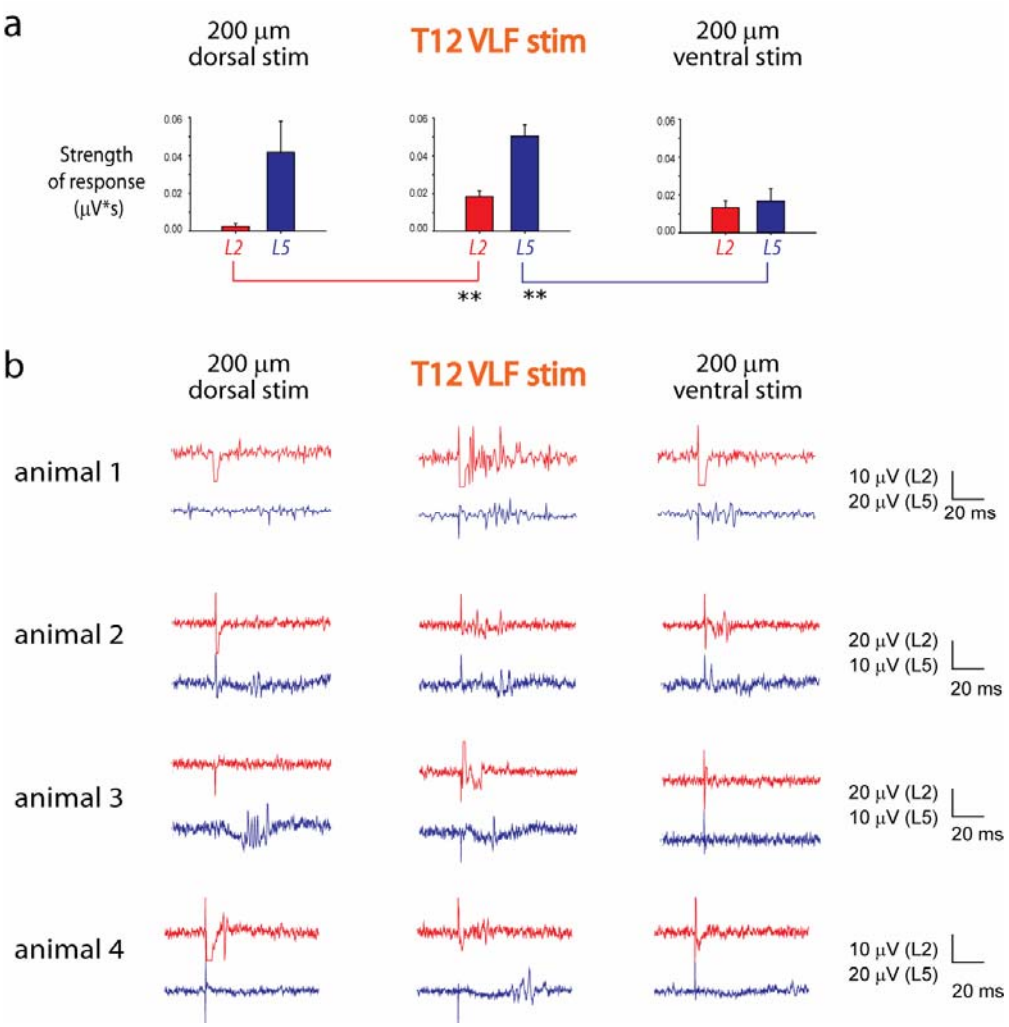

Figure 4.5: Stimulating within 200 µm of the T12 VLF stimulus site does not activate similar L2/L5 motor outputs.

a. Positioning of the stimulating micro-electrode in 200 µm in either lateral direction of the T12 VLF did not evoke combined ventral root L2/L5 responses of similar strengths (n=4 chronic-transected cords). Strengths of evoked responses for both CAPs and ventral-root responses were quantified by rectifying and integrating response signals for the time window of 100 ms post-stimulus, starting immediately after the end of a given stimulus artifact. To adjust for baseline noise, 100 ms worth of rectified, integrated pre-stimulus recording was subtracted from each value. Movement of stimulating electrode 200 µm closer to the dorsal column resulted in a significant reduction in the L2 response (paired student's T-test, ** indicates $p < 0.01$), whereas movement of the stimulating electrode 200 µm closer to the ventral aspect caused a significant reduction in the L5 response (paired student's T-test, ** indicates $p < 0.01$).

b. Example traces of stimulation responses for the four studied chronic-transected spinal cords are shown.

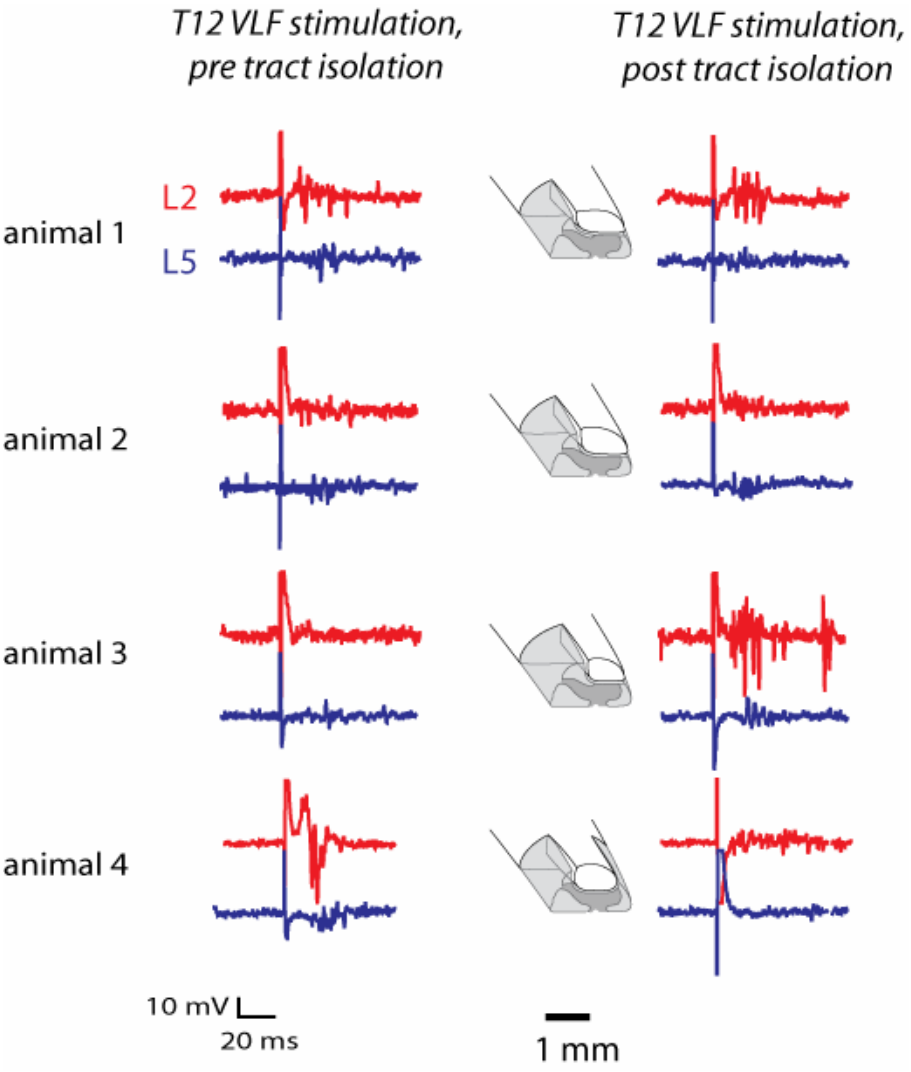

Figure 4.6: Surface stimulation of the isolated white matter subadjacent to T12 VLF is potentially sufficient for eliciting the observed L2/L5 stimulus-evoked response. The spinal cords of 4 chronic-transected animals were tested. Ventral root L2 and L5 responses to T12 VLF stimulation were elicited prior to, and then immediately following, isolation of the white matter tracts immediately below the T12 VLF. The extent and location of isolated tract was measured post-experiment, and are shown above. Tract isolation extended three spinal segments (T12 to L1, inclusive). For animals 1 and 2, evoked responses were essentially unchanged. For animal 3, the evoked responses increased post-isolation and for animal 4 the post-isolation evoked responses decreased. The variability in depth of the tract isolations should be noted, and may account for the variability in these preliminary results.

Lipophilic Dye Labeling and Analysis

In parallel studies, we used lipophilic dye labeling to investigate the projections of axons traveling in distinct white matter tract regions of the chronic-transected cord. First, animals were anesthetized, cords were isolated, and then preserved in 2% paraformaldehyde fixative. Cords were then suspended in agarose gel and labeled with the carbocyanine dye DiI. Crystals of DiI were placed at the cut surface of the VLF, LF, DLF, and VF at rostrocaudal levels T12, L4, and S1 (n = 24 control, 24 chronic-transected cords). (**Figure 4.7a**). Following dye migration, imaging studies initially focused on identifying which gray matter populations projected in the T12 VLF white matter in transected spinal cords vs. control cords (**Figure 4.7b**).

Dye was given 90 days to migrate fully, whereupon 100μm thick cross-sections of the cord were then imaged via fluorescent microscopy using the software program Neurolucida. Virtual slicing of the 100μm slices into 10 - 15 μm thick cross-sections was performed and the fluorescent labeling photographed for later reconstruction and cell counting using Neurolucida software. Labeled propriospinal neurons were hand counted and the results tabulated in Excel. Examples of dye placement and individual cell labeling are presented (**Figure 4.7c**), and demonstrate that DiI labeling of axonal tracts is capable of labeling individual cells with high-resolution. This precision allows for morphological analyses of the populations labeled via their axonal projections.

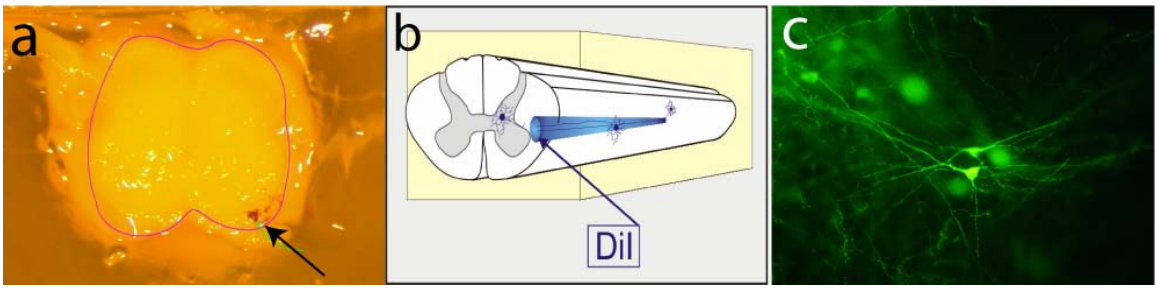

Figure 4.7: Axonal tract tracing procedure.
a. Spinal cords of p14-15 rats were fixed in 2 % paraformaldehyde (0.1M phosphate, pH 7.4), embedded in agar then sectioned at the T12 thoracic segment. Crystals of the carbocyanine dye DiI were placed at the cut surface of the VLF, LF, DLF, and VF at rostrocaudal levels T12, L4, and S1 (n = 24 control, 24 chronic-transected cords). Shown is labeling at the T12 VLF (at arrow).
b. DiI inserts into cell membranes and slowly diffuses both anterogradely and retrogradely throughout the projection territory of the dye-contacted axon (including to cell bodies and dendrites). Three months following crystal placement, the spinal cord was serially sectioned and the fluorescent labeling photographed for later reconstruction and cell counting using Neurolucida software.
c. Images of labeled cell membranes demonstrate that DiI axonal tract tracing method labels cells with satisfactory precision.

Results

Three major findings were obtained from the above experiments. First, it was determined that focal surface stimulation of the T12 VLF in the chronic-transected cord is capable of reliably activating ipsilateral L2 and L5 motor outputs that are of greater strength than those evoked in the intact (control) cord. Secondly, we found that T12 VLF stimulation also evokes longer-duration (>30 ms), synaptically-mediated surface compound action potentials caudal to L2/L5 motor neurons. Finally, we determined that the chronic-transected cord's L2/L5 responses to T12 VLF stimulation can be facilitated for creation of more complex, potentially rhythmic motor outputs. These findings demonstrate that the T12 VLF in the chronic-transected cord is a promising site for tapping into hindlimb-associated motor circuitry.

Part 1: Stimulation of the T12 VLF in the chronic-transected cord evokes a reliable, asynchronous response in L2 and L5 motor neuron populations.

Experiments were conducted to compare the response of spinal motor circuitry to T12 VLF stimulation in chronic-transected vs. non-transected cord (n=10 chronic-transected cords, 6 control cords). The T12 VLF was stimulated using 500 μA, 50 μs stimulus pulses (rectangular). Responses were recorded in the L2 and L5 ventral roots and at the L6 VLF. Response strengths were quantified by measuring the area under the rectified signal for duration of 100 ms immediately following stimulus artifact. To account for baseline activity, a similar area underneath the rectified signal was also measured prior to stimulus and subtracted from the response value.

We found that surface stimulation of the T12 VLF in the chronic-transected cord evokes stronger L2 and L5 motor outputs than those evoked by T12 VLF stimulation of control cords (**Figure 4.8**). Comparison of means using student's T-test (two-tailed distribution, assuming equal variance) shows that this difference in response strengths is

statistically significant (0.070 μV*ms vs. 0.029 μV*ms at L2, 0.036 μV*ms vs. 0.009 μV*ms at L5, p-values < 0.01).

To compare the overall responsiveness and viability of chronic-transected vs. control cords, reflexes were evoked at segmental L2 (dorsal root L2 stimulus pulse of 500 μA, 50 μs, rectangular) (**Figure 4.8c**). When baseline activity was accounted for, the average strength of evoked L2 reflexes was not greater for the chronic-transected cords. This indicates that the larger T12 VLF stimulus-evoked L2/L5 responses measured in the chronic-transected cords were not due to a global increase in responsiveness to stimulation in the tested chronic-transected cords.

In chronic-transected cords versus control cords, strength of T12 VLF stimulus-evoked response recorded at the L6 VLF was also greater (**Figure 4.9**, 7 chronic-transected cords and 3 intact cords measured). A comparison of means using Student's t-test shows that this difference in response strengths is statistically significant (mean of 0.22 μV*ms for chronic-transected cords, 0.15 μV*ms for control cords, student's T-test, two-tailed distribution assuming equal variance, p-value < 0.05). DLF CAP responses remained relatively unchanged and relatively weaker than the evoked VLF CAP response for both chronic-transected and control groups.

The observed T12 VLF stimulus-evoked responses at L2 and L5 displayed a consistent pattern, with the L2 response occurring earlier and lasting longer than the evoked L5 response (**Figure 4.10**, n=10 chronic-transected cords). Assuming a minimum synaptic delay of 2-3 ms (Meinck 1976), the latency-to onset of the evoked stimulus-responses leaves ample time for multi-synaptic activation of spinal circuits. Additionally, the fact that the activation of L2 and L5 motor neurons is non-synchronous suggests the possibility that we can tap into the reciprocally-inhibitory properties known to exist between flexor- and extensor-related motor neurons to evoke sustained alternating L2/L5 activity.

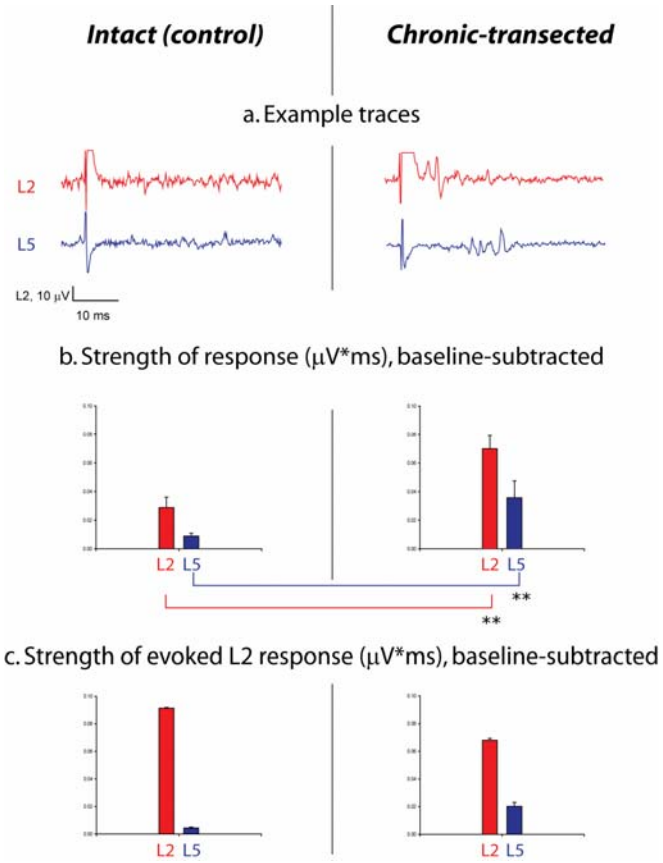

Figure 4.8: Chronic-transected vs. control animals: T-12 VLF stimulation evokes a combined L2/L5 response that is stronger in chronic-transected vs. control cords.
a. Example evoked responses. A total of 10 chronic-transected cords and 6 intact cords were stimulated. The T12 VLF was stimulated using 500 μA, 50 μs stimulus pulses (rectangular). Responses were recorded in the L2 and L5 ventral roots and at the L6 VLF.
b. Response strengths at L2 and L5 were quantified by measuring the area under the rectified response signal for duration of 100 ms immediately following stimulus artifact. To account for baseline activity, a similar area underneath the rectified signal was also measured prior to stimulus and subtracted from the response value. Comparison of means using student's t-test show that both the L2 and L5 evoked response strengths are significantly stronger in chronic-transected cords (** denotes $p < 0.01$).
c. As a comparison of overall responsiveness of chronic-transected vs. control cords, reflexes were evoked at segmental L2 (dorsal root L2 stimulus pulse of 500 μA, 50 μs, rectangular). The average strength of evoked L2 reflexes was not greater for the chronic-transected cords. This indicates that the larger evoked L2/L5 responses measured in the chronic-transected cords were not necessarily due to a global increase in responsiveness in chronic-transected cords.

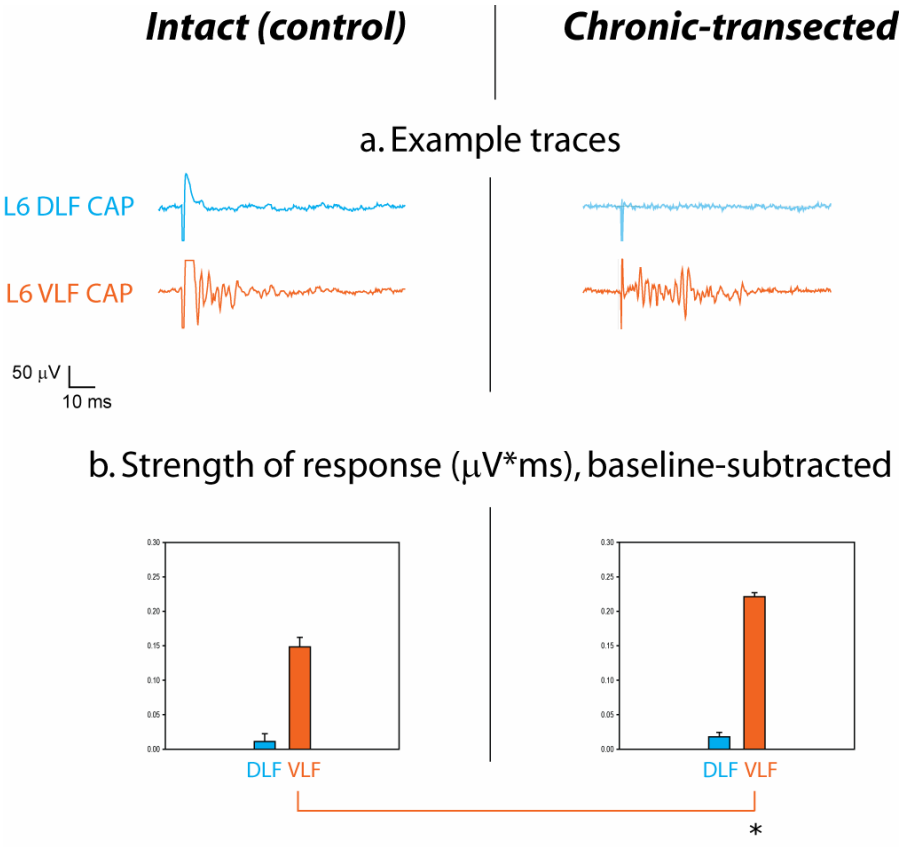

Figure 4.9: T12 VLF stimulus-evoked compound action potentials at segmental level L6 VLF are larger in chronic-transected cords.
a. Example evoked responses. A total of 7 chronic-transected cords and 3 intact cords were investigated. The T12 VLF was stimulated using 500 µA, 50 µs stimulus pulses (rectangular). Compound action potential (CAP) responses were recorded on the L6 VLF and L6 DLF surfaces and are shown above.
b. Comparison of mean responses (µV*ms) using Student's t-test shows that the chronic-transected cord responds with a significantly stronger VLF CAP (* denotes $p < 0.05$). DLF CAP responses remained relatively unchanged and relatively weaker than the evoked VLF CAP response for both chronic-transected and control groups.

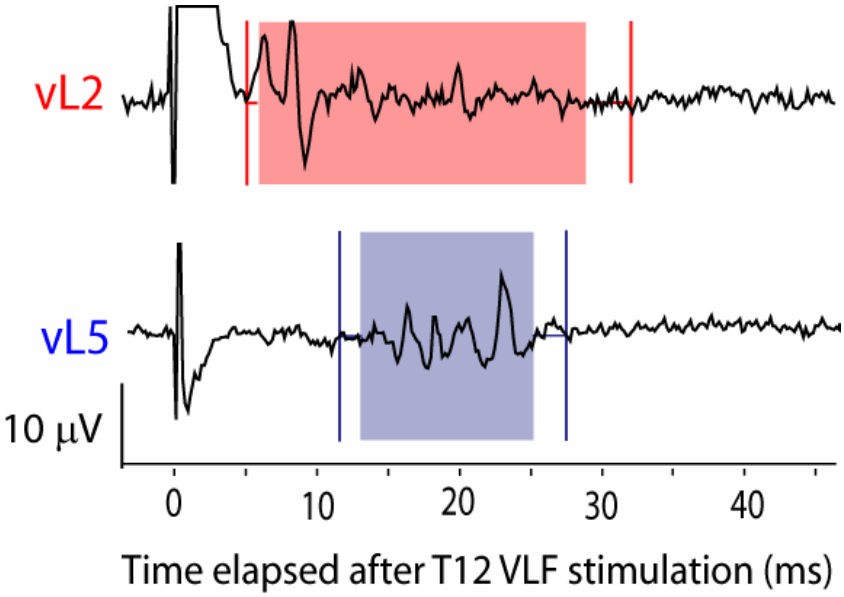

Figure 4.10: T12

VLF stimulation in the chronic-transected cord reliably evokes non-concomitant ventral root L2 and L5 responses.
Histogram bars with standard errors are shown for the average latency-to-onset and duration of evoked ventral root L5 (top) and L2 responses to stimulation of the T12 VLF (a total of 10 chronic-transected cords). Example traces from one of the ten studied cords overlay the reported averages.

Part 2: T12 VLF stimulation activates spinal circuitry at locations known to be significant to hindlimb motor coordination.

Additional experiments were performed to study the anatomical location of neurons and axons responding to T12 VLF stimulation. Information on the location and synaptic involvement of the activated circuits was then compared with what is known concerning known spinal systems within these regions. Such information serves as necessary starting points for the identification of the neuronal populations activated by T12 VLF stimulation in the chronic-transected cord.

The first series of experiments study the influence of T12 VLF stimulation on systems caudal to the activated L2 and L5 motor neurons. Ascending and propriospinal systems whose axons travel in the VLF from sites caudal to the L2/L5 motor neuron pools have known influence on hindlimb rhythm-generating circuitry (Lev-Tov, Delvolve et al. 2000; Dutton, Carstens et al. 2006; Reed, Shum-Siu et al. 2006). We investigated whether T12 VLF stimulation, when compared with T12 DLF and T12 LF stimulation, evoked compound action potentials in this region (**Figure 4.11,** n=7 chronic-transected cords). We found that surface stimulation of the T12 DLF evokes both L6 DLF and L6 VLF CAPs, which indicates that axonal populations traveling in both regions are activated by stimulation of the T12 DLF. Stimulation of the T12 LF evokes less of a L6 DLF but a similar-magnitude L6 VLF response, whereas stimulation of the T12 VLF evokes L6 VLF CAPs only. This suggests that stimulation of the T12 VLF is most successful in selectively activating the axons traveling in the L6 VLF.

Further investigation into the nature of the activated L6 VLF CAPs was performed to determine its synaptic contributions. This information is an important first step in identifying the activated spinal circuits. Results in **Figure 4.12** show that replacement of the aCSF with a high Mg^{2+}, low Ca^{2+} (synaptic transmission blocking) bath results in strong reduction of later components of the T12-VLF evoked L6 VLF

CAP response. This confirms that synaptic actions are involved in the observed responses. Synaptic activation may explain why L6 VLF CAP strength was similar regardless of funiculus stimulus site at T12.

Unique, non-rhythmic spiking activity, both spontaneous and in response to T12 DLF stimulation, was observed in recordings at the L6 DLF (n=6 total chronic-transected cords). This activity was influenced by stimulation (**Figure 4.13a**) but was also observed to occur spontaneously (**Figure 4.13b**). This activity was also recorded to a lesser extent at the L6 LF (n=3 out of 6 cords investigated), but was not seen on the L6 VLF for any of the studied cords. Axons transmitting signals in the L6 DLF include those that report on systems that experience hyperexcitability and/or spasticity following injury (Norton, Bennett et al. 2008). These results, while preliminary, suggest that we may have found a surface recording site that reports such behavior in chronic-transected cords.

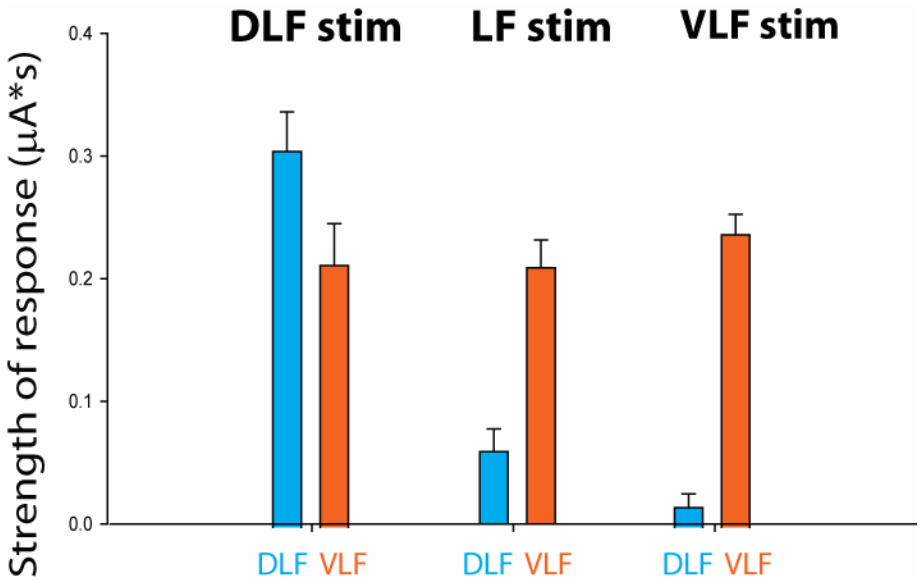

Figure 4.11: Stimulation of the VLF, LF, and DLF at segmental level T12 evokes surface compound action potentials (CAPs) at segmental level L6.
Shown are average strengths of L6 CAP responses to stimulation of the T12 DLF, T12 LF, and T12 VLF (n=7 chronic-transected cords). Standard error bars are shown. Surface stimulation of the T12 DLF evokes both L6 DLF and L6 VLF CAPs, which indicates that axons in both regions are activated by stimulation of the T12 DLF. Stimulation of the T12 LF evokes less of a L6 DLF but a similar-magnitude L6 VLF response, whereas stimulation of the T12 VLF evokes L6 VLF CAPs only. CAP strength was measured by calculating the area under the rectified response signal for duration of 100 ms immediately following stimulus artifact. To account for baseline activity, an area underneath 100 ms of rectified signal prior to stimulus measured prior and subtracted from the response value.

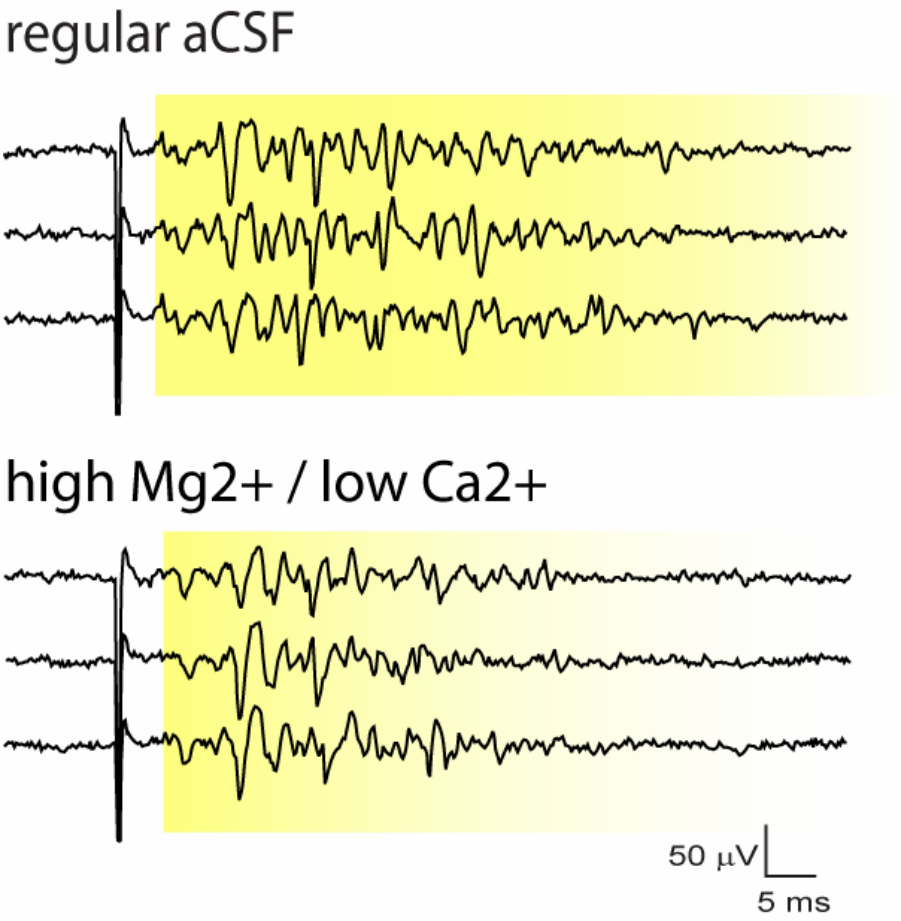

Figure 4.12: L6 VLF Compound action potential responses to stimulation at the T12 VLF, before and after synaptic transmission blockade.
Shown are 3 raw records of the evoked CAP in one animal before (top) and after minimizing synaptic transmission by exchange into a high Mg^{2+}/low Ca^{2+} aCSF (bottom). Longer latency events were lost when synaptic transmission was blocked. This demonstrates that a fraction of evoked events in the VLF occur via synaptic activation of spinal neurons with axons in the L6 VLF. Synaptic activation may explain why L6 VLF CAP strength was similar regardless of funiculus stimulus site at T12 (as shown in **Figure 4.11**).

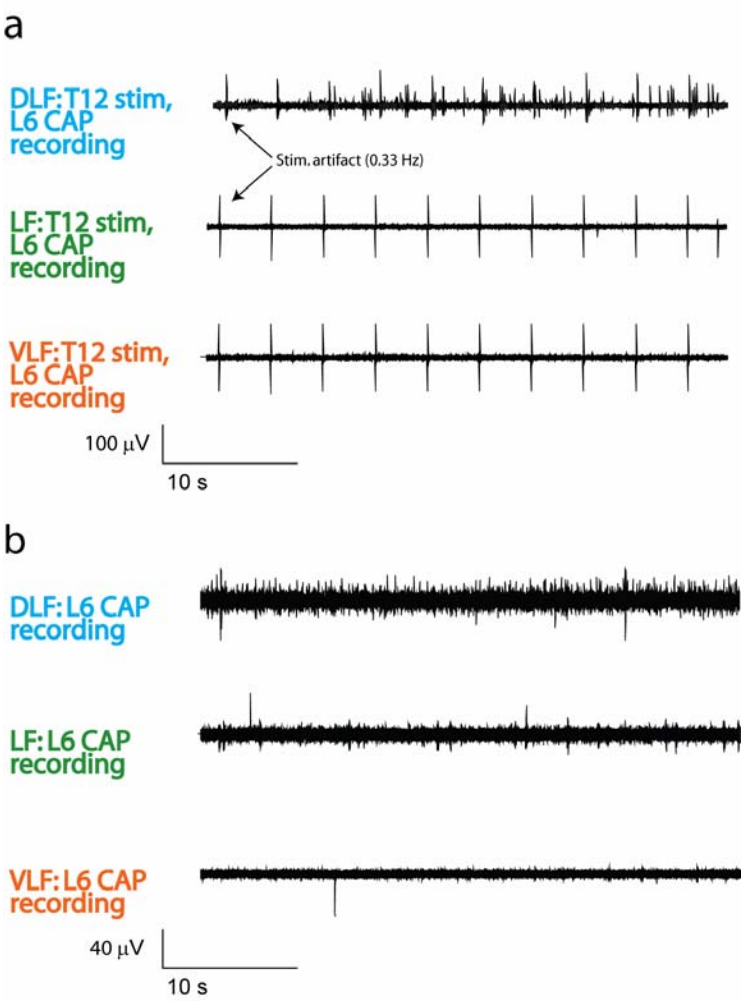

Figure 4.13: Recordings on the L6 DLF surface report spiking behavior in chronic-transected cords.
a. Shown are example compound action potential responses from stimulation at T12 at the DLF, LF, and VLF (n = 6 total chronic-transected cords). Shorter-term compound action potential responses were observed at each site but are not visible on the presented timescale. Stimulation of the T12 DLF consistently elicited longer-lasting, spiking behavior recorded at the L6 DLF.
b. Spontaneous activity was also recorded in chronic-transected cords at the L6 DLF (n=6 out of 6 cords investigated). This activity was also recorded to a lesser extent at the L6 LF (n=3 out of 6 cords investigated). This activity was not seen on the L6 VLF for any of the studied cords.

The location and number of propriospinal neurons labeled via lipophilic dye placement at the T12 VLF was then determined (**Figure 4.14**). For the two intact cords labeled at T12 VLF, a total number of 59 and 139 cells were labeled; for the two chronic-transected cords labeled at T12 VLF, a total number of 30 and 33 cells were labeled. In all four cases, the majority of labeled cells were found in the lower-thoracic or upper lumbar regions of the cord, and none extended beyond the lumbar enlargement. In analysis in other labeled tracts (data not shown), dye migration after 3 months was shown to continue beyond 10 segments, so it is not suspected that the observed terminations were a limitation of migration time.

The percentage of cells counted in each of the ipsilateral and contralateral gray matter lamina is shown in **Figure 4.15**. In both transected and control cords, T12 VLF-labeled axons arose predominantly from intermediate spinal cord regions (deep dorsal horn and intermediate gray). These labeled populations indicate that T12 VLF stimulation may access spinoreticular sensory-motor neurons (Danziger, Remy et al. 1996; Jordan 1998; Reed, Shum-Siu et al. 2008). However, populations were also labeled in the superficial dorsal horn, which is a region that contributes to pain sensation (Fields and Basbaum 1978). While both chronic-transected and control cords showed labeling in both of these areas, the rostro-caudal location, number and distribution of labeled neurons was distinct between chronic-transected versus control cords.

A total of 24 total locations in the chronic-transected and control spinal cords were labeled with axon-tracing dye. The reported results represent a subset of this total number of sites initially labeled. Over half of these cords have yet to be imaged, and will be described in future reports on this work as ongoing data acquisition and analysis continues. When completed, these results of may provide important insight into the nature of changes in axonal projection patterns in ascending and propriospinal systems in chronic-transected vs. intact cords.

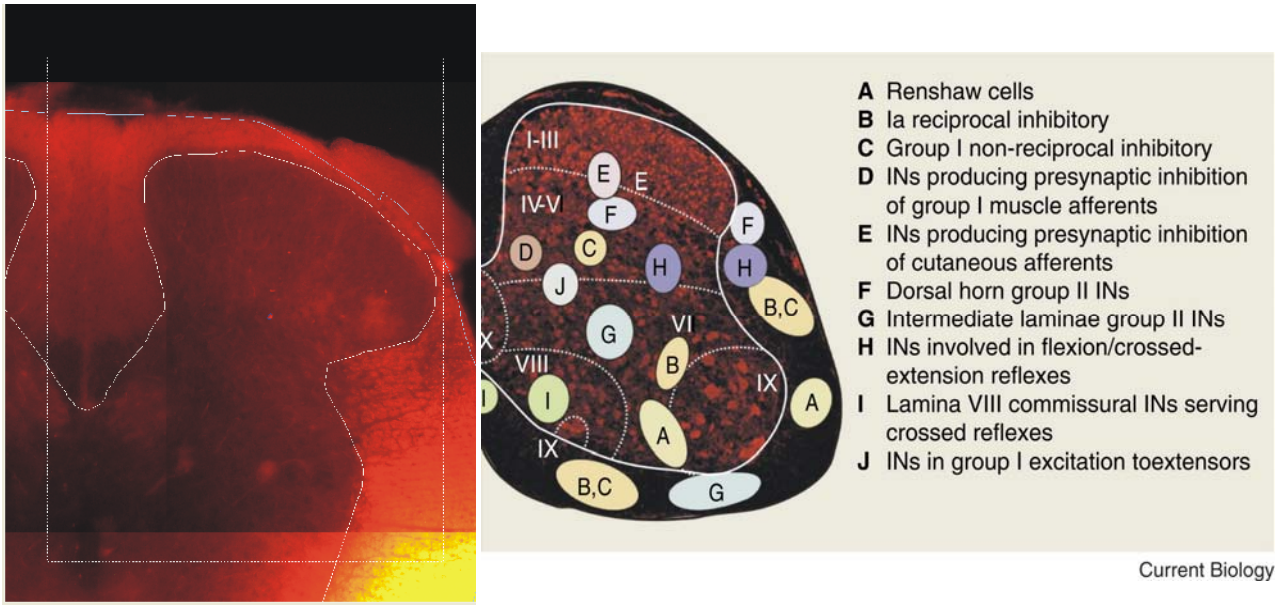

Figure 4.14 Imaging and analysis of dye-labeled axonal tracts.
Left: Example image showing dye-labeled neurons (small, bright dots) in the dorsal horn and intermediate region ipsilateral (and several segments caudal) to dye placement at the T12 VLF.
Right: The overall location of these labeled cells was quantified based on gray matter lamina. This schematic (Hochman 2007) summarizes the known locations of propriospinal populations within the different lamina, as well as in different white matter tracts.

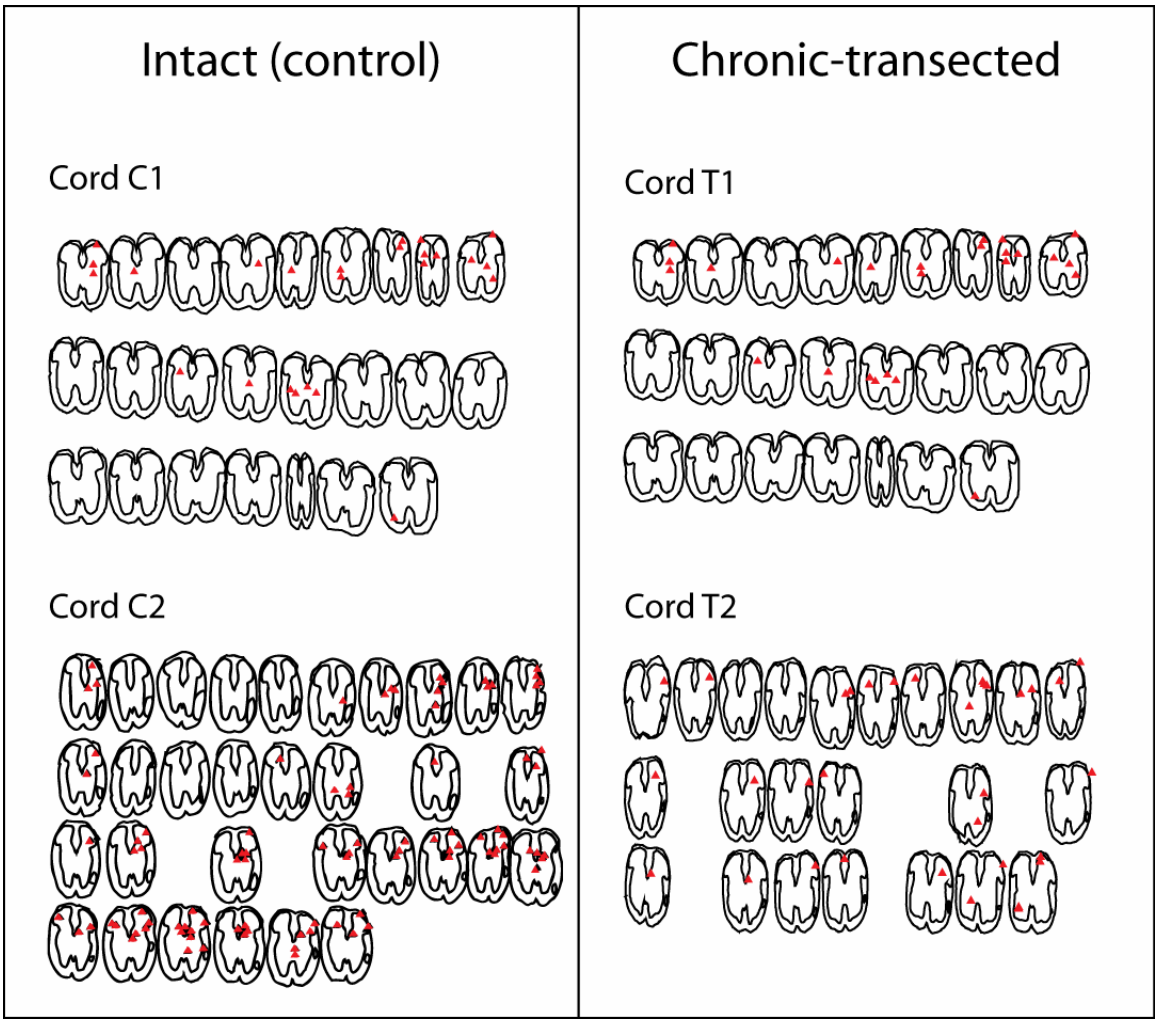

Figure 4.15: Location of propriospinal neurons with axons traveling in the T12 VLF.
Three-dimensional renderings showing the location of propriospinal neurons whose axonal projections were labeled via lipophilic DiI placement in the T12 VLF. The two left renderings are of control (intact) spinal cords (Cord C1 and Cord C2), and the two right renderings are of chronic-transected cords (Cord T1 and Cord T2).

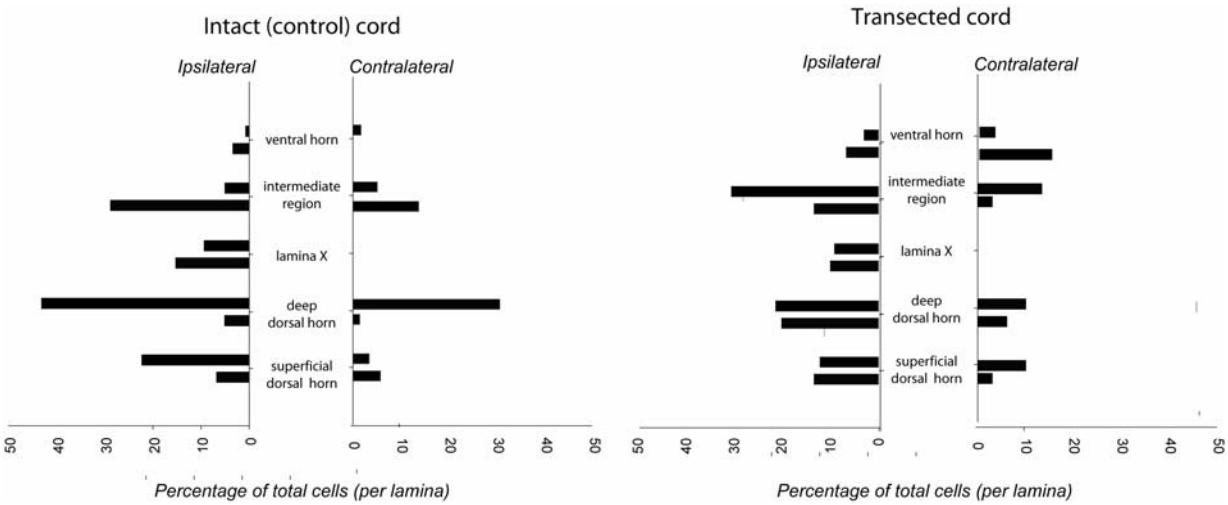

Figure 4.16: Distribution of neurons with axons that travel in the T12 VLF, grouped by lamina.
Total numbers of labeled cells in each lamina are shown for the transected (n=2; left) and control cords (n=2; right). Neuron number is presented as fraction of the total population and represents total neuron counts from caudal thoracic and rostral lumbar spinal segments.

Part 3: T12 VLF stimulus-evoked responses are responsive to spatial, pharmacologic, and temporal facilitation.

The contribution of T12 VLF stimulation to motor circuits at segmental level L2 was then studied. This region of the cord has been shown to contain critical circuitry for the initiation of fictive locomotor activity(Cazalets, Borde et al. 1995). Results from these studies (n = 4 chronic-transected cords) (**Figure 4.17a**) indicate that stimulation of the chronic-transected cord at T12 VLF is capable of spatial facilitation via stimulation of L2 afferents. The observed non-linear summation of the independent stimuli suggest that the observed facilitation involves convergent actions on common interneurons. In comparison, the evoked response in the L6 VLF was depressed following L2 dorsal root conditioning stimulation, which suggests inhibitory interactions. The potential for focal T12-VLF stimulation to evoke alternating flexor- and extensor- associated motor activity, when combined with sensory afferent activation, is also shown (**Figure 4.17b**).

Temporal facilitation of the T12-VLF evoked response was also demonstrated in all cords for which pulse trains were delivered (n = 5 chronic-transected cords, **Figure 4.18** and **Figure 4.19**). Compared to single pulses, double-pulse stimulation of the T12 VLF facilitates motor activity and response in the L6 VLF (**Figure 4.18**), which indicates that some synaptic actions are subthreshold and can only be accessed via T12 VLF stimulation when multi-pulse protocols are applied. **Figure 4.19** shows evoked responses to 15 pulses at 10 Hz and 25 pulses at 50 Hz that demonstrate that the activated circuitry does not fatigue readily and that, at 50 Hz, pulse trains at T12 VLF incites persistent post-stimulus firing.

The potential for pharmacologic facilitation of the evoked T12-VLF response using 20 μM serotonin (5HT) is also presented (**Figure 4.20**). In these experiments, 5HT was bath-applied and enhancement of the T12-VLF evoked responses at vL2 and vL5 was observed (n=4 chronic-transected animals). These results demonstrate that

stimulation of the chronic-transected cord at T12-VLF can be enhanced via serotonin, and suggests that future protocols that combine electrical stimulation of this site with pharmacological stimulus protocols may have synergistic effects for activation and refinement of motor output.

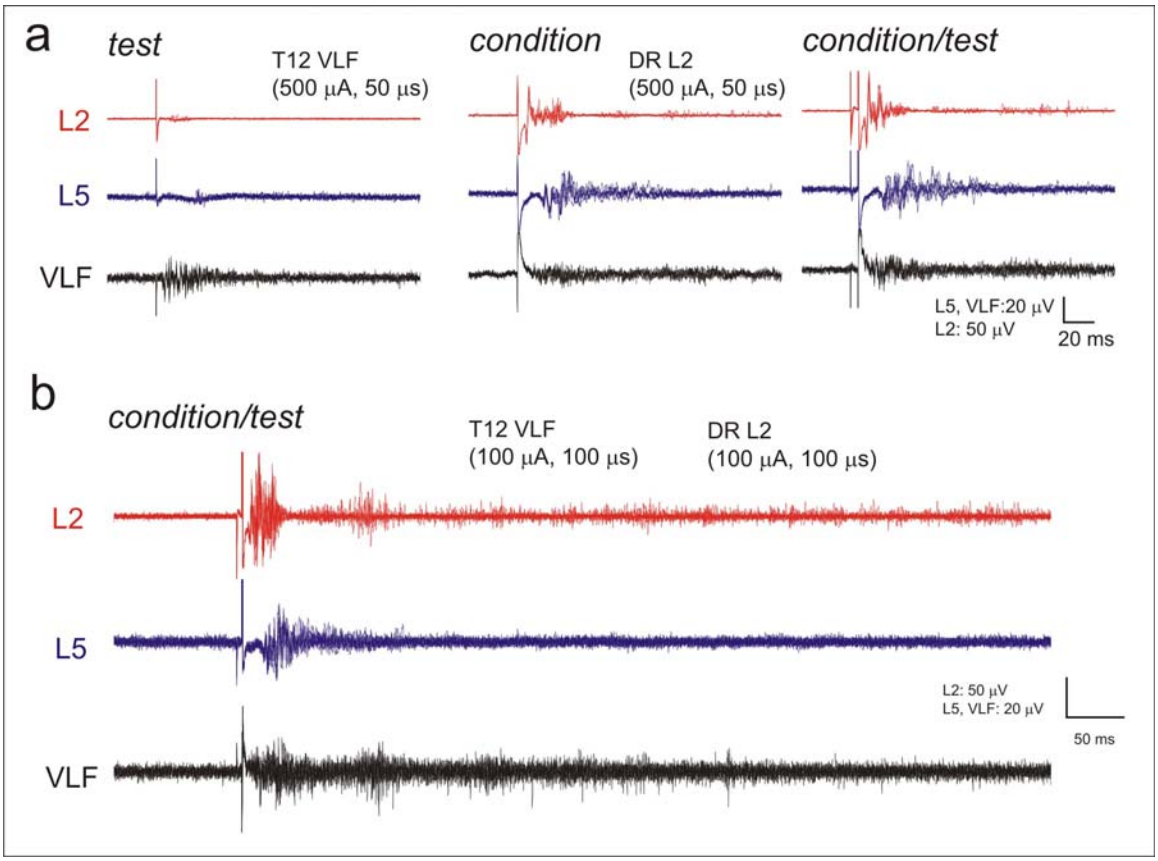

Figure 4.17: Spatial facilitation (via sensory co-stimulation) evokes a facilitated response that can include rhythmic patterns.
a. Evoked responses are shown in L2 and L5 ventral roots and L6 VLF following stimulation of the T13 VLF (left; test stimulus), the L2 dorsal root (middle; conditioning stimulus) or both (right; condition and test). Traces represent 5 raw records superimposed. Note that conditioned response in both nerve roots is greater than the sum of each independent evoked response, suggesting activation via common interneurons. In comparison, the evoked response in the L6 VLF was depressed following L2 dorsal root conditioning stimulation, supporting inhibitory interactions.
b. Another example of the condition test protocol that shows evidence of rhythmic evoked activity, particularly in the L2 VR and L6 VLF recordings.

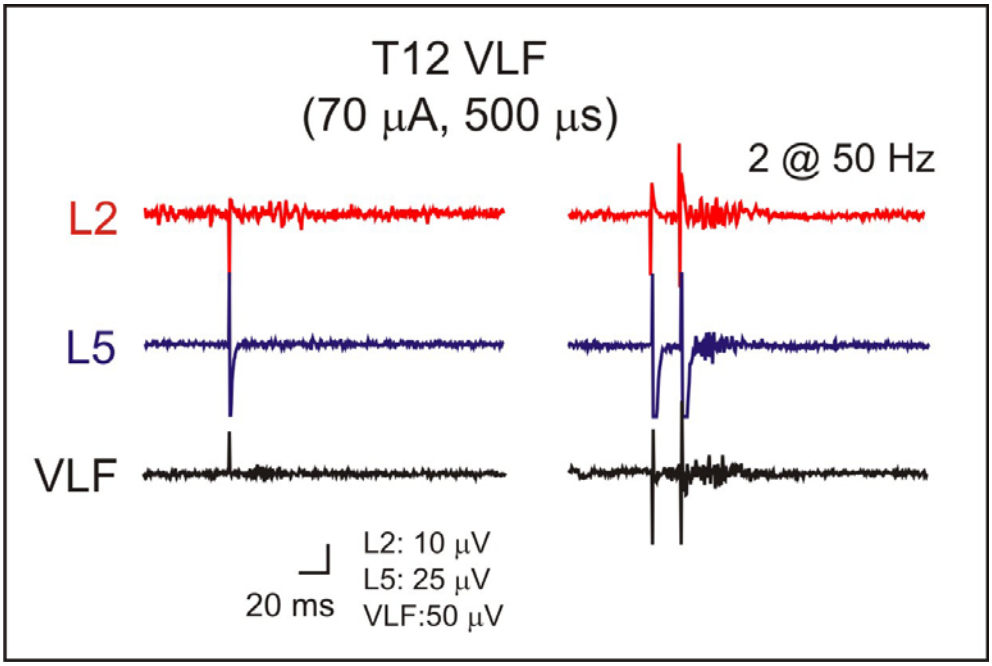

Figure 4.18: Temporal facilitation is achieved using multi-pulse stimuli at the T12 VLF.
a. Temporal facilitation of T12 VLF evoked activity is shown. Double pulse stimulation of the T12 VLF evokes responses in ventral roots L2 and L5 that were far greater than those evoked by single-pulse stimulus. Facilitated activity was also observed consistently in recordings at the L6 VLF surface (n=4 chronic-transected cords).

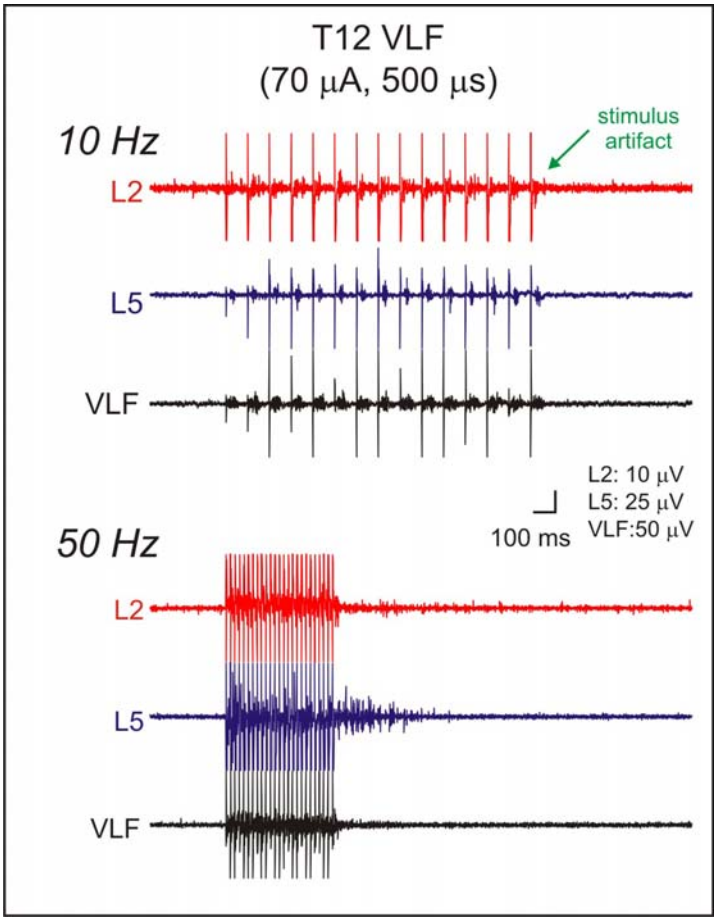

4.19: Temporal facilitation of T12 VLF evoked responses using pulse trains at 10 Hz and 50 Hz.
Top panel shows evoked responses to 15 pulses at 10 Hz, bottom panel is 25 pulses at 50 Hz. Large, constant amplitude responses are stimulus artifact. Note that comparable evoked responses are observed following each stimulus at 10 Hz. At 50 Hz, persistent firing is seen after stimulus terminations. Stimulus trains lasting as long as 10 seconds were tested with similar results.

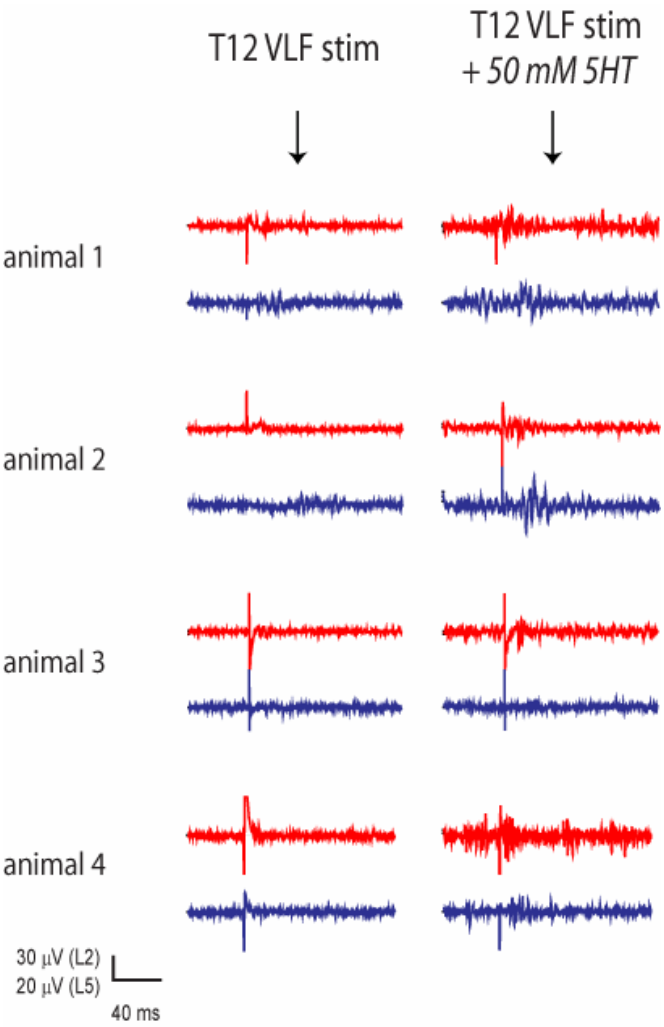

Figure 4.20: Bath application of Serotonin (5HT) facilitates T12 VLF-evoked motor activity.
Bath application of 5HT (20 µM) increased background activity in all recordings and evoked motor responses that were substantially facilitated.

Discussion

We have shown that T12 VLF stimulation of chronic-transected cords, produces significantly stronger responses from ventral root L2, ventral root L5 and the L6 VLF surface hen compared to intact control cords. In intact cords, both the VLF and the pre-lumbar enlargement are known to contain systems important for the activation of complex hindlimb motor output (Cazalets, Borde et al. 1995; Magnuson, Schramm et al. 1995; Kiehn and Kjaerulff 1998; Ichiyama, Gerasimenko et al. 2005). We hypothesized that, in spinal cords with chronic mid-thoracic transection, stimulation of the T12 VLF can be similarly used to tap into hindlimb-associated motor output. We verified our prediction that single-pulse stimulation at this site was capable of eliciting an asymmetric L2/L5 response. This demonstrates that the T12 VLF is a promising site for further investigation in the chronic-transected cord.

A potential explanation for why T12 VLF stimulation evokes larger responses in chronic-transected vs. intact cords is that, in the case of chronic-transected cords, descending tracts in the VLF, such as the reticulospinal, anterior spinocerebellar, and vestibulospinal tracts (Davidoff 1983), have degenerated post-SCI. With these tracts no longer taking up space on or near the T12 VLF surface, there might be improved surface stimulus access to remaining tracts. This hypothesis could be further tested through additional axon tract migration studies that identify the number and location of cell bodies whose axons travel through the T12 VLF in chronic-transected vs. intact cords. Such additional studies are described below in relation to current dye-labeling results.

Another explanation for the increased strength of L2, L5, and VLF CAP response to T12 VLF stimulation is that there might be an overall increase in excitability in the injured cord. Such increases in overall excitability are known to occur following SCI (Norton, Bennett et al. 2008). To account for this factor, however, we compared strengths of L2 ventral root response to L2 dorsal root stimulation. We found no increase in

average (baseline-subtracted) strength of L2 reflex response (**Figure 4.8c**), which suggests that the observed increases in responsiveness to T12 VLF stimulation were not specifically due to a global increase in responsiveness following SCI as recorded at segmental level L2.

We also found that T12 VLF surface stimulation in the chronic-transected spinal cord spinal includes activation of pathways caudal to L2 and L5 motor neuron pools, as reported by evoked CAPs in the L6 VLF. A subset of these observed CAPs in the L6 VLF was shown to result from Ca^{2+}-dependent synaptic actions in spinal neurons. Ascending and propriospinal systems whose axons travel in the VLF from sites caudal to the L2/L5 motor neuron pools have known influence on hindlimb rhythm-generating circuitry (Lev-Tov, Delvolve et al. 2000; Dutton, Carstens et al. 2006; Reed, Shum-Siu et al. 2006). The observed increase in recruitment of axons in the L6 VLF may also be influenced by an increased excitability of interneurons with axons in the VLF. As shown by Wall (Wall 1994), many axons in spinal cord white matter tracts are unmasked after $GABA_A$ receptor blockade. Alternately, some existing spinal axons may undergo plastic alteration in conduction velocity.

Recordings at the L6 DLF revealed unique, non-rhythmic spiking activity that was both spontaneous and in response to T12 DLF stimulation. This activity was also recorded to a lesser extent at the L6 LF (n=3 out of 6 cords investigated), but was not seen on the L6 VLF for any of the studied cords. Axons transmitting signals in the L6 DLF include those that report on systems that experience hyperexcitability and/or spasticity following injury (Norton, Bennett et al. 2008), so it is possible that the L6 DLF is reporting such behavior in chronic-transected cords. Future comparisons with L6 DLF recordings in intact cords would be an important first step in identifying this potentially novel reporter of spastic behavior in the chronic-transected cord.

Our lipophilic tract-tracing study results suggest that the T12 VLF contains axonal associated with propriospinal populations in both the dorsal horn and intermediate

regions of the spinal gray manner are activated by T12 VLF stimulation. These regions include those that have been labeled using biocytin tracing of tracts shown to evoke fictive locomotion in the neonatal rat (Antonino-Green, Cheng et al. 2002). It should be noted that, for both control and chronic-transected cords, DiI crystals labeled a smaller-than-expected total number of cells. It is thought that this is related to the placement of DiI crystals onto a very specific region of axons (an example of the degree of focal labeling can be seen in **Figure 4.7a** as it was at the time undetermined the degree of lateral spread this sort of dye labeling would incur). In the case in the 2 analyzed chronic-transected cords with DiI placement on the T12 VLF, a total of 30 and 33 cells were labeled. This is a small number in relation to the total number of 52,000 and 12,000 total propriospinal axons shown to travel in the lateral and ventral funiculi, respectively (Chung and Coggeshall 1983). Despite these limitations, our initial imaging studies were important in demonstrating the location of a subset of the axons activated by T12 VLF stimulation, and in showing preliminary evidence that the labeled cells were different for chronic-transected vs. intact cords.

In order to capture a more complete representation of the total number of axons activated by T12 VLF stimulation, cut tract resection techniques can be used to isolate the white matter in the T12 VLF prior to labeling. Results from preliminary use of this technique have been presented for use in electrophysiological studies (**Figure 4.6**). The DiI crystals can be dissolved in alcohol and pressure-injected through a large glass suction electrode encompassing the entire end of the isolated T12 VLF tract. In such a way, complete and consistent labeling of the cut end could be accomplished. It is expected that labeling the T12 VLF using this technique would provide a more thorough identification of cells with axons traveling through this funiculus.

The pattern of L2 (flexor-related) and L5 (extensor-related) motor neuron pools evoked by stimulation of the T12 VLF in chronic-transected cords was reliably asymmetric and asynchronous (**Figure 4.10**), but not strictly alternating. This indicates

that, while we appear to be activating the L2 and L5 motor neurons, but are not tapping directly into a system that involves ipsilateral inhibition between L2 and L5. T12 VLF stimulation evoked flexor activity (reported at lumbar level 2) followed by extensor activity (as reported by ventral root lumbar level 5), as might be expected in the case of low-level activation of rhythm-generating propriospinal circuitry, which is has been shown to be rostrocaudally driven (Kremer and Lev-Tov 1997). Further evidence concerning the rhythmicity of the motor outputs elicited by T12 VLF stimulation (potentially with longer-duration pulses or sensory co-stimulation) would have to be gathered before futher conclusions can be made.

It is thought that further studies that use pulse train stimuli at the T12 VLF might help uncover its potential to generate synergistic and/or rhythmic output. The reported successes for evoking rhythmic activity via surface stimulation all use trains of pulses, in comparison to the single-pulse stimuli used in the above investigations (Magnuson and Trinder 1997; Dimitrijevic, Gerasimenko et al. 1998; Saigal, Renzi et al. 2004; Ichiyama, Gerasimenko et al. 2005; Ichiyama, Gerasimenko et al. 2005; Guevremont, Renzi et al. 2006; Minassian, Persy et al. 2007) Additionally, other types of facilitation (spatial or pharmacological) might be applied in future studies of T12 VLF stimulation of the chronic-transected cord, as we have demonstrated that these methods are also effective in facilitating the evoked motor responses.

Taken together, the results from these studies support our hypothesis that single-pulse focal surface stimulation of the chronic-transected cord at T12 VLF can tap into hindlimb flexor- and extensor-related motor circuitry, and that the activated circuits can be potentially built upon to evoke synergistic, rhythmic output. The T12 VLF site has previously been difficult to selectively stimulate *in vivo*, but can be readily accessed (and stimulated in a focal manner) by the MEA technology presented in Chapter 2 and Chapter 3 of this thesis. We found in the above studies that effective T12 VLF surface stimulation required a minimum lateral spatial selectivity of 200 μm (**Figure 4.5**), which

is a spatial resolution achievable using current versions of our MEA electrode pattern (**Figure 3.5**). Further investigations that stimulate the chronic-transected cord's T12 VLF can therefore use this technology to access this, as well as other, surface locations *in vivo*. Findings from such work could make potentially significant contributions to the use of this more ventrally-located site for recovery of function post-SCI.

CHAPTER 5

DISCUSSION

Access to, and subsequent control of, spinal cord function is a critical consideration for design of optimal therapeutic strategies for SCI patients. Electrical stimulation of the spinal cord is capable of activating behaviorally-relevant populations of neurons for recovery of function, and is therefore an attractive target for potential devices. A promising method for accessing these spinal circuits is through their axons, which are organized as longitudinal columns of white matter funiculi along the cord exterior. For this thesis, I hypothesized that these funiculi can be selectively recruited via electrodes appropriately placed on the surface of the spinal cord for functional activation of relevant motor circuitry in a chronically-transected spinal cord.

Central to my hypothesis was that the motor outputs evoked through selective surface stimulation could occur via activation of propriospinal neurons via their white matter funiculi. These identified funiciuli are known to span over several segments and are active during locomotion (Jankowska 1992; Jankowska and Edgley 1993). A prediction, then, was that focal electrical stimulation of their axons in the white matter should actually be able to activate these same functional populations of interneurons distributed over several spinal segments. Because these interneurons coordinate motor output across hindlimb joints bilaterally (Baldissera, Hultborn et al. 1981; Jankowska 1992), organized motor patterns should be recruited by such stimuli.

The tandem design goal for my thesis was to fabricate and implement a conformable multi-electrode array (MEA) that would enable selective stimulation of the spinal cord surface. A current challenge among neural interfacing techniques is maximizing selectivity of activation while minimizing invasiveness and damage to the interfaced tissue. In this thesis, I proposed surface stimulation of axonal tracts as an

approach to achieving this balance for the activation of discrete pathways with actions on spinal cord functional systems.

In Chapter 2, I presented technique for stimulating surface tracts with an MEA that uses a conformable elastomer substrate in order to promote precise stimulus delivery to the cord surface. I use PDMS as my MEA electrode substrate not only because of its superior elasticity but also its well-characterized biocompatibility and recent developments in microfabrication capabilities. I described a new, scalable, fabrication process for creating a high electrode density, elastic MEA on PDMS substrate, which I developed in conjunction with R. Giuly. I also used electromechanical and *in vitro* interfacing experiments to demonstrate that this functional PDMS-based array exhibits properties that enable close, mechanically conformable contact with the surface of the spinal cord for selective stimulation of axonal tracts. In addition, I describe recent improvements to the fabrication and features of this MEA, which is capable of further isolating the electrode-tissue microenvironment via isolation wells around each electrode. I demonstrated that a MEA placed in contact with the surface of the spinal cord can be applied to selectively recruit spinal tracts and to selectively activate motor patterns.

In Chapter 3, I further assessed the fundamental capability of this novel, conformable MEA technology to stimulate white matter tracts in a precise, controlled, and functionally-relevant manner. This was assessed through in vitro experiments that explored the ability of this MEA to locally activate axons via single- and dual-site surface stimulation. Selectivity was tested in the isolated young rat spinal cord maintained *in vitro*, and three different capabilities of the MEA were assessed: anatomical selectivity, size selectivity, and 'functional' selectivity. Anatomical selectivity studies quantified the orthogonal (lateral) spread of activated white matter tracts, and compared results with those obtained with traditional rigid bipolar electrodes. Single-pulse MEA electrical stimulation was then tested on circuits that require synaptic activation by examining evoked responses in motor nerve roots. My results demonstrate that electrical stimulation

with the MEA can activate specific white matter regions with the dorsal column with a spatial selectivity that compared well to tests with a rigid, bipolar Tungsten electrode.

In order to thoroughly assess depth activation of our stimulus method, direct recordings of recruitment at different depths below the surface electrode would be required. However, due to the presence of stimulus artifacts that would overlap temporally with evoked responses, this may not be possible. This challenge may be surmounted in future studies via application of stimulus artifact elimination technologies (Blum) that facilitate analysis of responses that would otherwise be lost in stimulus artifact.

In addition, insight concerning the regional nature of the presented stimulus method can be gained by predictive modeling studies. For example, characterization of our MEA's current delivery profile and MEA-to-cord microenvironment could be applied to existing models for electrical activation of spinal cord circuits for better understanding of the influence of MEA stimulation on the spinal cord (Rutten 2002) (Ranck 1975; McNeal 1976; Struijk, Holsheimer et al. 1993; McIntyre and Grill 2001; Lertmanorat and Durand 2004; Rattay and Resatz 2007). Ideally, a combination of further experimental testing and predictive modeling will enable us to further characterize the regions of the cord which we would expect our MEA to activate.

Following single-site selectivity stimulation assessments using the MEA, I also demonstrated that dual-site stimulation of adjacent MEA electrode pairs could recruit spatially distinct populations of axons. Importantly, I also showed that the MEA is capable of site-specific stimulation of the ventrolateral funiculus for synaptic recruitment of motor circuits. These results, along with my demonstration that surface stimulation of the spinal cord by the conformable MEA functions analogously to rigid electrodes, allow me to translate studies using single rigid electrodes in a model of chronic SCI (Chapter 5) to the potential application of the MEA to stimulating chronic-transected cords

The aforementioned results suggest that future therapeutic and experimental

regimens may be able to use the MEA in place of rigid stimulating microelectrodes (either single or in arrays). For surface stimulation of the spinal cord, the MEA has clear advantages over rigid electrodes concerning accessibility of the spinal cord surface; for example, the MEA substrate is conformable enough to allow the MEA to wrap around the *in vitro* cord of juvenile rats to access ventral and lateral tracts. The MEA can also use its multiple electrodes to deliver interleaved stimulus patterns, which have shown to improve stimulation efficacy in both peripheral nerve (McDonnall, Clark et al. 2004) and spinal cord (Tai, Booth et al. 2000). Finally, it is expected that, when implanted, the presence of multiple electrodes will enable more adaptability in stimulating the cord, especially as longer-term adaptations develop in response to implantation and stimulation (Alo and Holsheimer 2002). Such features may be extremely beneficial to the long-term success of implantable electrode interfaces.

Before broader conclusions can be made concerning the functional capabilities of the above-described surface stimulation studies, further testing is necessary. In particular, it is essential to demonstrate successful applications following chronically implanting electrodes *in vivo* for the effective translation into therapeutic devices for spinal cord dysfunction. This is especially important since the functional properties of spinal circuits have been shown to change following injury (Dimitrijevic and Nathan 1968; Hultborn and Malmsten 1983; Hultborn and Malmsten 1983; Malmsten 1983; Edgerton, Tillakaratne et al. 2004; Rossignol, Barriere et al. 2008).

A critical component of successful control of the injured cord is understanding (and therefore potentially harnessing) the extensive plasticity that occurs in neural circuits in response to SCI. This includes the development of chronic pain syndromes and hyper-excitable spinal reflexes including spasticity (Dimitrijevic and Nathan 1968; Hultborn and Malmsten 1983; Hultborn and Malmsten 1983; Malmsten 1983; Mailis and Ashby 1990; Schouenborg, Holmberg et al. 1992; Levi, Hultling et al. 1995; Schouenborg, Weng et al. 1995; Cina and Hochman 2000). Fortunately, the

capacity for spinal cord plasticity can also be used as an advantage, and can undergo motor learning in an activity-dependent manner (Durkovic and Damianopoulos 1986; Barbeau and Rossignol 1987; Rossignol and Barbeau 1995; De Leon, Hodgson et al. 1998; Durkovic and Prokowich 1998; De Leon, Hodgson et al. 1999; De Leon, Tamaki et al. 1999; Edgerton, Leon et al. 2001; Edgerton, Tillakaratne et al. 2004). Clinically-relevant examples involve re-training the spinal cord to undertake coordinated stepping or standing (Edgerton, Tillakaratne et al. 2004; Rossignol, Bouyer et al. 2004). Since the spinal cord can revert to these behaviorally relevant motor states after SCI, the opportunity exists for neural prostheses (NPs) to interface with these circuits to provide for their external control. It is important that future studies evaluating spinal-cord stimulating technologies incorporate not only the short-term effects of stimulation, but also endeavor to understand how stimulation of spinal circuits by NPs is altered over longer periods of usage in SCI cords.

The hemisected, *in vitro* preparation that I use for functional response evaluation is limited in its representation of whole neural circuit-produced motor outputs. However, the reduced nature of this preparation also allows me to more precisely identify which axons are involved in generating the observed motor outputs. It is expected that, by stimulating the whole (vs. hemisected) cord and by applying the above T12 VLF surface stimulation to intact preparations, the motor outputs evoked would exhibit increasingly complex motor outputs as more neural connections remain intact. I propose that the MEA is uniquely capable of interfacing with the *in vivo* cord in such future studies to further implement the T12 VLF as a surface access point for eliciting coordinated motor outputs.

The imaging results that I present in Chapter 5 results indicate that surface tracts in the chronic-transected versus intact cords may project to regionally and functionally distinct neuronal populations within the gray matter. If he presence of a deep dorsal horn population in transects proves significant, an additional application for surface

stimulation at this site may involve using electrical stimulation as away to inhibit pain sensation (or block associated axonal propagation) in future applications.
egardless of potential anatomical changes due to tract degeneration, I have also shown in Chapter 5 that the chronic-transected cord responds to surface stimulation in significantly different ways than the intact cord. These distinctions warrant further study of the differences in response to surface stimulation between intact and SCI cords, and potentially also indicate the necessity of using transected subjects for future studies using surface stimulation to recover function following a spinal cord injury. The presence of a deep dorsal horn population in transects proves significant, surface stimulation could also be utilized to inhibit pain sensation in future applications.

In conclusion, the above studies provide essential starting point to further use of conformable MEAs to effectively activate and control spinal cord function from the surface of the spinal cord. The presented device development and assessments – along with analysis of the interfaced spinal systems in the chronic-transected cord – have been designed and analyzed for future potential incorporation into methods for therapeutic stimulation of the spinal cord. The findings that I present in this Thesis suggest that spinal-cord surface stimulation with this novel MEA technology may provide discrete, minimally-damaging management of neuronal subpopulations for therapeutic devices. Additionally, this technology may enable researchers to better control (and therefore study) modular elements of the spinal cord apparatus that are most critical for regaining function or limiting aberrant activity following injury.

References

Armani, D. L., C.; Aluru, N. (1999). Re-configurable fluid circuits by PDMS elastomer micromachining. Micro Electro Mechanical Systems, 1999. MEMS '99. Twelfth IEEE

http://www.ninds.nih.gov/disorders/sci/sci.htm. Most recent access date: January 2007.

Al-Majed, A. A., C. M. Neumann, et al. (2000). "Brief electrical stimulation promotes the speed and accuracy of motor axonal regeneration." J Neurosci **20**(7): 2602-8.

Alo, K. M. and J. Holsheimer (2002). "New trends in neuromodulation for the management of neuropathic pain." Neurosurgery **50**(4): 690-703; discussion 703-4.

Amaris, M. A., P. Z. Rashev, et al. (2002). "Microprocessor controlled movement of solid colonic content using sequential neural electrical stimulation." Gut **50**(4): 475-9.

Andersson, O. and S. Grillner (1983). "Peripheral control of the cat's step cycle. II. Entrainment of the central pattern generators for locomotion by sinusoidal hip movements during "fictive locomotion."" Acta Physiol Scand **118**(3): 229-39.

Antonino-Green, D. M., J. Cheng, et al. (2002). "Neurons labeled from locomotor-related ventrolateral funiculus stimulus sites in the neonatal rat spinal cord." J Comp Neurol **442**(3): 226-38.

Aoyagi, Y., V. K. Mushahwar, et al. (2004). "Movements elicited by electrical stimulation of muscles, nerves, intermediate spinal cord, and spinal roots in anesthetized and decerebrate cats." IEEE Trans Neural Syst Rehabil Eng **12**(1): 1-11.

Armani, D. L., C.; Aluru, N. (1999). Re-configurable fluid circuits by PDMS elastomer micromachining. Micro Electro Mechanical Systems, 1999. MEMS '99. Twelfth IEEE International Conference on.

Baldissera, F., H. Hultborn, et al. (1981). "Integration in spinal neuronal systems." Handbook of Physiology. Section I: The Nervous System Williams and Wilkins: pp. 509-595.

Bamford, J. A., C. T. Putman, et al. (2005). "Intraspinal microstimulation preferentially recruits fatigue-resistant muscle fibres and generates gradual force in rat." J Physiol **569**(Pt 3): 873-84.

Barbeau, H., M. Ladouceur, et al. (2002). "The effect of locomotor training combined with functional electrical stimulation in chronic spinal cord injured subjects: walking and reflex studies." Brain Res Brain Res Rev **40**(1-3): 274-91.

Barbeau, H. and S. Rossignol (1987). "Recovery of locomotion after chronic spinalization in the adult cat." Brain Res **412**(1): 84-95.

Barthelemy, D., H. Leblond, et al. (2007). "Characteristics and mechanisms of locomotion induced by intraspinal microstimulation and dorsal root stimulation in spinal cats." J Neurophysiol **97**(3): 1986-2000.

Belanger, M. C. and Y. Marois (2001). "Hemocompatibility, biocompatibility, inflammatory and in vivo studies of primary reference materials low-density polyethylene and polydimethylsiloxane: a review." Journal of Biomedical Materials Research(USA) **58**(5): 467-477.

Benabid, A. L., B. Wallace, et al. (2005). "Therapeutic electrical stimulation of the central nervous system." C R Biol **328**(2): 177-86.

Bizzi, E., M. C. Tresch, et al. (2000). "New perspectives on spinal motor systems." Nat Rev Neurosci **1**(2): 101-8.

Blum, R. A. R., J.D. Brown, E.A. DeWeerth, S.P. (2007). " An Integrated System for Simultaneous, Multichannel Neuronal Stimulation and Recording." Circuits and Systems I: Regular Papers, IEEE Transactions on [Circuits and Systems I: Fundamental Theory and Applications, IEEE Transactions on] **54**(12): 10.

Boppart, S. A., B. C. Wheeler, et al. (1992). "A flexible perforated microelectrode array for extended neural recordings." IEEE Trans Biomed Eng **39**(1): 37-42.

Boyer, S., M. Sawan, et al. (2000). "Implantable selective stimulator to improve bladder voiding: design and chronic experiments in dogs." IEEE Trans Rehabil Eng **8**(4): 464-70.

Branner, A., R. B. Stein, et al. (2004). "Long-term stimulation and recording with a penetrating microelectrode array in cat sciatic nerve." IEEE Trans Biomed Eng **51**(1): 146-57.

Branner, A., R. B. Stein, et al. (2001). "Selective stimulation of cat sciatic nerve using an array of varying-length microelectrodes." Journal of Neurophysiology **85**(4): 1585-94.

Branner, A., R. B. Stein, et al. (2001). "Selective stimulation of cat sciatic nerve using an array of varying-length microelectrodes." J Neurophysiol **85**(4): 1585-94.

Bras, H., P. Cavallari, et al. (1989). "Morphology of midlumbar interneurones relaying information from group II muscle afferents in the cat spinal cord." J Comp Neurol **290**(1): 1-15.

Brindley, G. S., C. E. Polkey, et al. (1982). "Sacral anterior root stimulators for bladder control in paraplegia." Paraplegia **20**(6): 365-81.

Brown, T. G. (1911). "The intrinsic factors in the act of progression in the mammal." Proc. R. Soc. Lond. B., 84: 308-319.

Bryz-Gornia, W. F., Jr. and D. J. Stelzner (1986). "Ascending tract neurons survive spinal cord transection in the neonatal rat." Exp Neurol **93**(1): 195-210.

Calancie, B., B. Needham-Shropshire, et al. (1994). "Involuntary stepping after chronic spinal cord injury. Evidence for a central rhythm generator for locomotion in man." Brain **117 (Pt 5)**: 1143-59.

Cater, H. L., D. Gitterman, et al. (2007). "Stretch-induced injury in organotypic hippocampal slice cultures reproduces in vivo post-traumatic neurodegeneration: role of glutamate receptors and voltage-dependent calcium channels." Journal of Neurochemistry **101**(2): 434-47.

Cazalets, J. R., M. Borde, et al. (1995). "Localization and organization of the central pattern generator for hindlimb locomotion in newborn rat." J Neurosci **15**(7 Pt 1): 4943-51.

Chae, J., F. Bethoux, et al. (1998). "Neuromuscular stimulation for upper extremity motor and functional recovery in acute hemiplegia." Stroke **29**(5): 975-9.

Chapin, J. K. (2000). "Neural prosthetic devices for quadriplegia." Currrent Opinion in Neurology **13**(6): 671-5.

Chapin, J. K. and K. A. Moxon (2001). "Neural prostheses for restoration of sensory and motor function." CRC Press: 1-296 pp.

Chung, K. and R. E. Coggeshall (1982). "Quantitation of propriospinal fibers in the tract of Lissauer of the rat." J Comp Neurol **211**(4): 418-26.

Chung, K. and R. E. Coggeshall (1983). "Propriospinal fibers in the rat." J Comp Neurol **217**(1): 47-53.

Chung, K. and R. E. Coggeshall (1988). "Propriospinal fibers in the white matter of the cat sacral spinal cord." J Comp Neurol **269**(4): 612-7.

Chung, K., G. A. Kevetter, et al. (1984). "An estimate of the ratio of propriospinal to long tract neurons in the sacral spinal cord of the rat." Neurosci Lett **44**(2): 173-7.

Chung, K., L. A. Langford, et al. (1987). "Primary afferent and propriospinal fibers in the rat dorsal and dorsolateral funiculi." J Comp Neurol **263**(1): 68-75.

Cina, C. and S. Hochman (2000). "Diffuse distribution of sulforhodamine-labeled neurons during serotonin-evoked locomotion in the neonatal rat thoracolumbar spinal cord." J Comp Neurol **423**(4): 590-602.

Clark, G. M. (1999). "Cochlear implants in the Third Millennium." Am J Otol **20**(1): 4-8.

Clark, G. M., Y. C. Tong, et al. (1977). "A multiple electrode cochlear implant." Journal of Laryngology and Otology **91**(11): 935-45.

Conway, B. A., H. Hultborn, et al. (1987). "Proprioceptive input resets central locomotor rhythm in the spinal cat." Exp Brain Res **68**(3): 643-56.

Cowley, K. C. and B. J. Schmidt (1997). "Regional distribution of the locomotor pattern-generating network in the neonatal rat spinal cord." J Neurophysiol **77**(1): 247-59.

Crone, C. and J. Nielsen (1994). "Central control of disynaptic reciprocal inhibition in humans." Acta Physiol Scand **152**(4): 351-63.

Czarkowska, J., E. Jankowska, et al. (1981). "Common interneurones in reflex pathways from group 1a and 1b afferents of knee flexors and extensors in the cat." J Physiol **310**: 367-80.

Dalmose, A., C. Bjarkam, et al. (2003). "Electrostimulation: a future treatment option for patients with neurogenic urodynamic disorders?" APMIS Suppl(109): 45-51.

Danziger, N., P. Remy, et al. (1996). "A clinical and neurophysiological study of a patient with an extensive transection of the spinal cord sparing only a part of one anterolateral quadrant." Brain **119 (Pt 6)**: 1835-48.

Davidoff, R. A. (1983). Handbook of the Spinal Cord.

Davis, R., T. Houdayer, et al. (1999). "Paraplegia: prolonged standing using closed-loop functional electrical stimulation and Andrews ankle-foot orthosis." Artif Organs **23**(5): 418-20.

De Leon, R. D., J. A. Hodgson, et al. (1998). "Full weight-bearing hindlimb standing following stand training in the adult spinal cat." J Neurophysiol **80**(1): 83-91.

De Leon, R. D., J. A. Hodgson, et al. (1999). "Retention of hindlimb stepping ability in adult spinal cats after the cessation of step training." J Neurophysiol **81**(1): 85-94.

De Leon, R. D., H. Tamaki, et al. (1999). "Hindlimb locomotor and postural training modulates glycinergic inhibition in the spinal cord of the adult spinal cat." J Neurophysiol **82**(1): 359-69.

DiMarco, A. F. (2001). "Neural prostheses in the respiratory system." Journal of Rehabilitation Research and Development **38**(6): 601-7.

Dimitrijevic, M. R., Y. Gerasimenko, et al. (1998). "Evidence for a spinal central pattern generator in humans." Ann N Y Acad Sci **860**: 360-76.

Dimitrijevic, M. R. and P. W. Nathan (1968). "Studies of spasticity in man. 3. Analysis of revlex activity evoked by noxious cutaneous stimulation." Brain **91**(2): 349-68.

Durkovic, R. G. and E. N. Damianopoulos (1986). "Forward and backward classical conditioning of the flexion reflex in the spinal cat." J Neurosci **6**(10): 2921-5.

Durkovic, R. G. and L. J. Prokowich (1998). "D-2-amino-5-phosphonovalerate, and NMDA receptor antagonist, blocks induction of associative long-term potentiation of the flexion reflex in spinal cat." Neurosci Lett **257**(3): 162-4.

Dutton, R. C., M. I. Carstens, et al. (2006). "Long ascending propriospinal projections from lumbosacral to upper cervical spinal cord in the rat." Brain Res **1119**(1): 76-85.

Eccles, J. C., R. M. Eccles, et al. (1960). "Types of neuron in and around the intermediate nucleus of the lumbosacral cord." J. Physiol. (Lond), 40 **154**: 89-114.

Edell, D. J., V. V. Toi, et al. (1992). "Factors influencing the biocompatibility of insertable silicon microshafts in cerebral cortex." IEEE Transactions on Biomedical Engineering **39**(6): 635-43.

Edgerton, V. R., G. Courtine, et al. (2008). "Training locomotor networks." Brain Res Rev **57**(1): 241-54.

Edgerton, V. R., R. D. Leon, et al. (2001). "Retraining the injured spinal cord." J Physiol **533**(Pt 1): 15-22.

Edgerton, V. R., R. D. Leon, et al. (2001). "Retraining the injured spinal cord." Journal of Physiology **533**(Pt 1): 15-22.

Edgerton, V. R., N. J. Tillakaratne, et al. (2004). "Plasticity of the spinal neural circuitry after injury." Annu Rev Neurosci **27**: 145-67.

Elefteriades, J. A., J. A. Quin, et al. (2002). "Long-term follow-up of pacing of the conditioned diaphragm in quadriplegia." Pacing Clin Electrophysiol **25**(6): 897-906.

Emmanuel Pierrot-Deseilligny, D. B. (2005). The Circuitry of the Human Spinal Cord: Its Role In Motor Control and Movement Disorders, Cambridge University Press.

Fedirchuk, B., J. Nielsen, et al. (1998). "Pharmacologically evoked fictive motor patterns in the acutely spinalized marmoset monkey (Callithrix jacchus)." Exp Brain Res **122**(3): 351-61.

Fields, H. L. and A. I. Basbaum (1978). "Brainstem control of spinal pain-transmission neurons." Annu Rev Physiol **40**: 217-48.

Fisher, L. E., M. E. Miller, et al. (2006). "Preliminary evaluation of a neural prosthesis for standing after spinal cord injury with four contact nerve-cuff electrodes for quadriceps stimulation." Conf Proc IEEE Eng Med Biol Soc **1**: 3592-5.

Fouad, K. and K. Pearson (2004). "Restoring walking after spinal cord injury." Prog Neurobiol **73**(2): 107-126.

Francisco, G., J. Chae, et al. (1998). "Electromyogram-triggered neuromuscular stimulation for improving the arm function of acute stroke survivors: a randomized pilot study." Arch Phys Med Rehabil **79**(5): 570-5.

Ganio, E., A. Masin, et al. (2001). "Short-term sacral nerve stimulation for functional anorectal and urinary disturbances: results in 40 patients: evaluation of a new option for anorectal functional disorders." Dis Colon Rectum **44**(9): 1261-7.

Garra, J., T. Long, et al. (2002). "Dry etching of polydimethylsiloxane for microfluidic systems." Journal of Vacuum Science & Technology a-Vacuum Surfaces and Films **20**(3): 975-982.

Gaunt, R. A., A. Prochazka, et al. (2006). "Intraspinal microstimulation excites multisegmental sensory afferents at lower stimulus levels than local alpha-motoneuron responses." J Neurophysiol **96**(6): 2995-3005.

Gerasimenko, Y., R. R. Roy, et al. (2008). "Epidural stimulation: comparison of the spinal circuits that generate and control locomotion in rats, cats and humans." Exp Neurol **209**(2): 417-25.

Gerasimenko, Y. P., V. D. Avelev, et al. (2003). "Initiation of locomotor activity in spinal cats by epidural stimulation of the spinal cord." Neurosci Behav Physiol **33**(3): 247-54.

Gerasimenko, Y. P., I. A. Lavrov, et al. (2005). "Formation of locomotor patterns in decerebrate cats in conditions of epidural stimulation of the spinal cord." Neurosci Behav Physiol **35**(3): 291-8.

Gerasimenko, Y. P., I. A. Lavrov, et al. (2006). "Spinal cord reflexes induced by epidural spinal cord stimulation in normal awake rats." J Neurosci Methods **157**(2): 253-63.

Gerasimenko, Y. P., I. A. Lavrov, et al. (2006). "Spinal cord reflexes induced by epidural spinal cord stimulation in normal awake rats." Journal of Neuroscience Methods **157**(2): 253-63.

Giszter, S. F., F. A. Mussa-Ivaldi, et al. (1993). "Convergent force fields organized in the frog's spinal cord." J Neurosci **13**(2): 467-91.

Gonzalez, C. and M. Rodriguez (1997). "A flexible perforated microelectrode array probe for action potential recording in nerve and muscle tissues." J Neurosci Methods **72**(2): 189-95.

Gordon, I. T., M. J. Dunbar, et al. (2008). "The Interaction Between Developing Spinal Locomotor Networks in the Neonatal Mouse." J Neurophysiol.

Gray, D. S., J. Tien, et al. (2004). "High-conductivity elastomeric electronics." Advanced Materials **16**(5): 393-+.

Grill, W. M., N. Bhadra, et al. (1999). "Bladder and urethral pressures evoked by microstimulation of the sacral spinal cord in cats." Brain Res **836**(1-2): 19-30.

Grill, W. M., M. D. Craggs, et al. (2001). "Emerging clinical applications of electrical stimulation: opportunities for restoration of function." Journal of Rehabilitation Research and Development **38**(6): 641-53.

Grill, W. M. and R. F. Kirsch (2000). "Neuroprosthetic applications of electrical stimulation." Assist Technol **12**(1): 6-20.

Grillner, S. (1981). "Control of locomotion in bipeds,tetrapods, and fish." Handbook of Physiology-The Nervous System II: pp. 1179-1236.

Grillner, S. and P. Zangger (1979). "On the central generation of locomotion in the low spinal cat." Exp Brain Res **34**(2): 241-61.

Guevremont, L., C. G. Renzi, et al. (2006). "Locomotor-related networks in the lumbosacral enlargement of the adult spinal cat: activation through intraspinal microstimulation." IEEE Trans Neural Syst Rehabil Eng **14**(3): 266-72.

Guo, L., Kathleen K. Williams, Richard J. Giuly, Stephen P. DeWeerth (2007). A PDMS-based Elastic Multi-Electrode Array for Spinal Cord Surface Stimulation and Its Electrode Modification to Enhance Performance. MRS Symposium on Advanced Materials for Neuroprosthetics, San Francisco, CA, USA.

Gustafsson, B. and E. Jankowska (1976). "Direct and indirect activation of nerve cells by electrical pulses applied extracellularly." J Physiol **258**(1): 33-61.

Gustafsson, B., M. J. Pinter, et al. (1986). "The effect of axotomy on posttetanic potentiation of group Ia synapses in the cat." J Neurophysiol **56**(4): 1174-84.

He, W. and R. V. Bellamkonda (2005). "Nanoscale neuro-integrative coatings for neural implants." Biomaterials **26**(16): 2983-90.

Hedo, G., J. M. Laird, et al. (1999). "Time-course of spinal sensitization following carrageenan-induced inflammation in the young rat: a comparative electrophysiological and behavioural study in vitro and in vivo." Neuroscience **92**(1): 309-18.

Hesse, S., F. Reiter, et al. (1998). "Botulinum toxin type A and short-term electrical stimulation in the treatment of upper limb flexor spasticity after stroke: a randomized, double-blind, placebo-controlled trial." Clin Rehabil **12**(5): 381-8.

Hetke, J. F., J.C. Williams, D.S. Pellinen, R.J. Vetter, D.R. Kipke (2003). 3-D Silicon Probe Array with Hybrid Polymer Interconnect for Cortical Recording. IEEE Proceedings of the First International Conference on Neural Engineering.

Heuschkel, M. O., M. Fejtl, et al. (2002). "A three-dimensional multi-electrode array for multi-site stimulation and recording in acute brain slices." Journal of Neuroscience Methods **114**(2): 135-48.

Hillman, T., A. N. Badi, et al. (2003). "Cochlear nerve stimulation with a 3-dimensional penetrating electrode array." Otol Neurotol **24**(5): 764-8.

Hillman, T., A. N. Badi, et al. (2003). "Cochlear nerve stimulation with a 3-dimensional penetrating electrode array." Otology and Neurotology **24**(5): 764-8.

Hochman, S. (2007). "Primer: Spinal Cord." Current Biology **17**(22): R950-955.

Hochman, S. (2007). "Spinal Cord." Current Biology **17**(22): 6.

Holman G., Y. H., R.C. Wyeth, A.O.D. Willows, D. Denton, K.F. Bohringer (2002). Silicon Micro-Needles with Flexible Interconnections. Second Annual International IEEE-EMBS Special Topic Conference on Microtechnologies in Medicine & Biology.

Hultborn, H. (2001). "State-dependent modulation of sensory feedback." J Physiol **533**(Pt 1): 5-13.

Hultborn, H., B. A. Conway, et al. (1998). "How do we approach the locomotor network in the mammalian spinal cord?" Ann. NY Acad. Sci. **860**: 70-82.

Hultborn, H. and J. Malmsten (1983). "Changes in segmental reflexes following chronic spinal cord hemisection in the cat. I. Increased monosynaptic and polysynaptic ventral root discharges." Acta Physiol Scand **119**(4): 405-22.

Hultborn, H. and J. Malmsten (1983). "Changes in segmental reflexes following chronic spinal cord hemisection in the cat. II. Conditioned monosynaptic test reflexes." Acta Physiol Scand **119**(4): 423-33.

Hursh, J. B. (1939). "Conduction Velocity and Diameter of Nerve Fibers." American Journal of Physiology **127**: 9.

Ichiyama, R. M., Y. Gerasimenko, et al. (2008). "Dose dependence of the 5-HT agonist quipazine in facilitating spinal stepping in the rat with epidural stimulation." Neurosci Lett **438**(3): 281-5.

Ichiyama, R. M., Y. P. Gerasimenko, et al. (2005). "Hindlimb stepping movements in complete spinal rats induced by epidural spinal cord stimulation." Neurosci Lett **383**(3): 339-44.

Ichiyama, R. M., Y. P. Gerasimenko, et al. (2005). "Hindlimb stepping movements in complete spinal rats induced by epidural spinal cord stimulation." Neurosci Lett.

Ichiyama, R. M., Y. P. Gerasimenko, et al. (2005). "Hindlimb stepping movements in complete spinal rats induced by epidural spinal cord stimulation." Neuroscience Letters **383**(3): 339-44.

Iwahara, T., Y. Atsuta, et al. (1992). "Spinal cord stimulation-induced locomotion in the adult cat." Brain Res Bull **28**(1): 99-105.

Jankowska, E. (1975). "Cortical motor representation in view of recent experiments on cortico-spinal relations." Acta Neurobiol Exp (Wars) **35**(5-6): 699-706.

Jankowska, E. (1992). "Interneuronal relay in spinal pathways from proprioceptors." Prog Neurobiol **38**(4): 335-78.

Jankowska, E. (2001). "Spinal interneuronal systems: identification, multifunctional character and reconfigurations in mammals." J Physiol **533**(Pt 1): 31-40.

Jankowska, E. and S. Edgley (1993). "Interactions between pathways controlling posture and gait at the level of spinal interneurones in the cat." Prog. Brain Res **97**: 161-171.

Jankowska, E., T. Johannisson, et al. (1981). "Common interneurones in reflex pathways from group 1a and 1b afferents of ankle extensors in the cat." J Physiol **310**: 381-402.

Jankowska, E., M. G. Jukes, et al. (1967). "The effect of DOPA on the spinal cord. 6. Half-centre organization of interneurones transmitting effects from the flexor reflex afferents." Acta Physiol Scand **70**(3): 389-402.

Jankowska, E., Y. Padel, et al. (1975). "The mode of activation of pyramidal tract cells by intracortical stimuli." J Physiol **249**(3): 617-36.

Jordan, L. M. (1998). "Initiation of locomotion in mammals." Ann N Y Acad Sci **860**: 83-93.

Kalb, R. G. and S. M. Strittmatter (2000). "Neurobiology of spinal cord injury." Humana Press, Totowa: 1-284 pp.

Kawashima, N., D. Nozaki, et al. (2008). "Shaping appropriate locomotive motor output through interlimb neural pathway within spinal cord in humans." J Neurophysiol **99**(6): 2946-55.

Kennedy, P. R., R. A. Bakay, et al. (2000). "Direct control of a computer from the human central nervous system." IEEE Trans Rehabil Eng **8**(2): 198-202.

Kennedy, P. R., S. S. Mirra, et al. (1992). "The cone electrode: ultrastructural studies following long-term recording in rat and monkey cortex." Neurosci Lett **142**(1): 89-94.

Kern, H., C. Hofer, et al. (2002). "Denervated muscles in humans: limitations and problems of currently used functional electrical stimulation training protocols." Artif Organs **26**(3): 216-8.

Kessler, D. K. (1999). "The CLARION Multi-Strategy Cochlear Implant." Annals of Otology, Rhinology, and Laryngology Supplement **177**: 8-16.

Kiehn, O. (2006). "Locomotor circuits in the mammalian spinal cord." Annu Rev Neurosci **29**: 279-306.

Kiehn, O. and S. J. Butt (2003). "Physiological, anatomical and genetic identification of CPG neurons in the developing mammalian spinal cord." Prog Neurobiol **70**(4): 347-61.

Kiehn, O., R. M. Harris-Warrick, et al. (1998). "Neuronal Mechanisms for Generating Locomotor Activity. Proceedings of a conference. New York City, New York, USA. March 20-23, 1998." Ann N Y Acad Sci **860**: 1-573.

Kiehn, O. and O. Kjaerulff (1996). "Spatiotemporal characteristics of 5-HT and dopamine-induced rhythmic hindlimb activity in the in vitro neonatal rat." J Neurophysiol **75**(4): 1472-82.

Kiehn, O. and O. Kjaerulff (1998). "Distribution of central pattern generators for rhythmic motor outputs in the spinal cord of limbed vertebrates." Ann N Y Acad Sci **860**: 110-29.

Kilgore, K. L., H. A. Hoyen, et al. (2008). "An implanted upper-extremity neuroprosthesis using myoelectric control." J Hand Surg [Am] **33**(4): 539-50.

Kinoshita, M. and T. Yamaguchi (2001). "Stimulus time-locked responses of motoneurons during forelimb fictive locomotion evoked by repetitive stimulation of the lateral funiculus." Brain Res **904**(1): 31-42.

Kipke, D. R., R. J. Vetter, et al. (2003). "Silicon-substrate intracortical microelectrode arrays for long-term recording of neuronal spike activity in cerebral cortex." IEEE Trans Neural Syst Rehabil Eng **11**(2): 151-5.

Kjaerulff, O. and O. Kiehn (1996). "Distribution of networks generating and coordinating locomotor activity in the neonatal rat spinal cord in vitro: a lesion study." J Neurosci **16**(18): 5777-94.

Kraft, G. H., S. S. Fitts, et al. (1992). "Techniques to improve function of the arm and hand in chronic hemiplegia." Arch Phys Med Rehabil **73**(3): 220-7.

Kralj, A., T. Bajd, et al. (1988). "Enhancement of gait restoration in spinal injured patients by functional electrical stimulation." Clin Orthop Relat Res(233): 34-43.

Kremer, E. and A. Lev-Tov (1997). "Localization of the spinal network associated with generation of hindlimb locomotion in the neonatal rat and organization of its transverse coupling system." J Neurophysiol **77**(3): 1155-70.

Kriellaars, D. J., R. M. Brownstone, et al. (1994). "Mechanical entrainment of fictive locomotion in the decerebrate cat." J Neurophysiol **71**(6): 2074-86.

Kumar, K., C. Toth, et al. (1997). "Deep brain stimulation for intractable pain: a 15-year experience." Neurosurgery **40**(4): 736-46; discussion 746-7.

Langlet, C., H. Leblond, et al. (2005). "Mid-lumbar segments are needed for the expression of locomotion in chronic spinal cats." J Neurophysiol **93**(5): 2474-88.

Lanmuller, H., S. Sauermann, et al. (1999). "Battery-powered implantable nerve stimulator for chronic activation of two skeletal muscles using multichannel techniques." Artif Organs **23**(5): 399-402.

Lapatki, B. G., J. P. Van Dijk, et al. (2004). "A thin, flexible multielectrode grid for high-density surface EMG." J Appl Physiol **96**(1): 327-36.

Lavrov, I., C. J. Dy, et al. (2008). "Epidural stimulation induced modulation of spinal locomotor networks in adult spinal rats." J Neurosci **28**(23): 6022-9.

Lavrov, I., Y. P. Gerasimenko, et al. (2006). "Plasticity of spinal cord reflexes after a complete transection in adult rats: relationship to stepping ability." J Neurophysiol **96**(4): 1699-710.

Lertmanorat, Z. and D. M. Durand (2004). "A novel electrode array for diameter-dependent control of axonal excitability: a simulation study." IEEE Transactions on Biomedical Engineering **51**(7): 1242-50.

Lev-Tov, A., I. Delvolve, et al. (2000). "Sacrocaudal afferents induce rhythmic efferent bursting in isolated spinal cords of neonatal rats." J Neurophysiol **83**(2): 888-94.

Leventhal, D. K. and D. M. Durand (2003). "Subfascicle stimulation selectivity with the flat interface nerve electrode." Annals of Biomedical Engineering **31**(6): 643-52.

Leventhal, D. K. and D. M. Durand (2004). "Chronic measurement of the stimulation selectivity of the flat interface nerve electrode." IEEE Transactions on Biomedical Engineering **51**(9): 1649-58.

Levi, R., C. Hultling, et al. (1995). "The Stockholm spinal cord injury study: 1. Medical problems in a regional SCI population." Paraplegia **33**(6): 308-15.

Levin, M. F. and C. W. Hui-Chan (1992). "Relief of hemiparetic spasticity by TENS is associated with improvement in reflex and voluntary motor functions." Electroencephalogr Clin Neurophysiol **85**(2): 131-42.

Li, Y., P. J. Harvey, et al. (2004). "Spastic long-lasting reflexes of the chronic spinal rat studied in vitro." J Neurophysiol **91**(5): 2236-46.

Liberson, W. T., H. J. Holmquest, et al. (1961). "Functional electrotherapy: stimulation of the peroneal nerve synchronized with the swing phase of the gait of hemiplegic patients." Arch Phys Med Rehabil **42**: 101-5.

Lidierth, M. (2007). "Long-range projections of Adelta primary afferents in the Lissauer tract of the rat." Neurosci Lett **425**(2): 126-30.

Loeb, G. E. and R. A. Peck (1996). "Cuff electrodes for chronic stimulation and recording of peripheral nerve activity." Journal of Neuroscience Methods **64**(1): 95-103.

Loeb, G. E. and R. A. Peck (1996). "Cuff electrodes for chronic stimulation and recording of peripheral nerve activity." J Neurosci Methods **64**(1): 95-103.

Lu, Y. and E. R. Perl (2003). "A specific inhibitory pathway between substantia gelatinosa neurons receiving direct C-fiber input." J Neurosci **23**(25): 8752-8.

Lundberg, A. (1967). "The supraspinal control of transmission in spinal reflex pathways." Electroencephalogr Clin Neurophysiol: Suppl 25:35-46.

Lundberg, A. (1969). "Half-centres revisited." Adv. Physiol. Sci(1): 155-167.

Lundberg, A. (1979). "Multisensory control of spinal reflex pathways." Prog Brain Res **50**: 11-28.

Lundberg, A., K. Malmgren, et al. (1987). "Reflex pathways from group II muscle afferents. 3. Secondary spindle afferents and the FRA: a new hypothesis." Exp Brain Res **65**(2): 294-306.

Madou, M. J. (2002). Fundamentals of Microfabrication: The Science of Miniaturization, Second Edition, CRC Press.

Maghribi, M., J. Hamilton, et al. (2002). Stretchable micro-electrode array [for retinal prostheses]. Microtechnologies in Medicine & Biology 2nd Annual International IEEE-EMB Special Topic Conference on, Madison, WI, IEEE, Piscataway.

Maghribi, M., J. Hamilton, et al. (2002). Stretchable micro-electrode array [for retinal prosthesis].

Maghribi M., J. H., D. Polla, K. Rose, T. Wilson, and P. Krulevitch (

2002). Stretchable Micro-Electrode Array. 2nd Annual International IEEE-EMBS Special Topic Conference on Microtechnologies in Medicine and Biology.

Magnuson, D. S., D. M. Green, et al. (1998). "Lumbar spinoreticular neurons in the rat: part of the central pattern generator for locomotion?" Ann N Y Acad Sci **860**: 436-40.

Magnuson, D. S., M. J. Schramm, et al. (1995). "Long-duration, frequency-dependent motor responses evoked by ventrolateral funiculus stimulation in the neonatal rat spinal cord." Neurosci Lett **192**(2): 97-100.

Magnuson, D. S., M. J. Schramm, et al. (1995). "Long-duration, frequency-dependent motor responses evoked by ventrolateral funiculus stimulation in the neonatal rat spinal cord." Neuroscience Letters **192**(2): 97-100.

Magnuson, D. S. and T. C. Trinder (1997). "Locomotor rhythm evoked by ventrolateral funiculus stimulation in the neonatal rat spinal cord in vitro." Journal of Neurophysiology **77**(1): 200-6.

Magnuson, D. S. and T. C. Trinder (1997). "Locomotor rhythm evoked by ventrolateral funiculus stimulation in the neonatal rat spinal cord in vitro." J Neurophysiol **77**(1): 200-6.

Mailis, A. and P. Ashby (1990). "Alterations in group Ia projections to motoneurons following spinal lesions in humans." J Neurophysiol **64**(2): 637-47.

Malmsten, J. (1983). "Time course of segmental reflex changes after chronic spinal cord hemisection in the rat." Acta Physiol Scand **119**(4): 435-43.

Marchetti, C., M. Beato, et al. (2001). "Alternating rhythmic activity induced by dorsal root stimulation in the neonatal rat spinal cord in vitro." J Physiol **530**(Pt 1): 105-12.

Maynard, E. M., C. T. Nordhausen, et al. (1997). "The Utah intracortical Electrode Array: a recording structure for potential brain-computer interfaces." Electroencephalogr Clin Neurophysiol **102**(3): 228-39.

McCrea, D. A. (1998). "Neuronal basis of afferent-evoked enhancement of locomotor activity." Ann N Y Acad Sci **860**: 216-25.

McCrea, D. A. (2001). "Spinal circuitry of sensorimotor control of locomotion." J Physiol **533**(Pt 1): 41-50.

McDonnall, D., G. A. Clark, et al. (2004). "Interleaved, multisite electrical stimulation of cat sciatic nerve produces fatigue-resistant, ripple-free motor responses." IEEE Transactions on Neural Systems and Rehabilitation Engineering **12**(2): 208-15.

McDonnall, D., G. A. Clark, et al. (2004). "Interleaved, multisite electrical stimulation of cat sciatic nerve produces fatigue-resistant, ripple-free motor responses." IEEE Trans Neural Syst Rehabil Eng **12**(2): 208-15.

McIntyre, C. C. and W. M. Grill (2001). "Finite element analysis of the current-density and electric field generated by metal microelectrodes." Ann Biomed Eng **29**(3): 227-35.

McKerracher, L. and R. Doucet, S. (2002). "Spinal Cord Trauma: Regeneration, Neural Repair and Functional Recovery." Elsevier, Amsterdam: 1-470 pp.

McNeal, D. R. (1976). "Analysis of a model for excitation of myelinated nerve." IEEE Trans Biomed Eng **23**(4): 329-37.

Meinck, H. M. (1976). "Occurrence of the H reflex and the F wave in the rat." Electroencephalogr Clin Neurophysiol **41**(5): 530-3.

Minassian, K., B. Jilge, et al. (2004). "Stepping-like movements in humans with complete spinal cord injury induced by epidural stimulation of the lumbar cord: electromyographic study of compound muscle action potentials." Spinal Cord **42**(7): 401-16.

Minassian, K., I. Persy, et al. (2007). "Human lumbar cord circuitries can be activated by extrinsic tonic input to generate locomotor-like activity." Hum Mov Sci **26**(2): 275-95.

Mirzadeh, H., M. T. Khorasani, et al. (1994). "Biocompatibility evaluation of laser-induced AAm and HEMA grafted EPR. Part 1: In-vitro study." Clin Mater **16**(4): 177-87.

Molenaar, I. and H. G. Kuypers (1978). "Cells of origin of propriospinal fibers and of fibers ascending to supraspinal levels. A HRP study in cat and rhesus monkey." Brain Res **152**(3): 429-50.

Mortimer, J. T., C. N. Shealy, et al. (1970). "Experimental nondestructive electrical stimulation of the brain and spinal cord." J Neurosurg **32**(5): 553-9.

Mushahwar, V. K., Y. Aoyagi, et al. (2004). "Movements generated by intraspinal microstimulation in the intermediate gray matter of the anesthetized, decerebrate, and spinal cat." Can J Physiol Pharmacol **82**(8-9): 702-14.

Mushahwar, V. K., D. M. Gillard, et al. (2002). "Intraspinal micro stimulation generates locomotor-like and feedback-controlled movements." IEEE Trans Neural Syst Rehabil Eng **10**(1): 68-81.

Mushahwar, V. K. and K. W. Horch (1997). "Proposed specifications for a lumbar spinal cord electrode array for control of lower extremities in paraplegia." IEEE Trans Rehabil Eng **5**(3): 237-43.

Mushahwar, V. K. and K. W. Horch (1998). "Selective activation and graded recruitment of functional muscle groups through spinal cord stimulation." Ann N Y Acad Sci **860**: 531-5.

Mushahwar, V. K. and K. W. Horch (2000). "Muscle recruitment through electrical stimulation of the lumbo-sacral spinal cord." IEEE Trans Rehabil Eng **8**(1): 22-9.

Mushahwar, V. K. and K. W. Horch (2000). "Selective activation of muscle groups in the feline hindlimb through electrical microstimulation of the ventral lumbo-sacral spinal cord." IEEE Trans Rehabil Eng **8**(1): 11-21.

Mushahwar, V. K., P. L. Jacobs, et al. (2007). "New functional electrical stimulation approaches to standing and walking." J Neural Eng **4**(3): S181-97.

Naples, G. G., J. T. Mortimer, et al. (1988). "A spiral nerve cuff electrode for peripheral nerve stimulation." IEEE Transactions on Biomedical Engineering **35**(11): 905-16.

Nashold, B. S., Jr. and H. Friedman (1972). "Dorsal column stimulation for control of pain. Preliminary report on 30 patients." J Neurosurg **36**(5): 590-7.

Nicol, D. J., M. H. Granat, et al. (1995). "Evidence for a human spinal stepping generator." Brain Res **684**(2): 230-2.

Nicolelis, M. A. (2001). "Actions from thoughts." Nature **409**(6818): 403-7.

Normann, R. A., D. J. Warren, et al. (2001). "High-resolution spatio-temporal mapping of visual pathways using multi-electrode arrays." Vision Res **41**(10-11): 1261-75.

Norton, J. A., D. J. Bennett, et al. (2008). "Changes in sensory-evoked synaptic activation of motoneurons after spinal cord injury in man." Brain **131**(Pt 6): 1478-91.

NSCISC (2008). Spinal Cord Injury Facts & Figures at a Glance 2008. Birmingham, AL, National Spinal Cord Injury Statistical Center. Last access: August 2008.

Oka, H., K. Shimono, et al. (1999). "A new planar multielectrode array for extracellular recording: application to hippocampal acute slice." Journal of Neuroscience Methods **93**(1): 61-7.

Peckham, P. H., M. W. Keith, et al. (2001). "Efficacy of an implanted neuroprosthesis for restoring hand grasp in tetraplegia: a multicenter study." Arch Phys Med Rehabil **82**(10): 1380-8.

Peckham, P. H. and J. S. Knutson (2005). "Functional electrical stimulation for neuromuscular applications." Annu Rev Biomed Eng **7**: 327-60.

Petersen, N., H. Morita, et al. (1999). "Modulation of reciprocal inhibition between ankle extensors and flexors during walking in man." J Physiol **520 Pt 2**: 605-19.

Peterson, S. L., A. McDonald, et al. (2005). "Poly(dimethylsiloxane) thin films as biocompatible coatings for microfluidic devices: cell culture and flow studies with glial cells." J Biomed Mater Res A **72**(1): 10-8.

Petko, M. and M. Antal (2000). "Propriospinal afferent and efferent connections of the lateral and medial areas of the dorsal horn (laminae I-IV) in the rat lumbar spinal cord." J Comp Neurol **422**(2): 312-25.

Polikov, V. S., P. A. Tresco, et al. (2005). "Response of brain tissue to chronically implanted neural electrodes." Journal of Neuroscience Methods **148**(1): 1-18.

Popovic, M. R., A. Curt, et al. (2001). "Functional electrical stimulation for grasping and walking: indications and limitations." Spinal Cord **39**(8): 403-12.

Prochazka, A., M. Gauthier, et al. (1997). "The bionic glove: an electrical stimulator garment that provides controlled grasp and hand opening in quadriplegia." Arch Phys Med Rehabil **78**(6): 608-14.

Prochazka, A., M. Gauthier, et al. (1997). "The bionic glove: an electrical stimulator garment that provides controlled grasp and hand opening in quadriplegia." Archives of Physical Medicine and Rehabilitation **78**(6): 608-14.

Prochazka, A. and V. K. Mushahwar (2001). "Spinal cord function and rehabilitation - an overview." J Physiol **533**(Pt 1): 3-4.

Prochazka, A., V. K. Mushahwar, et al. (2001). "Neural prostheses." J Physiol **533**(Pt 1): 99-109.

Prochazka, A., V. K. Mushahwar, et al. (2001). "Neural prostheses." The Journal of Physiology **533**(Pt 1): 99-109.

Raff, M. C., A. V. Whitmore, et al. (2002). "Axonal self-destruction and neurodegeneration." Science **296**(5569): 868-71.

Ranck, J. B., Jr. (1975). "Which elements are excited in electrical stimulation of mammalian central nervous system: a review." Brain Res **98**(3): 417-40.

Rashev, P. Z., M. Amaris, et al. (2002). "Microprocessor-controlled colonic peristalsis: dynamic parametric modeling in dogs." Dig Dis Sci **47**(5): 1034-48.

Rattay, F. and S. Resatz (2007). "Dipole distance for minimum threshold current to stimulate unmyelinated axons with microelectrodes." IEEE Transactions on Biomedical Engineering **54**(1): 158-62.

Reed, W. R., A. Shum-Siu, et al. (2008). "Reticulospinal pathways in the ventrolateral funiculus with terminations in the cervical and lumbar enlargements of the adult rat spinal cord." Neuroscience **151**(2): 505-17.

Reed, W. R., A. Shum-Siu, et al. (2006). "Inter-enlargement pathways in the ventrolateral funiculus of the adult rat spinal cord." Neuroscience **142**(4): 1195-207.

Rizzo, J. F., 3rd, J. Wyatt, et al. (2003). "Methods and perceptual thresholds for short-term electrical stimulation of human retina with microelectrode arrays." Invest Ophthalmol Vis Sci **44**(12): 5355-61.

Rizzo, J. F., 3rd, J. Wyatt, et al. (2003). "Perceptual efficacy of electrical stimulation of human retina with a microelectrode array during short-term surgical trials." Invest Ophthalmol Vis Sci **44**(12): 5362-9.

Roberts, A., S. R. Soffe, et al. (1998). "Central circuits controlling locomotion in young frog tadpoles." Ann N Y Acad Sci **860**: 19-34.

Rodger, D. C., Li, W., Fong, A.J., Ameri, H., Meng, E., Burdick, J.W., Roy, R.R., Edgerton, V.R., Weiland, J.D., Humayun, M.S., Tai, Y. (2006). Flexible Microfabricated Parylene Multielectrode Arrays for Retinal Stimulation and Spinal Cord Field Modulation. IEEE Engineering In Medicine and Biology Society Special Topic Conference on Microtechnologies in Medicine and Biology. Okinawa, Japan.

Rosenfeld, J. E., A. M. Sherwood, et al. (1995). "Evidence of a pattern generator in paralyzed subjects with spinal cord injury during spinal cord stimulation." Society for Neuroscience Abstracts **21**.

Rosenzweig, E. S. and J. W. McDonald (2004). "Rodent models for treatment of spinal cord injury: research trends and progress toward useful repair." Curr Opin Neurol **17**(2): 121-31.

Rossignol, I. S. and H. Barbeau (1995). "New approaches to locomotor rehabilitation in spinal cord injury." Ann Neurol **37**(5): 555-6.

Rossignol, S., G. Barriere, et al. (2008). "Plasticity of locomotor sensorimotor interactions after peripheral and/or spinal lesions." Brain Res Rev **57**(1): 228-40.

Rossignol, S., L. Bouyer, et al. (2004). "Determinants of locomotor recovery after spinal injury in the cat." Prog Brain Res **143**: 163-72.

Rossignol, S., N. Giroux, et al. (2001). "Pharmacological aids to locomotor training after spinal injury in the cat." J Physiol **533**(Pt 1): 65-74.

Rousche, P. J., D. S. Pellinen, et al. (2001). "Flexible polyimide-based intracortical electrode arrays with bioactive capability." IEEE Transactions on Biomedical Engineering **48**(3): 361-71.

Rousche, P. J., D. S. Pellinen, et al. (2001). "Flexible polyimide-based intracortical electrode arrays with bioactive capability." IEEE Trans Biomed Eng **48**(3): 361-71.

Rutten, W. L. (2002). "Selective electrical interfaces with the nervous system." Annu Rev Biomed Eng **4**: 407-52.

Rutten, W. L., J. P. Smit, et al. (1999). "Neuro-electronic interfacing with multielectrode arrays." IEEE Eng Med Biol Mag **18**(3): 47-55.

Sahin, M., M. A. Haxhiu, et al. (1997). "Spiral nerve cuff electrode for recordings of respiratory output." Journal of Applied Physiology **83**(1): 317-22.

Saigal, R., C. Renzi, et al. (2004). "Intraspinal microstimulation generates functional movements after spinal-cord injury." IEEE Trans Neural Syst Rehabil Eng **12**(4): 430-40.

Saxena, S. and P. Caroni (2007). "Mechanisms of axon degeneration: from development to disease." Prog Neurobiol **83**(3): 174-91.

Schmidt, S., K. Horch, et al. (1993). "Biocompatibility of silicon-based electrode arrays implanted in feline cortical tissue." Journal of Biomedical Materials Research **27**(11): 1393-9.

Schomburg, E. D., N. Petersen, et al. (1998). "Flexor reflex afferents reset the step cycle during fictive locomotion in the cat." Exp Brain Res **122**(3): 339-50.

Schouenborg, J., H. Holmberg, et al. (1992). "Functional organization of the nociceptive withdrawal reflexes. II. Changes of excitability and receptive fields after spinalization in the rat." Exp Brain Res **90**(3): 469-78.

Schouenborg, J. and O. Kiehn (2002). "The Segerfalk symposium on principles of spinal cord function, plasticity and repair." Elsevier Science. Brain Research Reviews. **40**: 1-329.

Schouenborg, J., H. R. Weng, et al. (1995). "A survey of spinal dorsal horn neurones encoding the spatial organization of withdrawal reflexes in the rat." Exp Brain Res **106**(1): 19-27.

Schuettler, M. and T. Stieglitz (2000). "18polar Hybrid Cuff Electrodes for Stimulation of Peripheral Nerves." 5th Annual International Conference of the International Functional Electrical Stimulation Society, Aalborg, Denmark: 18–20.

Schuettler, M., S. Stiess, et al. (2005). "Fabrication of implantable microelectrode arrays by laser cutting of silicone rubber and platinum foil." J Neural Eng **2**(1): S121-8.

Schuettler, M., S. Stiess, et al. (2005). "Fabrication of implantable microelectrode arrays by laser cutting of silicone rubber and platinum foil." Journal of Neural Engineering **2**: S121.

Schuettler, M., S. Stiess, et al. (2005). "Fabrication of implantable microelectrode arrays by laser cutting of silicone rubber and platinum foil." Journal of Neural Engineering **2**(1): S121-8.

Shao, J. and E. Miller. "Releasing Polydimethylsiloxane (PDMS) Replica Parts From Micromolds." 2007, from http://www.pnl.gov/microproducts/conferences/2004/posters/shao.pdf. Most recent access date: August 2008.

Shay, B. L., M. Sawchuk, et al. (2005). "Serotonin 5-HT2 receptors induce a long-lasting facilitation of spinal reflexes independent of ionotropic receptor activity." Journal of Neurophysiology **94**(4): 2867-77.

Shay, B. L., M. Sawchuk, et al. (2005). "Serotonin 5-HT2 receptors induce a long-lasting facilitation of spinal reflexes independent of ionotropic receptor activity." J Neurophysiol **94**(4): 2867-77.

Shealy, C. N., J. T. Mortimer, et al. (1970). "Dorsal column electroanalgesia." J Neurosurg **32**(5): 560-4.

Shealy, C. N., J. T. Mortimer, et al. (1967). "Electrical inhibition of pain by stimulation of the dorsal columns: preliminary clinical report." Anesth Analg **46**(4): 489-91.

Shealy, C. N., N. Taslitz, et al. (1967). "Electrical inhibition of pain: experimental evaluation." Anesth Analg **46**(3): 299-305.

Sherrington, C. S. (1910). "Flexion-reflex of the limb, crossed extension-reflex and reflex stepping and standing,." J. Physiol. (Lond), 40: 28-121.

Sillar, K. T. and A. Roberts (1992). "Phase-dependent Modulation of a Cutaneous Sensory Pathway by Glycinergic Inhibition from the Locomotor Rhythm Generator in Xenopus Embryos." Eur J Neurosci **4**(11): 1022-1034.

Silver, J. and J. H. Miller (2004). "Regeneration beyond the glial scar." Nat Rev Neurosci **5**(2): 146-156.

Spelman, F. A. (1999). "The past, present, and future of cochlear prostheses." IEEE Engineering in Medicine and Biology Magazine **18**(3): 27-33.

Spelman, F. A. (1999). "The past, present, and future of cochlear prostheses." IEEE Eng Med Biol Mag **18**(3): 27-33.

Spinelli, M., S. Malaguti, et al. (2005). "A new minimally invasive procedure for pudendal nerve stimulation to treat neurogenic bladder: description of the method and preliminary data." Neurourol Urodyn **24**(4): 305-9.

Stein, R. B., Y. Aoyagi, et al. (2004). "Encoding mechanisms for sensory neurons studied with a multielectrode array in the cat dorsal root ganglion." Can J Physiol Pharmacol **82**(8-9): 757-68.

Stein, R. B. and V. Mushahwar (2005). "Reanimating limbs after injury or disease." Trends in Neurosciences **28**(10): 518-24.

Stein, R. B. and K. G. Pearson (1971). "Predicted amplitude and form of action potentials recorded from unmyelinated nerve fibres." J Theor Biol **32**(3): 539-58.

Stein, R. B. and K. G. Pearson (1971). "Predicted amplitude and form of action potentials recorded from unmyelinated nerve fibres." Journal of Theoretical Biology **32**(3): 539-58.

Stieglitz, T. (2001). "Catalogue on Available Flexible, Light-weighted Microelectrodes." from www.ibmt.fraunhofer.de/gruppe_l/download/IBMT_Neuro%20Electrode%20Catalogue%20-%20July%202001.pdf. Most recent date accessed: January 2007.

Stieglitz, T., H. Beutel, et al. (1997). "[Flexible multichannel microelectrodes with integrated leads for use in neuroprosthetics]." Biomed Tech (Berl) **42 Suppl**: 449-50.

Strauss, I. and A. Lev-Tov (2003). "Neural pathways between sacrocaudal afferents and lumbar pattern generators in neonatal rats." J Neurophysiol **89**(2): 773-84.

Struijk, J. J., J. Holsheimer, et al. (1993). "Excitation of dorsal root fibers in spinal cord stimulation: a theoretical study." IEEE Trans Biomed Eng **40**(7): 632-9.

Struijk, J. J., M. Thomsen, et al. (1999). "Cuff electrodes for long-term recording of natural sensory information." IEEE Engineering Medicine Biology Magazine **18**(3): 91-8.

Subrebost, G. L., A. J. Rosenbloom, et al. (2002). In Situ Fabricated Microchannels Using Porous Polymer and Xenon Difluoride Etchant. Proceedings of the Sixth International Symposium on Micro Total Analysis System (mTAS 2002), Nara, Japan, Nov. 2-8, 2002.

Suzuki, Y. Y.-C. T. (2003). Micromachined high-aspect-ratio parylene beam and its application to low-frequency seismometer. Micro Electro Mechanical Systems, IEEE The Sixteenth Annual International Conference on. Kyoto.

Tai, C., A. M. Booth, et al. (1998). "Penile erection produced by microstimulation of the sacral spinal cord of the cat." IEEE Trans Rehabil Eng **6**(4): 374-81.

Tai, C., A. M. Booth, et al. (2001). "Colon and anal sphincter contractions evoked by microstimulation of the sacral spinal cord in cats." Brain Res **889**(1-2): 38-48.

Tai, C., A. M. Booth, et al. (2004). "Bladder and urethral sphincter responses evoked by microstimulation of S2 sacral spinal cord in spinal cord intact and chronic spinal cord injured cats." Exp Neurol **190**(1): 171-83.

Tai, C., A. M. Booth, et al. (1999). "Isometric torque about the knee joint generated by microstimulation of the cat L6 spinal cord." IEEE Trans Rehabil Eng **7**(1): 46-55.

Tai, C., A. M. Booth, et al. (2000). "Multimicroelectrode stimulation within the cat L6 spinal cord: influences of electrode combinations and stimulus interleave time on knee joint extension torque." IEEE Trans Rehabil Eng **8**(1): 1-10.

Tai, C., A. M. Booth, et al. (2003). "Multi-joint movement of the cat hindlimb evoked by microstimulation of the lumbosacral spinal cord." Exp Neurol **183**(2): 620-7.

Takeuchi, S. and I. Shimoyama (2004). "A radio-telemetry system with a shape memory alloy microelectrode for neural recording of freely moving insects." IEEE Trans Biomed Eng **51**(1): 133-7.

Tarler, M. D. and J. T. Mortimer (2004). "Selective and independent activation of four motor fascicles using a four contact nerve-cuff electrode." IEEE Trans Neural Syst Rehabil Eng **12**(2): 251-7.

Taylor, P. N., J. H. Burridge, et al. (1999). "Patients' perceptions of the Odstock Dropped Foot Stimulator (ODFS)." Clin Rehabil **13**(5): 439-46.

Thompson, S. W., A. E. King, et al. (1990). "Activity-Dependent Changes in Rat Ventral Horn Neurons in vitro; Summation of Prolonged Afferent Evoked Postsynaptic Depolarizations Produce a d-2-Amino-5-Phosphonovaleric Acid Sensitive Windup." Eur J Neurosci **2**(7): 638-649.

Tresch, M. C. and E. Bizzi (1999). "Responses to spinal microstimulation in the chronically spinalized rat and their relationship to spinal systems activated by low threshold cutaneous stimulation." Exp Brain Res **129**(3): 401-16.

Tresch, M. C., P. Saltiel, et al. (1999). "The construction of movement by the spinal cord." Nat Neurosci **2**(2): 162-7.

Tsay, C., Lacour, S.P., Wagner, S., Morrison, B., III (2005). Architecture, Fabrication, and Properties of Stretchable Micro-Electrode Arrays. Sensors, 2005 IEEE.

Tyler, D. J. and D. M. Durand (2002). "Functionally selective peripheral nerve stimulation with a flat interface nerve electrode." IEEE Trans Neural Syst Rehabil Eng **10**(4): 294-303.

Tyler, D. J. and D. M. Durand (2002). "Functionally selective peripheral nerve stimulation with a flat interface nerve electrode." IEEE Transactions on Neural Systems and Rehabilitation Engineering **10**(4): 294-303.

Veraart, C., W. M. Grill, et al. (1993). "Selective control of muscle activation with a multipolar nerve cuff electrode." IEEE Trans Biomed Eng **40**(7): 640-53.

Vetter, R. J., J. C. Williams, et al. (2004). "Chronic neural recording using silicon-substrate microelectrode arrays implanted in cerebral cortex." IEEE Trans Biomed Eng **51**(6): 896-904.

Wall, P. D. (1994). "Control of impulse conduction in long range branches of afferents by increases and decreases of primary afferent depolarization in the rat." Eur J Neurosci **6**(7): 1136-42.

Wallis, D. I., J. Wu, et al. (1993). "Is 5-hydroxytryptamine mediating descending inhibition in the neonatal rat spinal cord through different receptor subtypes?" Eur J Pharmacol **250**(3): 371-7.

Waltz, J. M. (1997). "Spinal cord stimulation: a quarter century of development and investigation. A review of its development and effectiveness in 1,336 cases." Stereotact Funct Neurosurg **69**(1-4 Pt 2): 288-99.

Warren, D. J., E. Fernandez, et al. (2001). "High-resolution two-dimensional spatial mapping of cat striate cortex using a 100-microelectrode array." Neuroscience **105**(1): 19-31.

Warren, D. J. and R. A. Normann (2005). "Functional reorganization of primary visual cortex induced by electrical stimulation in the cat." Vision Res **45**(5): 551-65.

Weingarden, H. P., G. Zeilig, et al. (1998). "Hybrid functional electrical stimulation orthosis system for the upper limb: effects on spasticity in chronic stable hemiplegia." Am J Phys Med Rehabil **77**(4): 276-81.

Willis, W. D., E. D. Al-Chaer, et al. (1999). "A visceral pain pathway in the dorsal column of the spinal cord." Proc Natl Acad Sci U S A **96**(14): 7675-9.

Willis, W. D., Coggeshall, R.E. (2004). Sensory Mechanisms of the Spinal Cord. New York, Kiuwer Academic/Plenum Publishers.

Wolpaw, J. R. and J. S. Carp (1993). "Adaptive plasticity in spinal cord." Adv Neurol **59**: 163-74.

Woodford, B. J., R. R. Carter, et al. (1996). "Histopathologic and physiologic effects of chronic implantation of microelectrodes in sacral spinal cord of the cat." J Neuropathol Exp Neurol **55**(9): 982-91.

Yamaguchi, T. (1986). "Descending pathways eliciting forelimb stepping in the lateral funiculus: experimental studies with stimulation and lesion of the cervical cord in decerebrate cats." Brain Res **379**(1): 125-36.

Yang, X., Grosjean, C., Tai, Y.C. (1998). A low power MEMS silicone/parylene valve. Solid-State Sensor and Actuator Workshop.

Zhong, Y., X. Yu, et al. (2001). "Stabilizing electrode-host interfaces: a tissue engineering approach." J Rehabil Res Dev **38**(6): 627-32.

Zhong, Y., X. Yu, et al. (2001). "Stabilizing electrode-host interfaces: a tissue engineering approach." Journal of Rehabilitation Research and Development **38**(6): 627-32.

Branner, A., R. B. Stein, et al. (2001). "Selective stimulation of cat sciatic nerve using an array of varying-length microelectrodes." Journal of Neurophysiology **85**(4): 1585-94.

Brindley, G. S., C. E. Polkey, et al. (1982). "Sacral anterior root stimulators for bladder control in paraplegia." Paraplegia **20**(6): 365-81.

Cater, H. L., D. Gitterman, et al. (2007). "Stretch-induced injury in organotypic hippocampal slice cultures reproduces in vivo post-traumatic neurodegeneration: role of glutamate receptors and voltage-dependent calcium channels." Journal of Neurochemistry **101**(2): 434-47.

Chapin, J. K. (2000). "Neural prosthetic devices for quadriplegia." Currrent Opinion in Neurology **13**(6): 671-5.

Clark, G. M., Y. C. Tong, et al. (1977). "A multiple electrode cochlear implant." Journal of Laryngology and Otology **91**(11): 935-45.

DiMarco, A. F. (2001). "Neural prostheses in the respiratory system." Journal of Rehabilitation Research and Development **38**(6): 601-7.

Edell, D. J., V. V. Toi, et al. (1992). "Factors influencing the biocompatibility of insertable silicon microshafts in cerebral cortex." IEEE Transactions on Biomedical Engineering **39**(6): 635-43.

Garra, J., T. Long, et al. (2002). "Dry etching of polydimethylsiloxane for microfluidic systems." Journal of Vacuum Science & Technology a-Vacuum Surfaces and Films **20**(3): 975-982.

Gerasimenko, Y. P., I. A. Lavrov, et al. (2006). "Spinal cord reflexes induced by epidural spinal cord stimulation in normal awake rats." Journal of Neuroscience Methods **157**(2): 253-63.

Gray, D. S., J. Tien, et al. (2004). "High-conductivity elastomeric electronics." Advanced Materials **16**(5): 393-+.

Grill, W. M., M. D. Craggs, et al. (2001). "Emerging clinical applications of electrical stimulation: opportunities for restoration of function." Journal of Rehabilitation Research and Development **38**(6): 641-53.

He, W. and R. V. Bellamkonda (2005). "Nanoscale neuro-integrative coatings for neural implants." Biomaterials **26**(16): 2983-90.

Heuschkel, M. O., M. Fejtl, et al. (2002). "A three-dimensional multi-electrode array for multi-site stimulation and recording in acute brain slices." Journal of Neuroscience Methods **114**(2): 135-48.

Hillman, T., A. N. Badi, et al. (2003). "Cochlear nerve stimulation with a 3-dimensional penetrating electrode array." Otology and Neurotology **24**(5): 764-8.

Holman G., Y. H., R.C. Wyeth, A.O.D. Willows, D. Denton, K.F. Bohringer (2002). Silicon Micro-Needles with Flexible Interconnections. Second Annual International IEEE-EMBS Special Topic Conference on Microtechnologies in Medicine & Biology.

Ichiyama, R. M., Y. P. Gerasimenko, et al. (2005). "Hindlimb stepping movements in complete spinal rats induced by epidural spinal cord stimulation." Neuroscience Letters **383**(3): 339-44.

Kessler, D. K. (1999). "The CLARION Multi-Strategy Cochlear Implant." Annals of Otology, Rhinology, and Laryngology Supplement **177**: 8-16.

Kraft, G. H., S. S. Fitts, et al. (1992). "Techniques to improve function of the arm and hand in chronic hemiplegia." Arch Phys Med Rehabil **73**(3): 220-7.

Kralj, A., T. Bajd, et al. (1988). "Enhancement of gait restoration in spinal injured patients by functional electrical stimulation." Clin Orthop Relat Res(233): 34-43.

Leventhal, D. K. and D. M. Durand (2003). "Subfascicle stimulation selectivity with the flat interface nerve electrode." Annals of Biomedical Engineering **31**(6): 643-52.

Leventhal, D. K. and D. M. Durand (2004). "Chronic measurement of the stimulation selectivity of the flat interface nerve electrode." IEEE Transactions on Biomedical Engineering **51**(9): 1649-58.

Liberson, W. T., H. J. Holmquest, et al. (1961). "Functional electrotherapy: stimulation of the peroneal nerve synchronized with the swing phase of the gait of hemiplegic patients." Arch Phys Med Rehabil **42**: 101-5.

Loeb, G. E. and R. A. Peck (1996). "Cuff electrodes for chronic stimulation and recording of peripheral nerve activity." Journal of Neuroscience Methods **64**(1): 95-103.

Madou, M. J. (2002). Fundamentals of Microfabrication: The Science of Miniaturization, Second Edition, CRC Press.

Maghribi, M., J. Hamilton, et al. (2002). Stretchable micro-electrode array [for retinal prostheses]. Microtechnologies in Medicine & Biology 2nd Annual International IEEE-EMB Special Topic Conference on, Madison, WI, IEEE, Piscataway.

Maghribi, M., J. Hamilton, et al. (2002). Stretchable micro-electrode array [for retinal prosthesis].

Magnuson, D. S., M. J. Schramm, et al. (1995). "Long-duration, frequency-dependent motor responses evoked by ventrolateral funiculus stimulation in the neonatal rat spinal cord." Neuroscience Letters **192**(2): 97-100.

Magnuson, D. S. and T. C. Trinder (1997). "Locomotor rhythm evoked by ventrolateral funiculus stimulation in the neonatal rat spinal cord in vitro." Journal of Neurophysiology **77**(1): 200-6.

McDonnall, D., G. A. Clark, et al. (2004). "Interleaved, multisite electrical stimulation of cat sciatic nerve produces fatigue-resistant, ripple-free motor responses." IEEE Transactions on Neural Systems and Rehabilitation Engineering **12**(2): 208-15.

Naples, G. G., J. T. Mortimer, et al. (1988). "A spiral nerve cuff electrode for peripheral nerve stimulation." IEEE Transactions on Biomedical Engineering **35**(11): 905-16.

Oka, H., K. Shimono, et al. (1999). "A new planar multielectrode array for extracellular recording: application to hippocampal acute slice." Journal of Neuroscience Methods **93**(1): 61-7.

Polikov, V. S., P. A. Tresco, et al. (2005). "Response of brain tissue to chronically implanted neural electrodes." Journal of Neuroscience Methods **148**(1): 1-18.

Prochazka, A., M. Gauthier, et al. (1997). "The bionic glove: an electrical stimulator garment that provides controlled grasp and hand opening in quadriplegia." Arch Phys Med Rehabil **78**(6): 608-14.

Prochazka, A., V. K. Mushahwar, et al. (2001). "Neural prostheses." The Journal of Physiology **533**(Pt 1): 99-109.

Rodger, D. C., Li, W., Fong, A.J., Ameri, H., Meng, E., Burdick, J.W., Roy, R.R., Edgerton, V.R., Weiland, J.D., Humayun, M.S., Tai, Y. (2006). Flexible Microfabricated Parylene Multielectrode Arrays for Retinal Stimulation and Spinal Cord Field Modulation. IEEE Engineering In Medicine and Biology

Society Special Topic Conference on Microtechnologies in Medicine and Biology. Okinawa, Japan.

Rousche, P. J., D. S. Pellinen, et al. (2001). "Flexible polyimide-based intracortical electrode arrays with bioactive capability." IEEE Transactions on Biomedical Engineering **48**(3): 361-71.

Sahin, M., M. A. Haxhiu, et al. (1997). "Spiral nerve cuff electrode for recordings of respiratory output." Journal of Applied Physiology **83**(1): 317-22.

Schmidt, S., K. Horch, et al. (1993). "Biocompatibility of silicon-based electrode arrays implanted in feline cortical tissue." Journal of Biomedical Materials Research **27**(11): 1393-9.

Schuettler, M. and T. Stieglitz (2000). "18polar Hybrid Cuff Electrodes for Stimulation of Peripheral Nerves." 5th Annual International Conference of the International Functional Electrical Stimulation Society, Aalborg, Denmark: 18–20.

Schuettler, M., S. Stiess, et al. (2005). "Fabrication of implantable microelectrode arrays by laser cutting of silicone rubber and platinum foil." Journal of Neural Engineering **2**(1): S121-8.

Schuettler, M., S. Stiess, et al. (2005). "Fabrication of implantable microelectrode arrays by laser cutting of silicone rubber and platinum foil." Journal of Neural Engineering **2**: S121.

Schuettler, M., S. Stiess, et al. (2005). "Fabrication of implantable microelectrode arrays by laser cutting of silicone rubber and platinum foil." J Neural Eng **2**(1): S121-8.

Shao, J. and E. Miller. "Releasing Polydimethylsiloxane (PDMS) Replica Parts From Micromolds." 2007, from http://www.pnl.gov/microproducts/conferences/2004/posters/shao.pdf. Most recent access date: August 2008.

Shay, B. L., M. Sawchuk, et al. (2005). "Serotonin 5-HT2 receptors induce a long-lasting facilitation of spinal reflexes independent of ionotropic receptor activity." Journal of Neurophysiology **94**(4): 2867-77.

Spelman, F. A. (1999). "The past, present, and future of cochlear prostheses." IEEE Engineering in Medicine and Biology Magazine **18**(3): 27-33.

Stein, R. B. and V. Mushahwar (2005). "Reanimating limbs after injury or disease." Trends in Neurosciences **28**(10): 518-24.

Stein, R. B. and K. G. Pearson (1971). "Predicted amplitude and form of action potentials recorded from unmyelinated nerve fibres." Journal of Theoretical Biology **32**(3): 539-58.

Stieglitz, T. (2001). "Catalogue on Available Flexible, Light-weighted Microelectrodes." from www.ibmt.fraunhofer.de/gruppe_l/download/IBMT_Neuro%20Electrode%20Catalogue%20-%20July%202001.pdf. Most recent access date: January 2007.

Struijk, J. J., M. Thomsen, et al. (1999). "Cuff electrodes for long-term recording of natural sensory information." IEEE Engineering Medicine Biology Magazine **18**(3): 91-8.

Subrebost, G. L., A. J. Rosenbloom, et al. (2002). In Situ Fabricated Microchannels Using Porous Polymer and Xenon Difluoride Etchant. Proceedings of the Sixth International Symposium on Micro Total Analysis System (mTAS 2002), Nara, Japan, Nov. 2-8, 2002.

Suzuki, Y. Y.-C. T. (2003). Micromachined high-aspect-ratio parylene beam and its application to low-frequency seismometer Micro Electro Mechanical Systems, IEEE The Sixteenth Annual International Conference on. Kyoto.

Taylor, P. N., J. H. Burridge, et al. (1999). "Patients' perceptions of the Odstock Dropped Foot Stimulator (ODFS)." Clin Rehabil **13**(5): 439-46.

Tsay, C., Lacour, S.P., Wagner, S., Morrison, B., III (2005). Architecture, Fabrication, and Properties of Stretchable Micro-Electrode Arrays. Sensors, 2005 IEEE.

Tyler, D. J. and D. M. Durand (2002). "Functionally selective peripheral nerve stimulation with a flat interface nerve electrode." IEEE Transactions on Neural Systems and Rehabilitation Engineering **10**(4): 294-303.

Weingarden, H. P., G. Zeilig, et al. (1998). "Hybrid functional electrical stimulation orthosis system for the upper limb: effects on spasticity in chronic stable hemiplegia." Am J Phys Med Rehabil **77**(4): 276-81.

Yang, X., Grosjean, C., Tai, Y.C. (1998). A low power MEMS silicone/parylene valve. Solid-State Sensor and Actuator Workshop.

Zhong, Y., X. Yu, et al. (2001). "Stabilizing electrode-host interfaces: a tissue engineering approach." Journal of Rehabilitation Research and Development **38**(6): 627-32.